

UNITED STATES DEPARTMENT OF THE INTERIOR  
GEOLOGICAL SURVEY

MORPHOLOGY, SEDIMENTATION, AND SEISMIC CHARACTERISTICS OF AN ARCTIC  
BEACH, NOME, ALASKA -- WITH ECONOMIC SIGNIFICANCES

REC'D. COLLEGE

JUN 8 1970

DIV. MINES & GEOLOGY

By

H. Gary Greene

RECEIVED  
JUN 10 1970  
GEOLOGICAL SURVEY

Open-file report

1970

This report is preliminary  
and has not been edited or  
reviewed for conformity with  
Geological Survey standards

#### ABSTRACT

Arctic beaches exhibit characteristics that do not occur on beaches in more temperate zones. In the summer of 1967 morphological, sedimentological, and seismic refraction studies were made on an arctic beach near Nome, Alaska, in order to better define these distinguishing characteristics.

Several distinct microrelief structures are developed during ice break-up and the melting of ice and snow on the beaches including ice-pushed ridges, kaimoo ridge and deposits, sea-ice kettles, sea-ice sand and sea-ice gravel cones, micro-outwash deposits, and microdeltaic deposits.

Sedimentological studies showed that sediment distribution along the beach is random with no increasing or decreasing median diameters, or sorting coefficients, or sand-gravel percentages, either along the strandline or along the beach profile. This random grain size distribution is attributed to the relatively low energy along the coast of the Seward Peninsula. Further, the beaches are insulated from the elements by ice for about 6 months out of the year and the beach sediments are disturbed annually by ice-push. Longshore drift appeared to vary from east to west during the summer of 1967 with a net transport to the east.

The seismic refraction study on the Nome beach indicated that internal stratigraphy of the overburden could be interpreted and correlated with known onshore and offshore stratigraphic units. Bedrock was well defined in the seismograms and exhibited a gently

undulating topography with several buried channels that may be sites of gold placer deposits.

## TABLE OF CONTENTS

	PAGE
INTRODUCTION.....	1
I. General.....	1
II. Purpose and Scope of Investigation.....	3
III. Location.....	4
IV. Equipment.....	7
V. Geologic Setting.....	7
VI. Previous Investigations.....	10
<u>PART I - BEACH MORPHOLOGY</u>	
I. Introduction.....	12
II. Beach Profile.....	14
III. Beach Features.....	14
Rill Marks.....	14
Swash Marks.....	14
Cusps.....	16
IV. Microrelief Structures.....	18
Microrelief Features of the Lower Beach.....	19
Ice-pushed Ridges.....	19
Kaimoo Ridge and Deposits.....	20
Sea-ice Kettles.....	25
Sea-ice Sand Cones and Sea-ice Gravel Cones.....	27
Microrelief Features of the Upper Beach.....	34
Microfluvial Deposits.....	34
1. Micro-outwash Deposits.....	35
2. Micro-deltaic Deposits.....	35
<u>PART II - ASPECTS OF BEACH SEDIMENTATION AND TRANSPORT</u>	
I. Introduction.....	37
II. Procedures and Sampling Methods.....	37
Procedures.....	37
Methods.....	40
III. Grain Size Distribution.....	41
Swash Zone.....	44
Foreshore (or Lower Foreshore).....	44
Kaimoo Ridge Deposits and Kaimoo Deposits.....	45
Backshore (or Upper Foreshore).....	45
Micro-outwash Deposits.....	46
Stream Deposits.....	46
Offshore.....	47

	PAGE
IV. Processes Affecting Coastal Features.....	48
Wind.....	48
Waves.....	48
Littoral Currents.....	54
Ice.....	57
V. Offshore Features.....	57
River Mouth Bars and Spits.....	57
Longshore.....	59
VI. Conclusions.....	62
PART III - SEISMIC INVESTIGATION	
I. Introduction.....	69
II. Equipment and Procedures.....	69
Description of Equipment.....	70
Procedures.....	70
Summary.....	76
III. Interpretation of Seismograms.....	77
Theory.....	78
Analysis of Data.....	79
IV. Results.....	83
General.....	83
Beach Profile.....	84
Seismic Velocities.....	84
Depths.....	85
Bedrock Topography.....	85
Tundra Survey.....	89
Seismic Velocities.....	89
Depths.....	92
V. Discussion and Conclusions.....	92
General.....	92
Interpretation.....	95
Potential Placer Sites.....	99
Conclusions.....	99
PART IV - SUMMARY.....	100
BIBLIOGRAPHY.....	103
APPENDIX	
Table I. Grain Size Analysis of Nome Beach Sediment Samples.....	105
Table II. Textural Analysis of Nome Beach Sediment Samples by Folk and Ward Method.....	138

# LIST OF FIGURES

FIGURE	PAGE
1. Index map of Alaska.....	5
2. Map of southwestern Seward Peninsula.....	6
3. Generalized geologic map and cross section of coastal plain at Nome.....	8
4. View of the Nome coastal plain and beaches.....	12 13
5. General beach profile.....	15
6. Swash marks near Snake River.....	16
7. Cusps on the Nome Beach.....	17 18
8. Ice-pushed ridges.....	20
9. Kaimoo.....	21
10. Scarp of kaimoo ridge.....	23
11. Diagram illustrating the formation of kaimoo ridge, kaimoo deposit, and micro-outwash deposit.....	24
12. Sea-ice kettles in swash zone.....	25
13. Sea-ice kettle with chunk of melting ice.....	26
14. Diagram illustrating the formation of sea-ice kettles.....	28
15. Sea-ice sand cone.....	29
16. Sea-ice gravel cone.....	30
17. Formation of sea-ice sand and sea-ice gravel cones by melting of sediment-laden brash ice.....	32
18. Melting block of sea-ice showing sand flowing down sides to form a sand ridge.....	33
19. Fairy-castle structured ridges.....	33
20. Micro-deltaic deposit.....	36

FIGURE		PAGE
21.	Grain size distribution map of the Nome beach between Penny and Snake Rivers.....	38 39
22.	Mean Size vs. Standard Deviation plot for swash zone, longshore trough and longshore bar samples.....	42
23.	Mean Size vs. Sorting plot for swash zone, longshore trough and bar, foreshore, and backshore samples.....	43
24.	Small crashing breakers on the Nome beach.....	50 51
25.	Generalized wave refraction diagram of the northwestern Norton Sound area.....	52
26.	Storm wave-cut escarpment.....	53
27.	Nome dump.....	55
28.	The Snake River jetties showing accumulation of sediment on the west side and erosion on the east.....	56
29.	River mouth bars and spits.....	58 59
30.	Barrier spit with small lagoon built at the mouth of a stream east of Nome.....	60
31.	Old barrier spit and previous outlet of Penny River.....	61
32.	Mean Size vs. Sorting plot for kaimoo, kaimoo ridge and micro-outwash deposits samples.....	68
33.	Seismograms obtained with blasting caps and dynamite sound sources.....	72
34.	Time-distance graph and schematic representation of refraction of seismic energy at three acoustical interfaces and the resultant time- distance graph.....	80
35.	Refraction seismograms showing how first-arrival times are picked and plotted on a time-distance graph.....	81

FIGURE	PAGE
36. Beach survey. Map showing location of beach seismic stations and composite basement contours, with cross section, expanded beach profile, and geophone spreads.....	86
37. Time-distance graphs constructed from data of beach station 49.....	87
38. Time-distance graphs constructed from data of beach station 27.....	88
39. Time-distance graphs constructed from data of beach station 45.....	88
40. Profile of beach seismic refraction line relating travel-time curves to bedrock topography.....	90 91
41. Tundra survey. Map showing location of tundra seismic line and USSR&M drill-hole lines with block diagram and geophone spread.....	93
42. Profile of tundra seismic refraction line relating travel-time curves with bedrock topography.....	94
43. Idealized cross sections and stratigraphic column of Nome beach and tundra survey areas.....	98



## INTRODUCTION

### I. GENERAL

Field work on the beaches of Nome, Alaska, was conducted as part of the U.S. Geological Survey's Heavy Metals program on the Seward Peninsula during the summer of 1967. This was one of several independent explorations of sedimentary processes, Pleistocene stratigraphy, and gold resources of the Nome area offshore and on the beach. The investigation of the beaches included a study of beach morphology, a study of size distribution and sediment transport, and a seismic refraction survey.

Arctic beaches, unlike beaches at lower latitudes, are affected by wave action for only 6 months or less each year; during the remainder of the year they are protected by layers of snow, ice and gravel with a frozen matrix. Beaches in the Nome region are narrow, 200 feet wide or less, and includes only a foreshore backed by wave-eroded cliffs consisting of outwash, alluvium, colluvium, wind-blown silt, and peat which accumulated during Wisconsin and Holocene time. The cliffs range in height from 10 to 20 feet and are capped by tundra. A snowbank typically covers the base of the cliffs through late July and only during severe storms do waves reach the base of the cliffs. Slumping and solifluction are active in local areas.

Beaches along the peninsula are generally formed under conditions of low energy because the Bering Sea is shallow and has a relatively short fetch to the Seward Peninsula. Moreover, a

persistent ice cover precludes heavy seas and strong surf action along the beaches during the winter. Tidal range along the Seward Peninsula is very small and tides do not significantly influence beach processes. Sea-level changes caused by winds sometimes exceed those caused by lunar tides.

The most notable feature of the Nome beaches is its rough and commonly hummocky microtopography; this irregular beach surface persisted throughout the summer of 1967. Formation of most of the microrelief features is controlled by the pronounced seasonal temperature differences common in the arctic. When air temperatures fall below freezing in the fall, salt water begins to freeze on the surface of the beach and forms a protective layer of ice and gravel called a kaimoo (Moore, 1966, p. 593). Shorefast sea-ice (Sea-ice frozen to the ocean bottom near shore) forms during the winter and effectively prevents surf action. During spring break-up, when air temperatures begin to rise, sea-ice may grind ashore and forcefully disturb the beach sediments. Most of the microrelief features found on arctic beaches form in the spring. Summer storms usually wash away such structures shortly after they form; although, occasionally they may last throughout the summer until fall storms destroy them.

The microtopography was observed in 1967 to be produced during May and early June by sea-ice break-up, the melting of the kaimoo, permafrost, and blocks of ice stranded on the beach, and the addition of new sand and gravel to the beach by a spring storm.

Weather and sea conditions were unusual at Nome during the spring and summer of 1967 and a large shore-lead (that area that is open, without ice, between the shore and sea-ice offshore) opened early, evidently well before the last snow and prior to the last freezing weather. This allowed wave deposition of new sand and gravel onto the ice covered beach. As a result, microrelief produced by the ice and snow on the beach during this time was unusually well developed. Nevertheless, the features described in this report recurred, in less abundance in 1968, and similar features were seen around the south shore of Kotzebue Sound in the summer of 1966 (D. M. Hopkins, oral communication, 1968). In both years, the ice- and snow-formed microrelief persisted through July; the date and extent of destruction is unknown.

## II. PURPOSE AND SCOPE OF INVESTIGATION

Results of a study of beach morphology, a study of sedimentary processes, and a seismic refraction survey of an arctic beach near Nome, Alaska are reported here. Determination of mechanisms responsible for the unusual microrelief features found on the beach in 1967 and the determination of the type of dynamic processes acting on the beach and direction of longshore drift were major objectives in the investigation. The purpose of the seismic survey was to determine the beach thickness and bedrock topography under the beach. With the help of the results of the seismic survey correlation with onshore and offshore bedrock information could be made by the U.S. Geological Survey in their investigation for

detrital deposits of heavy metals. Field work was conducted between June 15, and September 1, 1967.

Generally both sediment sampling stations and seismic stations had a 1/2 to 1 mile spacing. The stations made offshore and sampled with the use of SCUBA had a 100 foot spacing. A total of 35 sediment stations and 37 seismic stations were made during the investigation.

About 5 pounds of sediment was collected at each of the sampling stations at various points along the beach profile for grain size analysis. Observations at each of these stations included wave direction and angle of attack, breaker type, general outline of beach profile, slope of beach face, beach width, type and coarseness of surface material, and morphologic and microrelief features present on the beach surface. Where possible the internal stratigraphy was noted. At each seismic station several seismograms were obtained to determine depth to bedrock and internal stratigraphy of the overburden.

### III. LOCATION

Areas of investigation are located in Alaska, on the Nome coastal plain, on the Seward Peninsula facing Norton Sound (Fig. 1). The beach region under consideration extends from Cape Rodney to Cape Nome. Detailed sediment and morphologic observations and the seismic study were confined to 10 miles of beach between Penny River and Snake River. An experimental seismic line across the tundra was located approximately 1 1/2 miles due north of Nome, Alaska, on Dry Creek (Fig. 2).

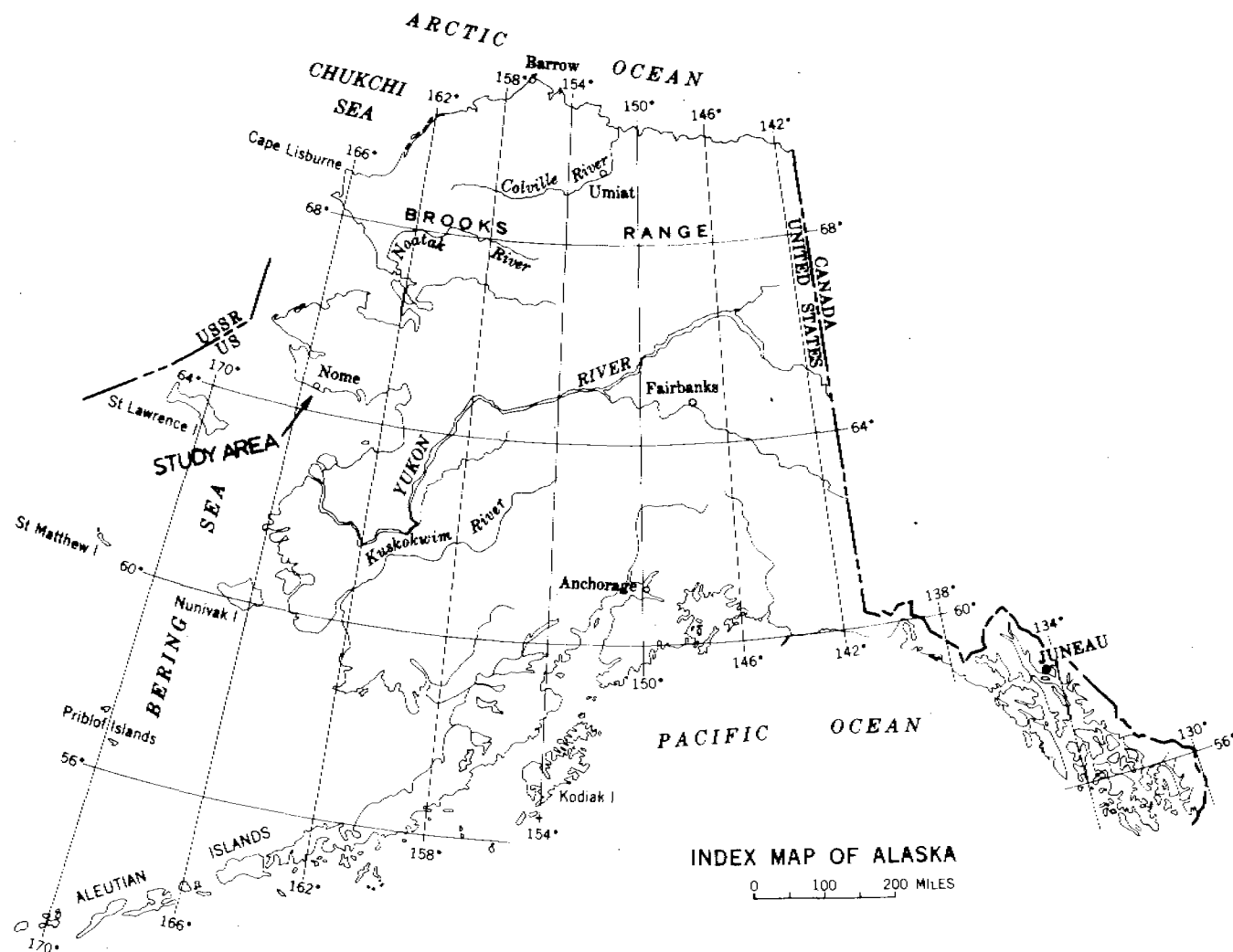


Figure 1. Index map of Alaska with Location of Study Area.

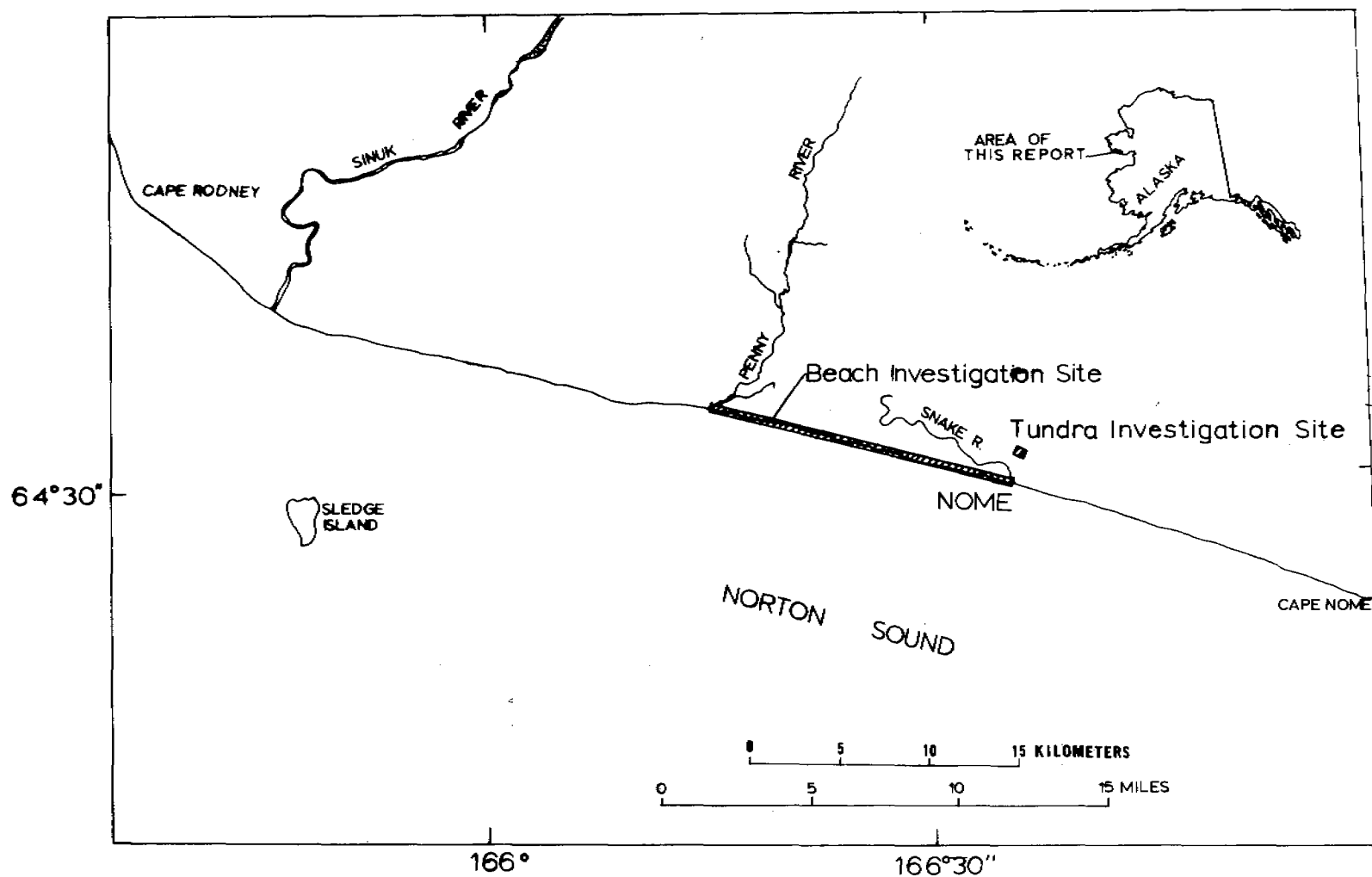


Figure 2.-Map of southwestern Seward Peninsula showing location of beach and tundra investigation sites.

#### IV. EQUIPMENT

A helicopter was used for reconnaissance, general surveillance, and sampling at remote places along the beach. Two tracked vehicles, a "Bombardier" and a "Weasel", were used at different times to travel between stations and to transport samples. The beach is too soft and too rough for wheeled vehicles. A portable seismograph was used to obtain seismic refraction data.

#### V. GEOLOGIC SETTING

The Nome coastal plain is covered with Pliocene and Pleistocene marine and glacial sand and gravel. Four marine units, locally known as Submarine Beach, Fourth Beach, Third Beach, and Second Beach, are recognized, each representing different sea level stands during the late Pliocene and Pleistocene time (Hopkins, 1960, p. 46). Submarine Beach, Second Beach, and Third Beach are separated by glacial drift of the Iron Creek (pre-Illinoian) and the Nome River (Illinoian) Glaciations. Covering the glacial drifts and the youngest marine sediments are outwash, alluvium, colluvium, wind blown silt, and peat accumulated during Wisconsin and Holocene time (Fig. 3). Beneath the sediments of the coastal plain and cropping out behind the coastal plain is Paleozoic schist and limestone bedrock that is faulted in many places (Collier and others, 1908, p. 149). Hopkins (1967, p. 49-50) describes the stratigraphy in greater detail.

The geology of Submarine Beach was extrapolated to the modern beach and used in the interpretations of the present beach stratigraphy. Submarine Beach consists of two strips (Inner and

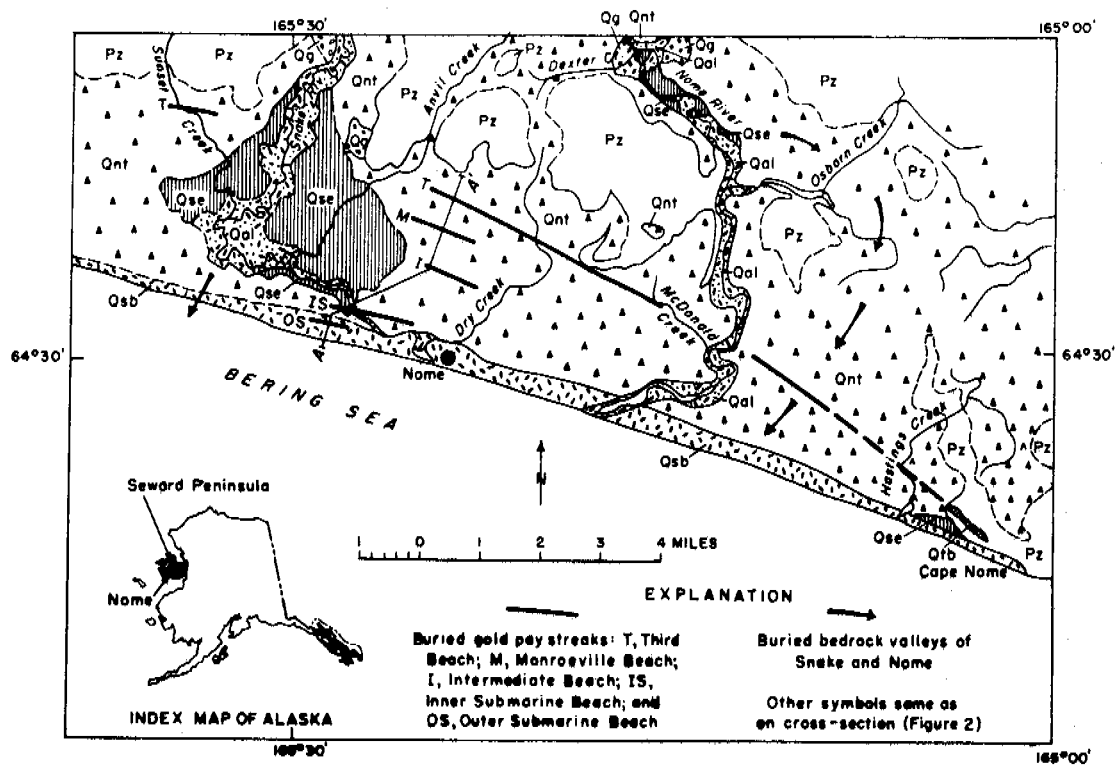


Figure 3A Generalized geologic map of the coastal plain at Nome.  
After Hopkins, 1960

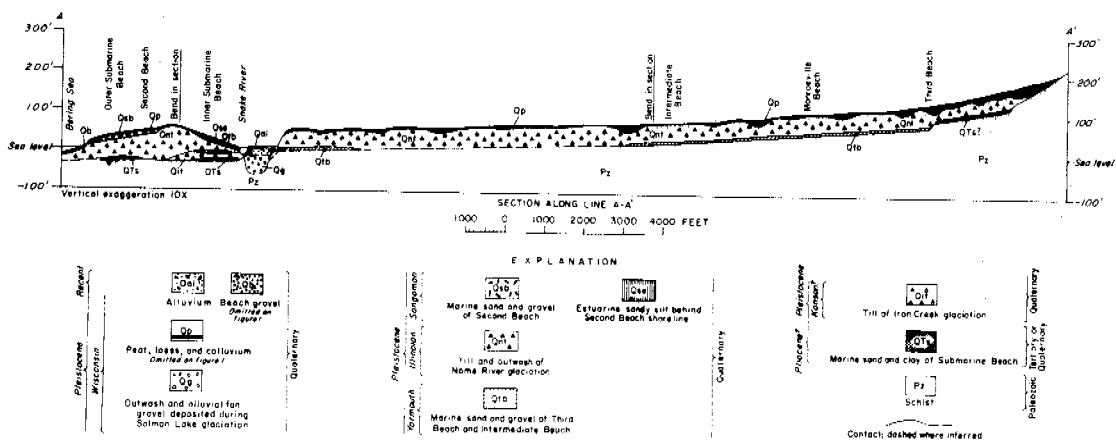


Figure 3B Cross section through the coastal plain at Nome along line AA', figure 3A.  
After Hopkins, 1960



Outer) of marine sediments oriented parallel to the present coast near the lower course of the Snake River (Fig. 3). The sediments consist of 1 to 3 feet of sand and pebbly sand resting upon bedrock where bedrock is high and on a shell rich clay where bedrock is low; these sediments appear to represent nearshore deposits rather than true beach deposits (Hopkins, 1967, p. 46). Geology of the beach was summarized by Brooks (1901, p. 85-91) from his examination of mining pits on the beach in 1898. Brooks observed a blue-clay bed found close to the tundra that sloped toward the sea and was referred to by the miners as a "false bedrock." About halfway down the beach (seaward) the clay bed was recognized beneath 5 to 7 feet of sand and gravel. Brooks could not trace the clay bed, or determine its thickness along the entire length of the beach, even though seams of clay appeared at several different locations. Evidence of similar clay beneath the beach in several places was found during the seismic survey and was interpreted as an offshore, shallow-water sediment deposited during Second Beach time. In addition, fine sands and coarse gravels were found with occasional thin lenses of clay immediately above the clay stratum.

In the vicinity of Dry Creek a thin layer of Wisconsin peat, loess, and colluvium overlies till and outwash of the Nome River glaciation which rests upon Paleozoic schist bedrock (Hopkins, 1960, p. 48) (Fig. 3). At the location of the tundra seismic line, Dry Creek has cut through the Wisconsin material and into about 20 feet of the Nome River till and outwash. Although the creek bed contains

boulders of schist, no bedrock outcrops were visible.

#### VI. PREVIOUS INVESTIGATIONS

The well known gold rush at Nome took place between 1889 and 1900 and accelerated geological investigations of the area by the U.S. Geological Survey (Brooks and others, 1901; Collier and others, 1908; Moffit, 1913). Later investigations of the Nome coastal plain were undertaken by the United States Smelting, Refining and Mining Co. (USSR&M) (Metcalf, J. B., and Tuck, Ralph, 1942, Placer Gold deposits of the Nome district, Alaska: Unpublished report, U.S. Smelting, Refining and Mining Company, p. 4-30) and by the U.S. Geological Survey (MacNeil and others, 1943, p. 69-96; Hopkins and others, 1960).

Except for the papers of Hume and Schalk, 1964; Moore, 1966; Rex, 1964; and Schalk, 1961, focused mostly on Point Barrow, Alaska, arctic beaches have received little study. There have been no detailed analyses of beach processes on the beaches of Nome, Alaska.

Beach placers of the Nome region extended along the shores of the Bering Sea from Cape Nome to Cape Rodney, a distance of 36 miles. Gold concentrations along the beach were found lying just above a false bedrock of silt, sand, and gravel; true bedrock could be found at a depth of 10 to 100 feet beneath the beach (Collier and others, 1908, p. 151). "Although only the most primitive methods were employed, over a million dollars were taken out (of the beaches) in a period of about two months. During the height of the excitement over 2,000 men were engaged in beach mining. Many of them made from

\$20 to \$100 per day. By the end of the summer (1899) the richest spots on the beach were practically exhausted" (Metcalf and Tuck, 1942, p. 4). Today, only very fine gold can be found in the beach sands. Over 2 million dollars of gold has been taken from the present beach, figured at the 1900 gold price of \$20.67 per ounce (Metcalf and Tuck, 1942, p. 30; Collier and others, 1908, p. 151). At \$20.67 gold, two million dollars of gold would be equivalent to approximately 100,000 ounces. To update this price figure, 100,000 ounces sold at today's price of \$35.00 an ounce would equal 3 1/2 million dollars. It has been estimated that 5,000,000 ounces of gold has been taken from the entire Nome area (Arthur Daily, oral communication to A. R. Tagg, 1968).

## PART I

## BEACH MORPHOLOGY

## I. INTRODUCTION

That portion of the coast of the Seward Peninsula studied would be classified by Johnson (1919) as a neutral, outwash plain coast or by Shepard (1963, p. 156), as a cusped foreland and glacial deposition coast with partially submerged drift features. Types of beaches found along this coast consist of shingled beaches and tideless, smooth profile sand beaches with a shingled base (King, 1961, p. 277) (Fig. 4A and B).

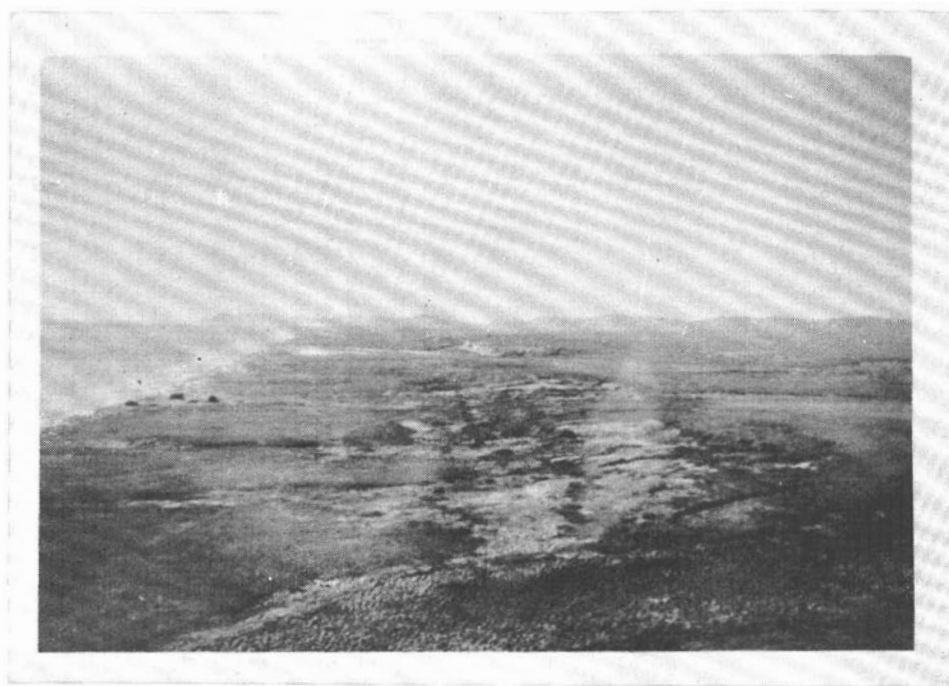


Figure 4.--A. View of the Nome coastal plain, looking west from Cape Nome toward Cape Rodney.



Figure 4.--B. Close-up view of the Nome beach. Photo clearly shows the extension of the Kaimoo ridge deposit. Cape Rodney at top of photo.

The general configuration of the coast of the Nome coastal plain is controlled by prevailing wind and wave direction and dynamic processes associated with ice. The beach surface along the Seward Peninsula near Nome is generally rugged but contains the common beach features such as rill marks, swash marks, and cusps. Microrelief features created by ice and associated mechanisms produce the rugged and hummocky beach surface.

## II. BEACH PROFILE

The beaches near Nome consist of only a foreshore except near Penny, Snake, and Nome Rivers, and other small streams along the beach where poorly developed berms and backshores are present (Fig. 5). The average slope of the beach face was about  $10^{\circ}$  and superimposed on the face were small storm beach ridges, kaimoo ridges, kaimoo deposits, all of which tended to increase the face angle. The average elevation or average height of the highest point on the beach, or height of berm when one existed, was 12 feet.

## III. BEACH FEATURES

### Rill marks

Rill marks are defined by Shepard (1963, p. 170) as "Small drainage channels forming in the lower portion of a beach at low tide." At Nome there is only about an 18 inch tidal range and as rill marks do not form at low tide they are rare here. Occasionally, when an offshore wind blows, sea level has been reported to drop as much as 4 feet. During the summer of 1967, on several occasions, a north or northeast wind blew offshore lowering sea level about 1 foot at which time drainage of the beach developed rill marks.

### Swash marks

Shepard (1963, p. 170) defined a swash mark as "The thin wavy line of fine sand, mica, or fucus left by the uprush of water along a beach." Swash marks were common on the Nome beaches and were especially well developed after a storm (Fig. 6).

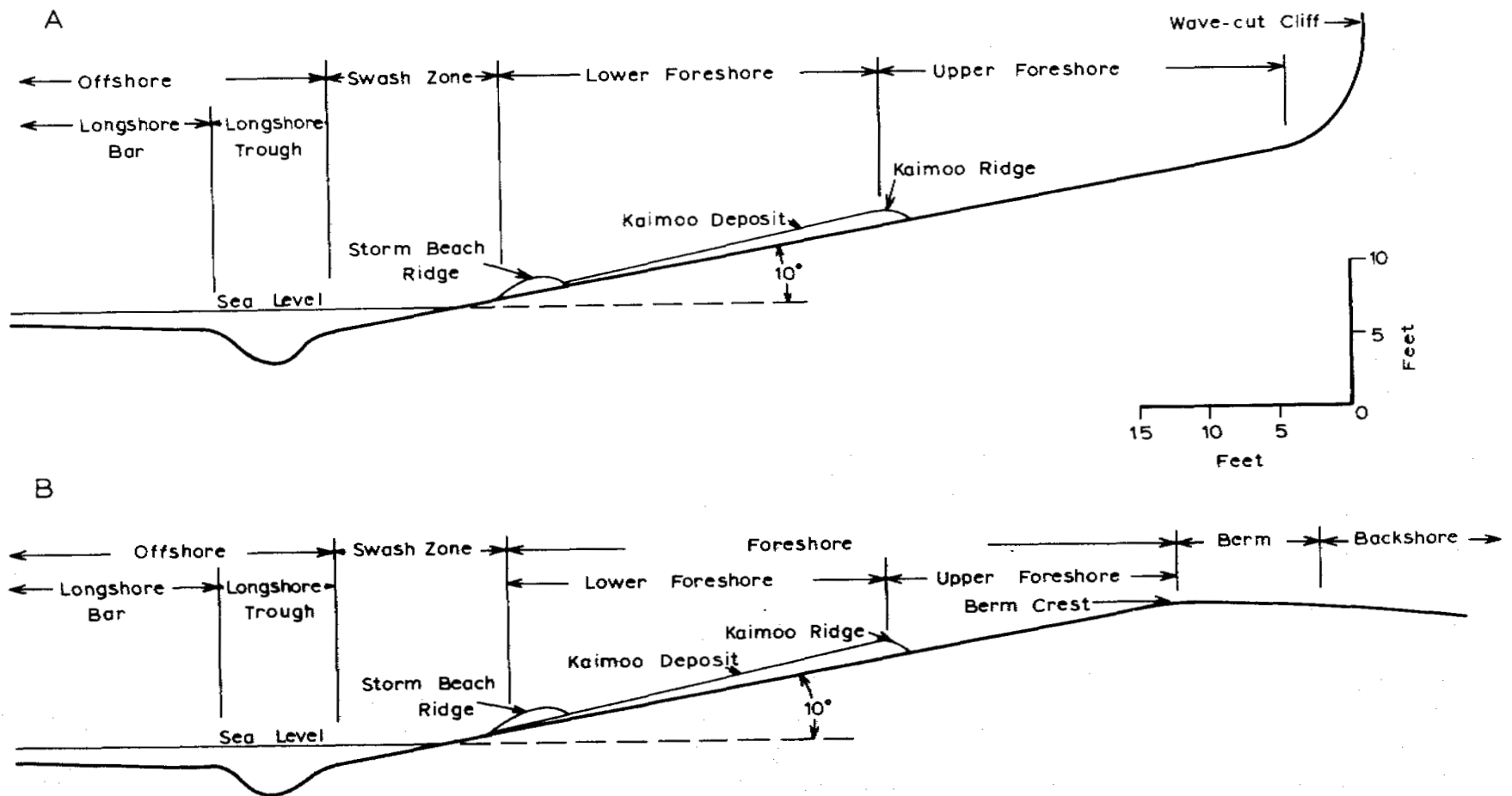


Figure 5. General beach profiles characteristic of most of the Nome beach.



Figure 6.--Swash marks near Snake River.

### Cusps

A cusp is defined by Shepard (1963, p. 169) as "One of a series of short ridges on the foreshore extending transverse to the beach and occurring at more or less regular intervals depending in spacing on wave height." At Nome cusps were unusually well developed and were found in both sand and gravel beaches (Fig. 7). Observations during the summer of 1967 at Nome supported Kuenen's



hypothesis of erosion of material in the bay by swash action with deposition of the coarser material at the back and on the horns of the cusp (Kuenen, 1948).



Figure 7.--A. Short period cusps on a coarse grained sandy beach near Nome, Alaska. Cape Rodney at top of photo.



Figure 7.--B. Long period cusps on a coarse gravel beach near Nome, Alaska. Horns of cusps consist of coarse gravel and bays consist of sand. Top of photo is west.

#### IV. MICRORELIEF STRUCTURES

A number of microrelief features distinctive of arctic and subarctic beaches were seen at Nome. Six microrelief features discussed in this report are either directly or indirectly created by interaction of surf, freezing seawater, and melting or break-up of sea-ice, snow, and permafrost. The beach environments in which the different microrelief is found depend on their originating mechanism and can be divided into two zones: (1) a lower beach zone, and (2) an upper beach zone. Microrelief features found on the lower beach are produced by the combination of deposition by wave action and melting of stranded ice fragments or brash ice and consist of ice-pushed ridges, kaimoo ridge and deposits, sea-ice

kettles, sea-ice gravel cones and sea-ice sand cones. Microrelief features found on the upper beach are developed by melt waters from surficial thawing of permafrost and melting snow-banks on the backshore and consist of microfluvial deposits made up of micro-outwash and micro-deltaic deposits.

#### Microrelief Features of the Lower Beach

Microrelief features of the lower beach form in the swash zone, but are preserved only if they form during storms when the swash zone extends higher on the beach than usual. The major portion of the microrelief features of this zone were seen well above the 1967 summer swash zone, probably as a result of storms from the south or southwest during the early spring.

#### Ice-pushed Ridges

Ice-pushed ridges on the Alaska coast have been discussed by Schalk (1961), Hume and Schalk (1964), Rex (1964), and Moore (1966). Hume and Schalk (1964, p. 267-268) state that "...buckling [ice] usually causes gouging, transportation, and deposition of the beach sediments in irregular mounds or ridges which have been called ice-pushed or ice-shoved mounds or ridges." Grounding of wind driven ice-floes which slide up and across the beach can produce relief of considerably different scale. For example, Hume and Schalk (1964, p. 267) described ice-pushed ridges as much as 15 feet high at Barrow, Alaska; in contrast, the author has observed ice-pushed ridges less than 6 inches high at Unalakleet, Alaska, in 1967. The few ice-pushed ridges seen on the beaches of Nome gave the appearance

of mounds of sand and gravel pushed up by a bulldozer. Ice-pushed ridges typical of arctic beaches are shown in figure 8.



Figure 8.--Ice-pushed ridges about 3 feet high, on a beach near Kotzebue, Alaska in the summer of 1966. Photo by Hans Nelson of the U.S. Geological Survey.

#### Kaimoo Ridge and Deposits

Moore (1966, p. 593) defines a kaimoo as "...the name given by the Eskimo to an ice and gravel rampart formed in winter on the surface of arctic beaches; it is extensively used by local people

as a smooth, flat trail." The kaimoo at Nome consist of a bed of ice approximately 1 meter thick and interlayered with thin beds of gravel and sand (Fig. 9).



Figure 9.--Kaimoo consisting of interlayers of ice, sand, and gravel. Scale indicated by shovel handle in left foreground, June, 1967.

Rex (1964, p. 391) describes a similar feature from Barrow, Alaska as "Spray from waves freezes to the beach in the fall. This frozen spray coats the beach with a glaze that may extend more than a hundred feet inland." Rex also states that "...the usual effect of glaze is to act as a coat of armor protecting beaches from

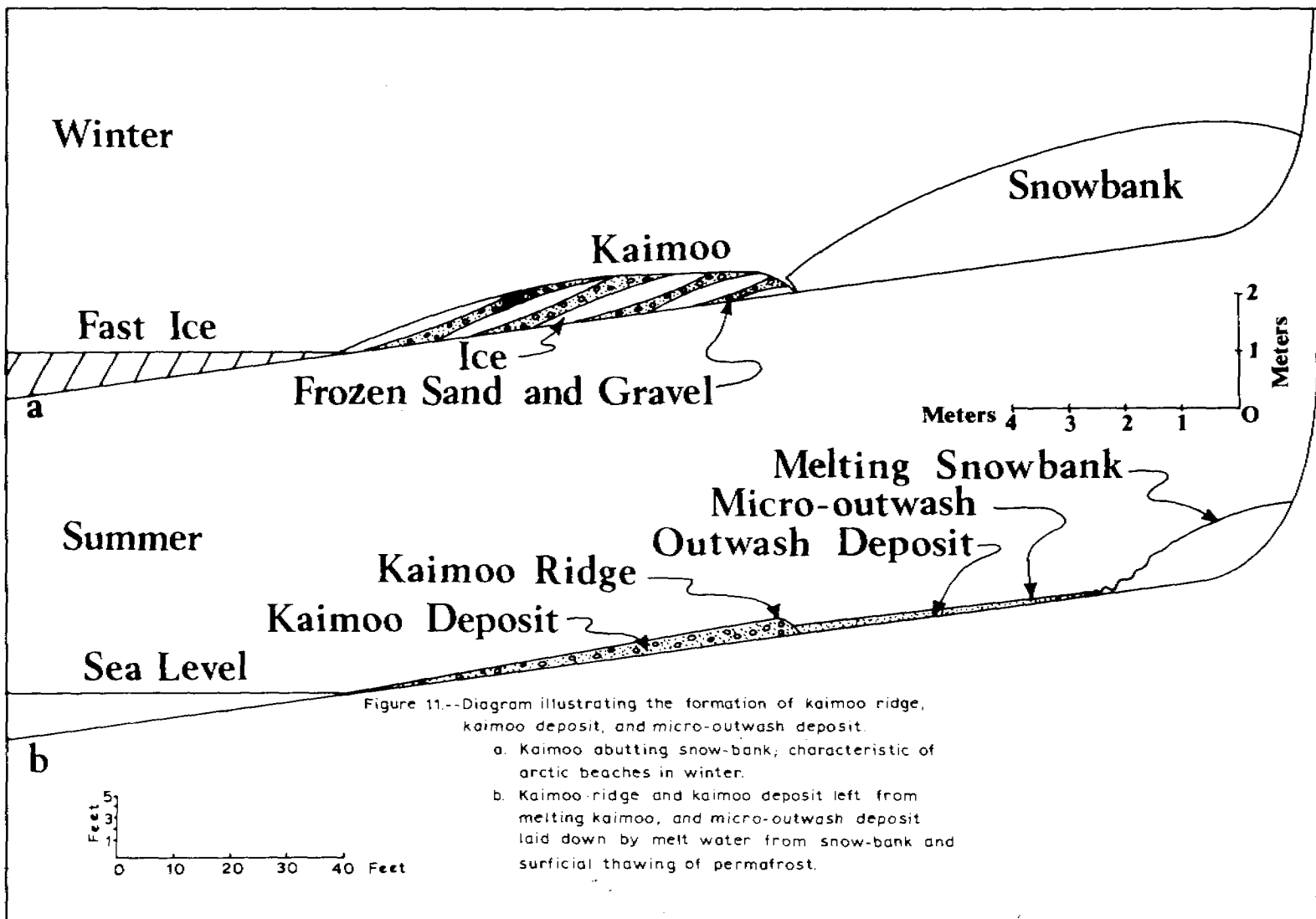
mechanical deformation by ice shove, etc." The kaimoo should not be confused with the storm-ice foot described by Rex (1964, p. 392). In this paper the kaimoo is defined as a bed of ice and frozen sand and gravels extending from the water line shoreward toward the backshore. Ice-foot is here defined as a fringe of ice bordering the land and extending seaward from the waterline.

Upon melting of interstitial ice, sand and gravel that make up the frozen kaimoo collapses upon the beach to form a kaimoo ridge and deposit. At Nome a distinctly corrugated, fairly continuous ridge on the beach, resembling an ice-pushed ridge that was reshaped by wind and surf action, represented a typical kaimoo ridge and deposit (Fig. 10). Although the ridge appeared as an ice-pushed ridge, it exhibited depositional structures and did not contain the disturbed stratification that is often characteristic of ice-pushed ridges. A kaimoo ridge has a gentle but corrugated slope toward the strand and a convex, steep scarp toward the backshore that contain numerous horizontal furrows. The landward scarp of the ridge represents the landward edge of the former kaimoo, where it most likely abutted against a snowbank (Fig. 11A); in other words, this scarp represents the boundary between the gravel-rich kaimoo and the sediment-free snow-drift on the beach. Probably the snow bank had a wave-cut scarp eroded into it that later became occupied by the kaimoo. This landward scarp of the kaimoo ridge is analogous with ice-contact scarps in glacial deposits.



Figure 10.--Scarp of kaimoo ridge, about 2 feet high, consisting of residual coarse-grained sand and gravel. Kaimoo deposit extends to swash zone in right background. Snowbank can be seen in left background with adjacent micro-outwash deposit. Collapse sea-ice sand cone superimposed on the kaimoo scarp, July, 1967.

Kaimoo deposits have an overall shingled profile with a thick landward edge forming the kaimoo ridge (Fig. 11A). Material that make up these deposits are loosely compacted and consist of sediment contained in the former kaimoo that has been let down by the melting of the ice. Each individual clast within the kaimoo deposit remain precariously balanced against other grains until disturbed, thus the loose packing.





### Sea-ice Kettles

Small holes or pits, here called sea-ice kettles, were observed in and above the swash zones of the Nome beaches (Fig. 12). These pits appear as collapse structures and are commonly as much as 1 to 3 feet in diameter and 0.5 to 1 foot deep. Many of the pits observed contained chunks of melting ice (Fig. 13).



Figure 12.--Sea-ice kettles in swash zone. Largest sea-ice kettle in foreground is about 1 foot in diameter. Fairy-castle ridges surround a small kettle in right foreground formed by melting ice block that was covered, but not buried, by sand, July, 1967.



Figure 13.--Sea-ice kettle with chunk of melting ice, June, 1967.  
Diameter of kettle is about 2 feet.

Chunks and blocks of sea-ice along with isolated fragments of the kaimoo are left stranded on the beach to melt during spring breakup (Fig. 14A). Surf action deposits sand and gravel around and on the melting chunks of ice in the swash zone and occasionally large waves or storms will cover blocks of ice on the forebeach with sediment well above the normal swash zone (Fig. 14B, C). As the ice melts the sediment collapses to form a pit or sea-ice kettle (Figs. 12, 13, and 14D, E, F). Sea-ice kettles are analogous to ice-block holes commonly associated with active glaciers.

Sea-ice kettles are prone to subsequent destruction by wave action as they occur mostly in the swash zone. However, several sea-ice kettles were still present in the upper forebeach at Nome late in the summer of 1967 and could possibly be preserved in the stratigraphic cross-section of the beach.

A similar feature was described by Nichols (1961, p. 697) as pitted beaches. Pits described by Nichols are much larger than sea-ice kettles, about 15 feet in diameter and 1 to 2 feet deep, and represent collapse features closely associated with active glaciers. Pitted beaches are commonly built against terminal ice cliffs where blocks of ice can fall from the glacier and be buried by beach gravels; later melting of these blocks of ice form pits.

#### Sea-ice Sand Cones and Sea-ice Gravel Cones

Small, conical mounds, consisting of fairly well sorted sand and gravel, 0.5 to 1 foot high, were common on the Nome Beach in 1967 (Figs. 15 and 16). Some contained a core of ice. The mounds, here called sea-ice gravel or sea-ice sand cones, occupy shallow depressions on the back beach. Constituent grains commonly contrast in size to those in the surrounding beach (Fig. 16). Many are surrounded by a precariously piled, unstable ridge of sand (a few inches high) and some of the sand ridges exhibit fairy-castle structures. (Fairy-castle structure is a complex gravel-pile form of packing where grains are frequently supported by only one or two adjacent grains).

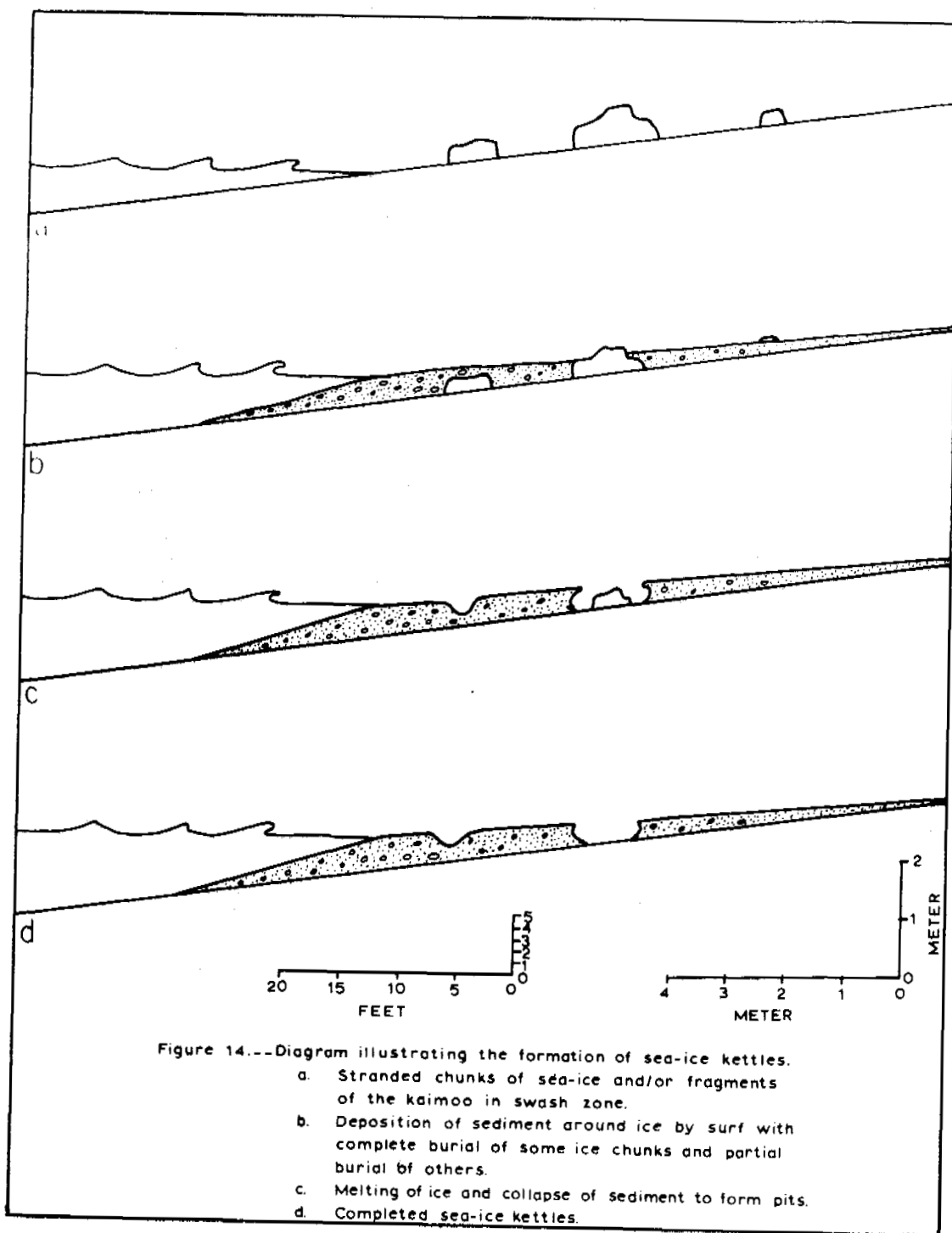




Figure 15.--Sea-ice sand cone in a small depression on a gravel beach. Note pen near base of cone for scale, August, 1967.

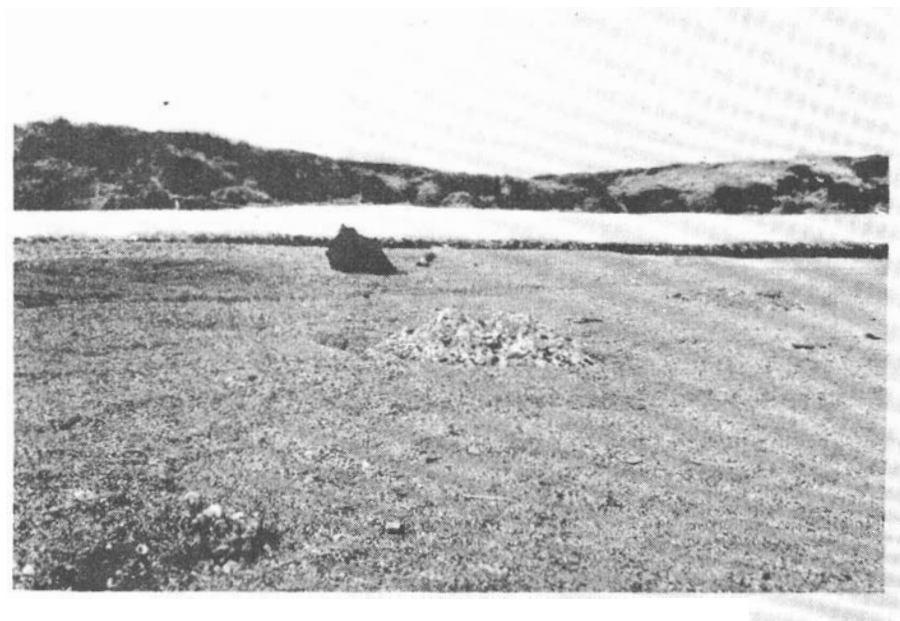


Figure 16.--Sea-ice gravel cone 1 foot high, located in a small depression on sandy kaimoo deposit, August, 1967.

Sea-ice sand or gravel cones presumably mark sites of stranded fragments of the storm ice-foot or stranded blocks of sea-ice that contained considerable sand or gravel picked-up in previous groundings (Fig. 17A). Rex (1964, p. 392) points out that wave distributed sand and gravel is commonly incorporated in the storm-ice foot which often become stranded on the beach during the fall thaw. Rex (1964, p. 391) also states that sea-ice accumulated layers of sediment by freezing to the bottom, breaking free with a load of sand or gravel and then freezing again in another place, thus, one or more sand or gravel layers may be added to ice cakes. Once

stranded on the beach, the ice begins to melt and the sediment released from the melting ice blocks flows down to form drapes of debris against the ice (Figs. 17B and 18). The decreasing size of the ice chunks is chronicled by deposition of concentric, recessional fairy-castle ridges on the beach surrounding the base of the ice blocks (Figs. 18 and 19). Eventually the ice completely melts, leaving in its place a cone of sand or gravel (Figs. 15, 16, and 17D). Sea-ice sand cones that lack marginal ridges probably are produced by fragments of the kaimoo containing abundant amounts of sand. Material forming these sea-ice sand cones are probably sorted by wave action and accumulate in shallow wells or cisterns in the kaimoo during the spring thaw. These are analogous to kames formed in moulins on glaciers. Other sea-ice gravel cones may form in the following way: after the sea-ice moves away from the shore, and during the melting of the kaimoo, sediment trapped in the kaimoo is reworked by wave action resulting in winnowing of sand and concentration of gravel in melt holes. This ultimately forms a small cone of gravel as the ice melts (Fig. 15).

Sea-ice sand and sea-ice gravel cones are analogous to debris covered ice cones described by Sharp (1949, p. 296). Debris-covered ice cones are usually much larger (40 to 50 feet high) than sea-ice sand and sea-ice gravel cones found on the beach of Nome in 1967 and are formed by ablation rather than by melting of stranded sediment laden brash ice.

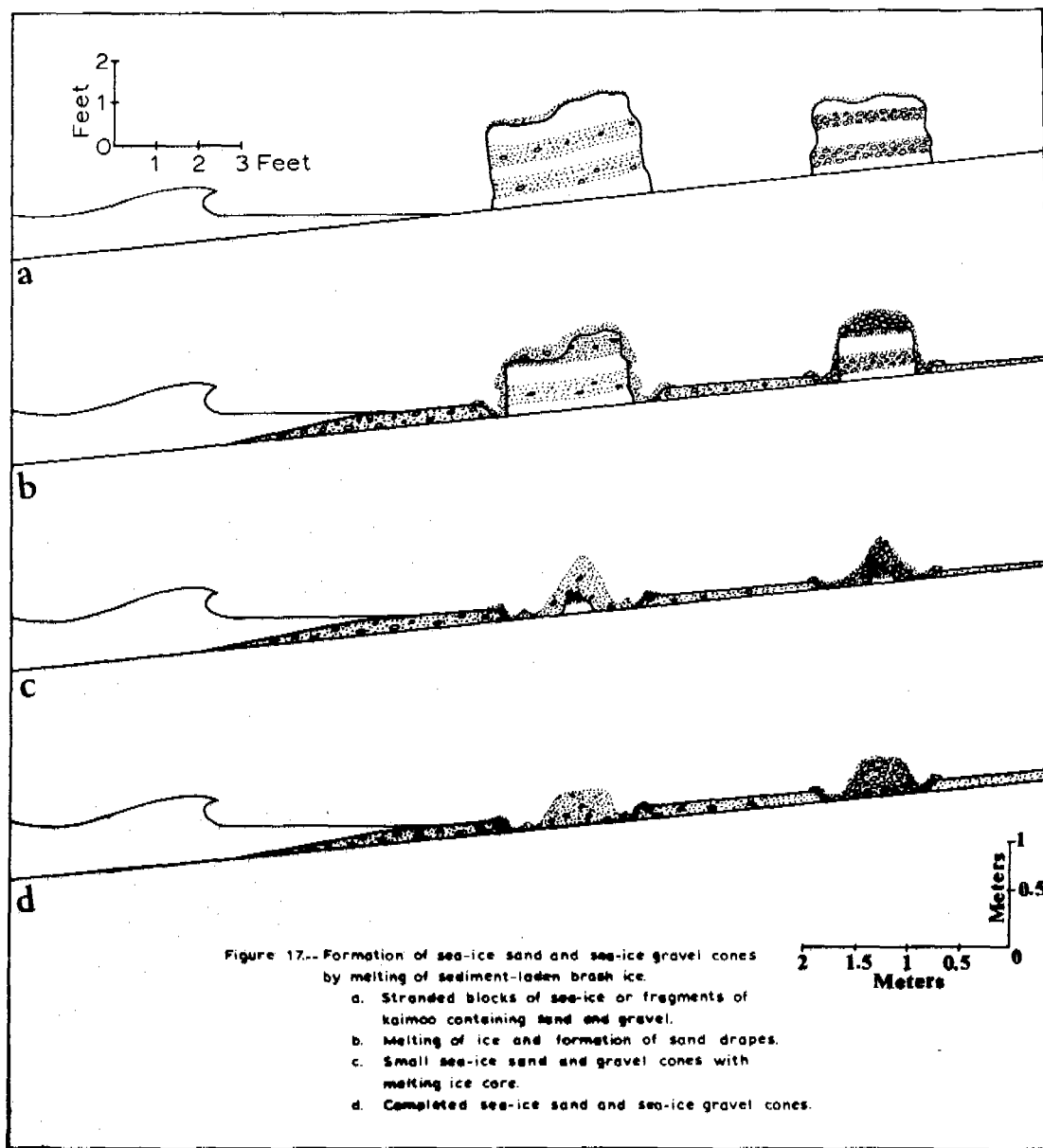






Figure 18.--Melting block of sea-ice showing sand flowing down sides to form a sand ridge. Ice is about 1 foot long, July, 1967.



Figure 19.--Fairy-castle structured ridges of sand showing former locations of stranded blocks of sea-ice. Boulder in right foreground is about 10 inches across, July, 1967.

### Microrelief Features of the Upper Beach

Microfluvial features of the upper beach are found between the landward limit of the swash zone or upper foreshore and the base of the wave cut cliffs and are mostly formed by fluvial processes. These structures are commonly preserved for more than 1 year as they form well above normal surf activity. Polymict masses of mud, sand, gravel, and driftwood that probably represent microfluvial deposits are exposed in cross-section near the rear of Sangamon beaches on the east and south shores of Kotzebue Sound (D. M. Hopkins, written communication, 1968).

### Microfluvial Deposits

Features that are constructed by fluvial processes on the Nome beaches can be divided into two types: (1) micro-outwash deposits, and (2) micro-deltaic deposits. Micro-deltaic deposits are commonly superimposed on micro-outwash deposits.

The coast of Nome is adjoined in many places by bluffs consisting of glacial drift or silt and fine sand. Both types of deposits are capped by a foot or two of loess, and the unconsolidated deposits commonly are perennially frozen. Collapse structures related to permafrost thawing are not seen on the beaches, indicating that permafrost does not extend out under the Nome beaches. Surficial thawing during warm summers result in mass-wasting or flowage of the drift, loess, and associated marine silt and sand onto the beach. In addition, melt water from snow drifts transport sand and silt onto the beach and small scale fluvial deposits are formed.

### 1. Micro-outwash Deposits

Micro-outwash deposits consist of mud, fine- to medium-grained sand and gravel deposited on the upper foreshore or backshore area (Fig. 10). In 1967 micro-outwash covered the beach between the seaward edge of the melting snowbanks and the midbeach line that is commonly marked by the kaimoo ridge (Figs. 11A and 11B). The thickness of these deposits ranged from about 3 inches on the backshore to about 2 feet near the kaimoo ridge.

### 2. Micro-deltaic Deposits

Micro-deltaic deposits form on the micro-outwash where major drainage lines within the snowbanks coalesce to form sluiceways to the sea. These micro-deltaic deposits consist of sheets of mud and medium-grained sand (Fig. 20). The deltaic sheets range from 3 to 15 feet across its seaward foot and 1 to 3 feet thick. Most of the micro-deltaic deposits were restricted to the backshore, but some spread into the foreshore area where they abut either a storm beach ridge or the kaimoo ridge.

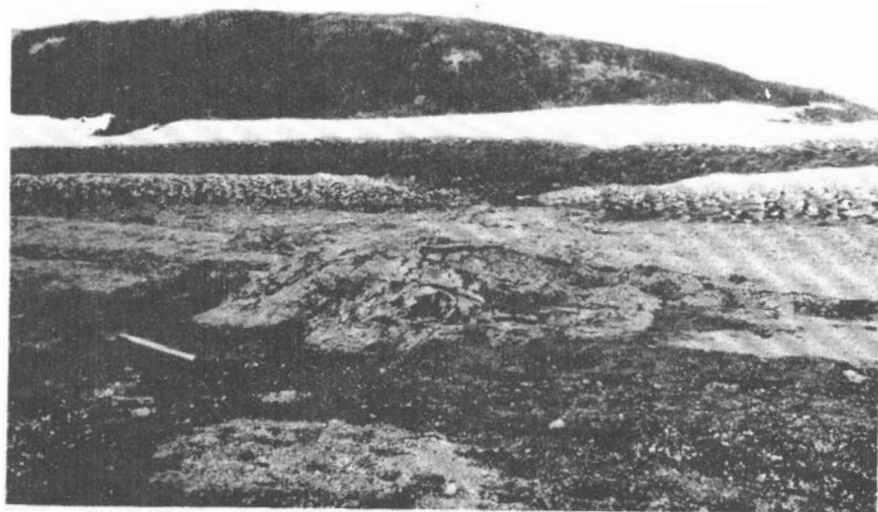


Figure 20.--Micro-deltaic deposit formed where drainage from snowbank coalesce to form a sluiceway to the sea, August, 1967. Ice-tunnel at apex of delta. Note shovel for scale.

PART II  
ASPECTS OF BEACH SEDIMENTATION AND TRANSPORT

I. INTRODUCTION

Sediment on the beaches of the Nome coastal plain varies from coarse gravel to fine- to medium-grained sand. Detailed sampling has never been done along the Nome beaches, even though the area has been a large producer of placer gold.

II. PROCEDURES AND SAMPLING METHODS

Procedures

Surface samples were collected from 22 stations located between Penny and Snake Rivers, most of which were associated with the seismic stations, and spaced approximately 1/2 mile apart (Fig. 21). At each beach station, about 5 pounds of sediment was hand scraped from the beach surface at points located at the swash zone, at the foreshore or lower foreshore, and at the backshore or upper foreshore. Additional sediment samples were collected at some of the stations from the kaimoo ridge deposits, kaimoo deposits, micro-outwash deposits, and stream deposits.

An underwater sampling grid was laid out on the sea bottom offshore of Station 35 (Fig. 21). A yellow nylon rope was extended perpendicular to the coastline from fixed points onshore to points 600 feet offshore and held in position by anchors located at each end. Every 100 feet on the rope was marked by a red fluorescent rag. Using SCUBA, divers collected about 5 pounds of sample in buckets from the sea bottom at the points marked by the pieces of rags on the rope. Upon obtaining a sample the diver would surface



directly above the mark and a man on shore established the diver's position with a transit. After completing one line the rope was moved 100 feet east and sampling continued. The first station on each line was located 50 feet offshore in the longshore trough. Due to deterioration of good weather only 13 points could be sampled.

#### Methods

Two methods were used in the mechanical analysis of the beach sands and gravels. First, all samples were sieved down to 2 mm and the gravel separated into 64, 32, 16, 8, 4, and 2 mm fractions. The fractions smaller than 2 mm was run through an Emery Settling Tube (Emery, 1938; Poole and others, 1951; Poole, 1957) for rapid analysis of sizes in the sand and coarse silt range. Several samples were run through the Emery Settling Tube twice; the results showed a reproducibility error of 1 to 2%.

Histograms and cumulative frequency curves were constructed from the grain size analysis data (see Table I in Appendix). From the graphed cumulative curves, median diameters, coefficients of sorting and skewness (Trask, 1932), and percentage of sand and gravel were calculated. A grain size distribution map, including sorting coefficient and sand and gravel percentages was compiled from these data (Fig. 21). Mean size, standard deviation, and skewness were calculated by the Folk and Ward method (1957, p. 12-15) for sediment samples collected in the swash zone, the longshore trough, and on the longshore bar (see Table II in Appendix). These data were compared with mean size, sorting coefficient, and skewness

data calculated by the Trask method for the same samples and it was found that little discrepancy, if any, existed between the two methods (Figs. 22 and 23). In comparing the Mean Size vs. Standard Deviation plot (Fig. 22) constructed from Folk and Ward data with the Mean Size vs. Sorting plot (Fig. 23) constructed from Trask data, it can be seen that an equal amount of separation exist on both plots between the concentration of points representing swash zone, longshore trough and longshore bar. As the sediment data is not refined with the Folk and Ward method, the Trask method was used throughout this investigation.

### III. GRAIN SIZE DISTRIBUTION

Considering all samples collected, there is a random distribution of grain sizes along the overall beach with no set direction of increasing or decreasing median diameters, sand-gravel percentages, or sorting coefficients. Starting at Penny River, where the average median diameter is 2.33 mm and the average sorting coefficient is 3.13 there is generally a decrease in grain sizes and an improvement in sorting eastward to Station 20. Between Stations 41 and 20 the average median diameter is 0.68 mm and the average sorting coefficient is 2.34. From Station 20 through Station 29 grain sizes and median diameters are higher and sorting is poor. Between Stations 20 and 29 the average median diameter is 2.87 mm and the average sorting coefficient is 1.99. Continuing eastward from Station 29 grain sizes and median diameters decrease and sorting improves. Average median diameter between Stations 29 and 34 is



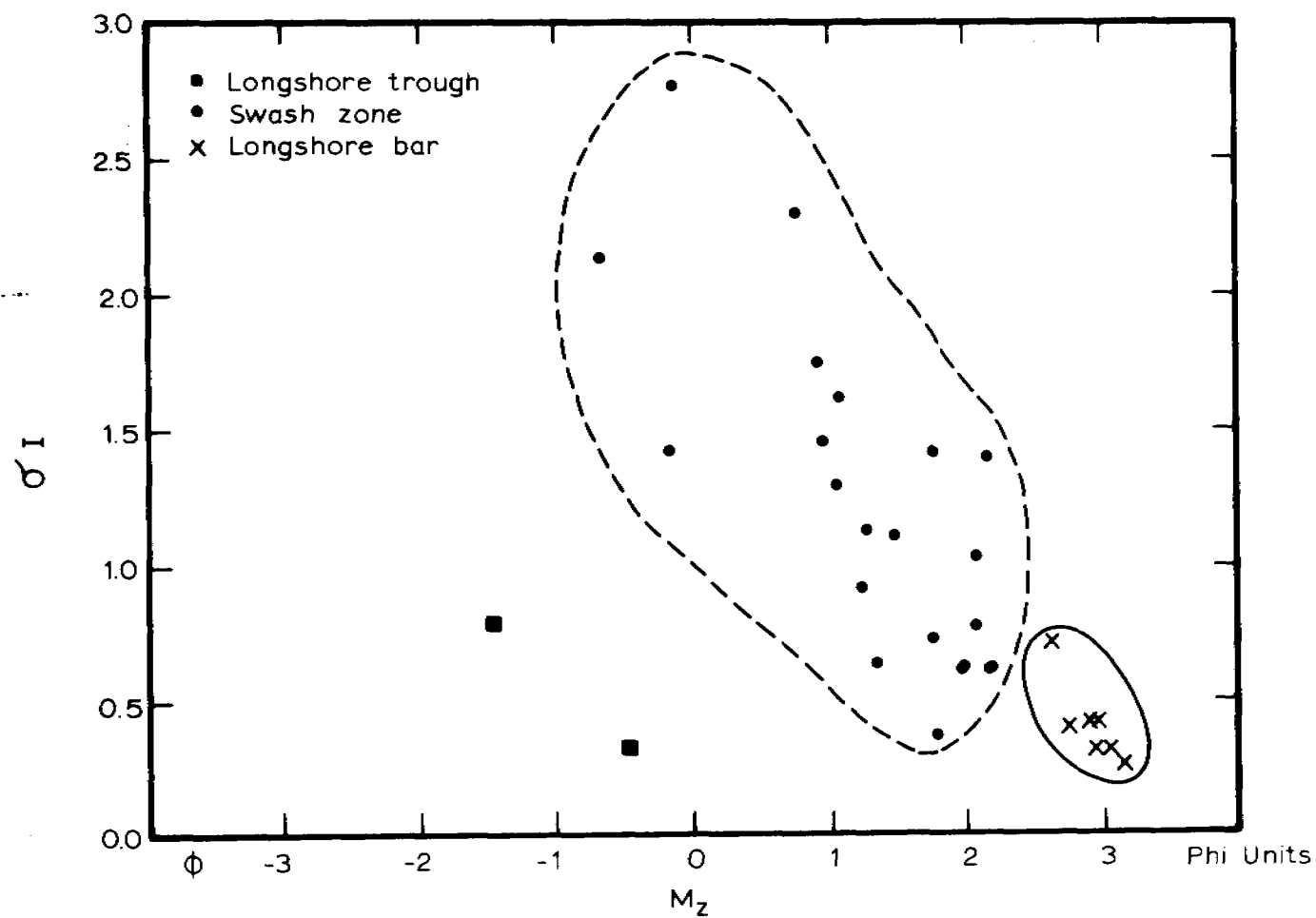


Figure 22.--Mean Size vs. Standard Deviation plot for samples collected in the swash zone, the longshore trough, and the longshore bar on the Nome Beach. Graph constructed by Folk and Ward method.



2.04 mm and the sorting coefficient is 1.78. Grain size and median diameters again increase and sorting becomes poorer between Stations 34 and 47 where the average median diameter is 3.14 mm and the average sorting coefficient is 2.26. Stations 48 and 49, on the Snake River spit, exhibit medium grain sizes with fair sorting. Average median diameter here is 1.10 and average sorting coefficient is 2.20.

#### Swash Zone

Sediment samples were collected from the swash zone at most of the stations. The swash zone at Nome in June and July, 1967 was 4 to 8 feet wide.

Except for 2 stations near the eastern end of the investigation area (Stations 39 and 45) grain size, sand-gravel percentages, and sorting coefficients remained fairly constant in the swash zone throughout the entire length of the beach. Median diameters range from a low of 0.20 mm to a high of 1.50 mm and variation in sorting coefficients range from 1.20 to 8.40. Average median diameter for the swash zone along the entire beach is 0.39 mm and the average sorting coefficient is 2.17.

#### Foreshore (or Lower Foreshore)

Sediment samples were collected from the foreshore or lower foreshore at all stations. Shepard (1963, p. 169) defines the foreshore as "the sloping part of the beach lying between the berm and the lower water mark." On the Nome beach, however, only a fore-

berm and backshore were poorly developed. Where there was no berm and backshore, samples were taken from the lower foreshore, in the position that the foreshore would be if a berm and backshore existed.

Grain sizes distribution along the lower foreshore of the beach was entirely random and varied from a median diameter of 0.34 mm to 17.00 mm with an average median diameter of 3.15 mm. Sorting varied from 1.20 to 6.60 with an average of 2.27. There were no patterns or direction of increasing or decreasing grain sizes or sand-gravel percentages, and no direction for changes in sorting.

#### Kaimoo ridge deposits and kaimoo deposits

Kaimoo ridge deposits and kaimoo deposits were commonly located on the lower foreshore and at several stations where they were conspicuous and well developed they were sampled separately. The eight different kaimoo ridge deposits that were sampled had median diameters ranging from 0.40 mm to 40.00 mm with an average of 8.16 mm. Sorting coefficient ranged from 1.40 to 2.30 with an average of 1.65. Five different kaimoo deposits were also sampled and exhibit median diameters ranging from 0.30 mm to 0.90 mm with an average of 0.58 mm. Sorting coefficients ranged from 1.30 to 4.70 with an average of 2.28.

#### Backshore (or Upper Foreshore)

The backshore or upper foreshore was sampled at all stations. Shepard (1963, p. 168) defines the backshore as "the zone of the beach lying between the foreshore and the coastline." As the Nome beach has only a foreshore in most places, most samples were

collected on the upper foreshore where the position of the backshore would be if a berm existed. At many stations the upper foreshore was masked by microfluvial deposits, and these had to be scraped away in order to correctly sample the upper foreshore deposits.

Grain size distribution along the upper foreshore varied from station to station and didn't differ greatly from the lower foreshore. The median diameter ranged from 0.45 mm to 10.00 mm with an average of 2.49 mm. Sorting varied from 1.20 to 4.20 with an average of 2.13. As on the lower foreshore, the upper foreshore showed no patterns or direction of increasing or decreasing grain sizes or sand-gravel percentages, and no distinct changes in sorting.

#### Micro-outwash deposits

Micro-outwash deposits were commonly located on the upper foreshore and were sampled separately at eight different stations. The median diameter ranged from 0.43 mm to 4.50 mm with an average of 1.61 mm; sorting varied from 1.40 to 4.00 with an average of 1.97.

#### Stream Deposits

Three different streams were sampled in order to determine the size of terrestrial sediments being added to the beach. Grain size was quite variable with median diameters ranging from 2.00 to 16.00 mm and an average of 6.13 mm. Sorting ranged from 1.20 to 2.80 with an average of 1.83. If the sediments brought down to the beach by Penny River were considered along with the streams the average median diameter would be reduced to 4.23 mm and the sorting coefficient would rise to 2.48. Penny River is one of the major

mediums for transporting terrestrial sediments to that portion of Nome beach sampled especially between stations 14 and 20, and material collected at the mouth of Penny River has an average median diameter of 2.33 mm with an average sorting coefficient of 3.13. However, cliff erosion is probably equally important in supplying new material all along the beach.

#### Offshore

Offshore of Station 35, thirteen samples were collected by using SCUBA. Shepard (1963, p. 169) defines offshore as "The breaker zone directly seaward of the low tide line." The offshore area sampled included the longshore trough and longshore bar but never extended beyond the longshore bar.

Grain size distribution in the offshore was very uniform and well sorted. For the overall offshore area median diameter varied from 0.12 mm to 2.80 mm with an average of 0.66 mm and the coefficient of sorting ranged from 1.02 to 2.80 with an average of 1.19. In the longshore trough median diameter ranged from 1.40 mm to 2.80 mm with an average of 2.06 and the sorting coefficient varied from 1.00 to 1.20 with an average of 1.13. The longshore bar had a median diameter range of 0.12 mm to 0.16 mm with an average of 0.13 mm and a sorting coefficient range of 1.10 to 1.30 with an average of 1.20.

#### IV. PROCESSES AFFECTING COASTAL FEATURES

The principal processes which control the formation of the coastal features in the Nome area are wind, waves, littoral currents, and ice. Salient characteristics of each of these features is described below.

##### Wind

Prevailing winds affecting the beaches of Nome during the summer of 1967 were from the north and northeast (determined from unofficial records of the U.S. Weather Bureau at Nome, Alaska, and from the logs of the U.S. Bureau of Mines Research Vessel Virginia City). These prevailing winds transported dry beach sands eastward along the beach and formed microdunes within the driftwood at the base of the wave cut cliffs. During storms, the wind blew from the south or southwest.

##### Waves

Energy that is produced by wind generated waves --

"Wind waves are classified by whether or not active wave generation includes the point where observations are being made. If a wind is generating waves locally, waves constitute a "sea". Waves which have propagated longer distances beyond the region of their active generation are manifest as ocean "swell". In contrast to sea, swell can be present at a location where there is no local wind."  
(Roberts and others, 1967, p. 14) --

is often the most important factor in shaping beaches (Roberts and others, 1967, p. 14). Roberts and others (1967, p. 14) state that

"The amount of wave energy that actually contributes to the dynamics

of a beach is a function of how much wave energy is available in deep water, less that amount dissipated, principally through refractions, bottom friction, breaking, and internal friction." However, at Nome wind generated waves are not the only major factor in shaping the beaches, sea-ice also plays an important role.

The waves affecting the Nome beaches during the period of this investigation were low energy, small rolling types with small crashing breakers no more than 1 or 2 feet high (Fig. 24). Waves of this type prevail during early summer (June and July), but heavier surf is common during August and September. Fetch is limited in the Bering Sea and Norton Sound and only wind blowing from the south has a fetch long enough to produce heavy surf on the beaches of the Seward Peninsula near Nome. The average angle of wave attack is about  $27^{\circ}$  to the coastline when wave direction is southeast. There generally is a small amount of wave refraction around Cape Rodney and interference patterns develop around Sledge Island (Fig. 25), but these appear to have no affect upon the beaches.

The wave direction is commonly north or northwest during storms with the angle of wave attack perpendicular to the coastline. At times of storms, erosion takes place on the beaches; at one point during a storm a 2 foot escarpment was cut locally into the beach (Fig. 26).



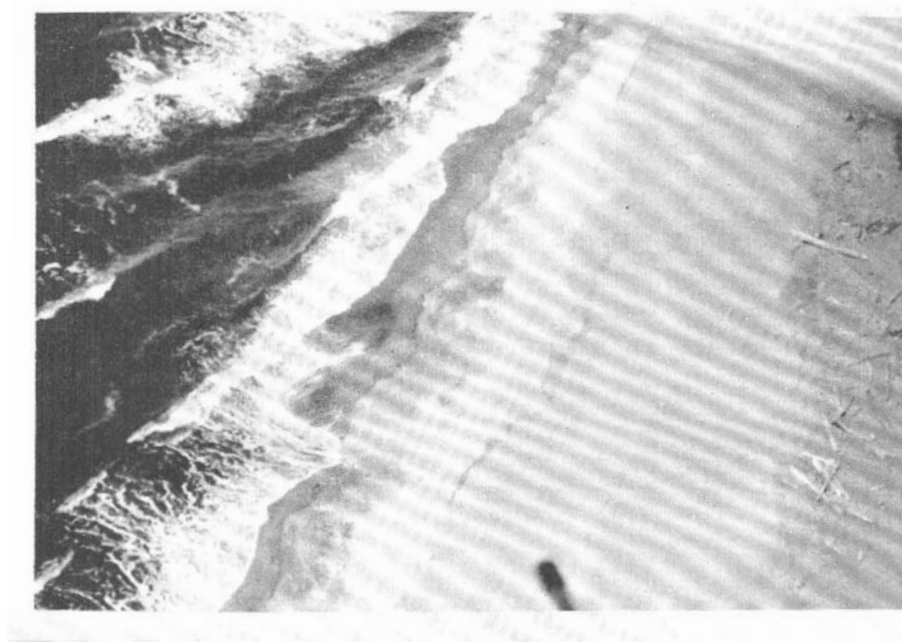


Figure 24.--A. Small crashing breakers on the Nome beach showing prevailing wave attack angle and refraction. Height of breakers is approximately 1 foot. Top of photo is west.

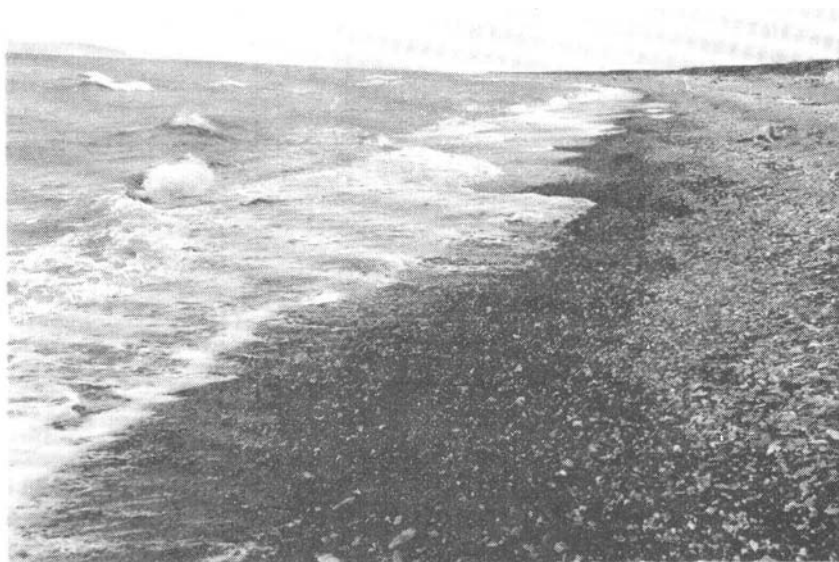


Figure 24.--B. Small crashing breakers on a coarse gravel beach near Nome. Height of breakers is about 1 foot. Top of photo is west, Sledge Island in upper left hand corner.

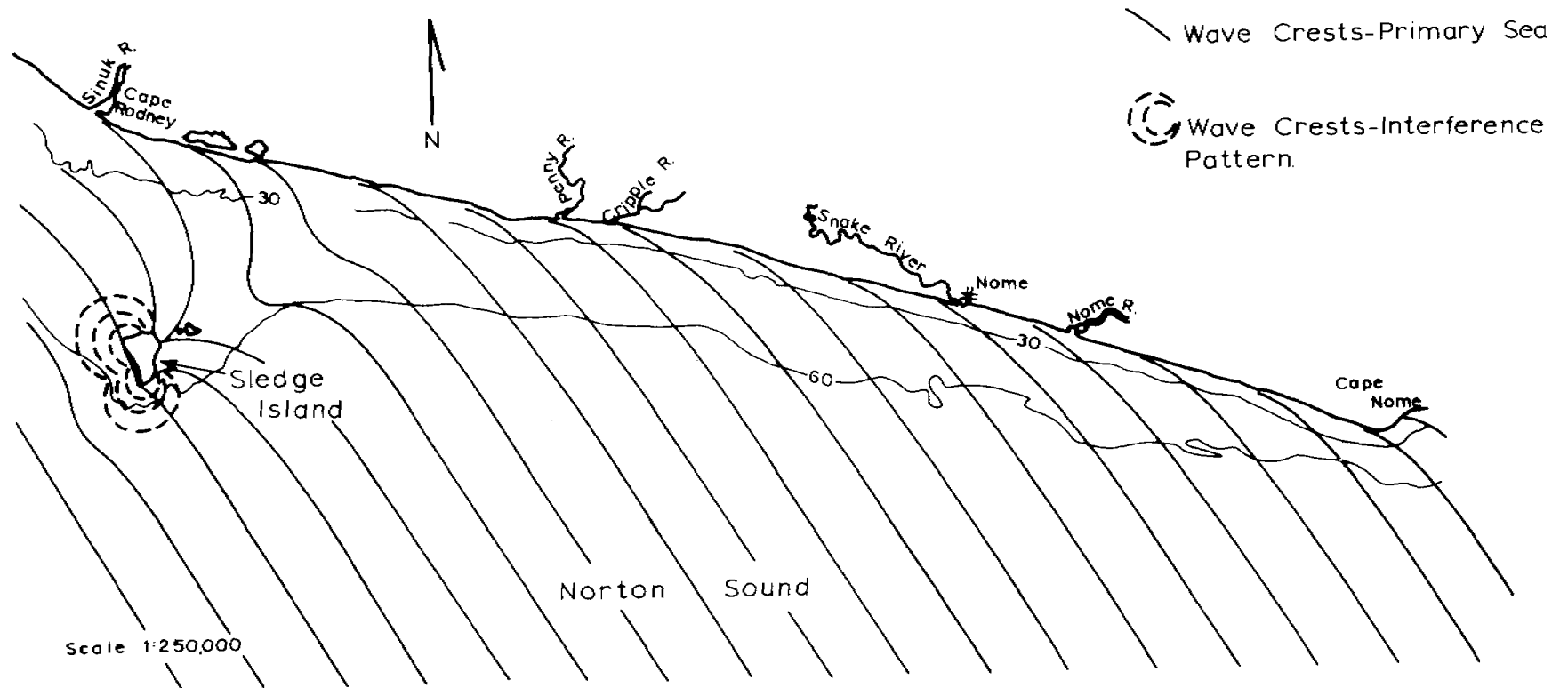


Figure 25. Generalized wave refraction diagram of the northwestern Norton Sound area.



Figure 26.--Storm wave-cut escarpment about 2 feet high, near Station 35 on the Nome beach. Looking north.

### Littoral Currents

Regional effects of the littoral current are shown in the net transport of sediments. During the summer of 1967 longshore drift varied from east to west with a mostly prevailing eastward direction. As longshore drift at Nome is dependent on the angle of wave incidence to the beach, and the waves are mostly from the northwest, the prevailing coastal current has an easterly set. Refraction of sea and swell appear to have little influence on littoral currents which seem to be more closely related to local winds.

A good aid in studying the effects and direction of longshore drift was given by the Nome dumps. One of Nome's dumps is located on the beach about 1/2 mile east of Snake River where trash, garbage and tin cans, are actively worked by waves (Fig. 27). The other dump is located about 1 mile west of Snake River. The tin cans proved to be the best item for studying transportation of material along the beach, as they are fairly uniform in size and quite plentiful. Cans were noticeable for some distance on both sides of the dumps, thus the evidence for a variable longshore drift. However, tin cans from the west dump could be seen as far east as the Snake River jetties where they have accumulated in fairly large concentrations. How much further eastward they would have gone if the jetties were not there is unknown. To the west, numerous tin cans could be seen for approximately 1/2 mile, but a few cans apparently had been carried as far as 3/4 of a mile. As ice considerably disturbs the beach surface when it comes in during

the winter and when it breaks up in the spring, the beach surface is a "clean slate" upon which the processes affecting the beach can be "written" each summer. Thus, the concentrations of tin cans observed along the beach during the summer of 1967 were distributed that same year. This led to the obvious conclusion that a net transport along the beach for the summer of 1967 was eastward.



Figure 27.--East Nome dump showing large amounts of debris trailing off toward the east with little or no debris trailing off toward the west indicating an eastward net longshore drift. **The town of Nome and Cape Rodney in the background.**

Accumulation of sand against the west jetty of the Snake River and erosion of material on the east side of the east jetty of the Snake River, where a seawall has been constructed to prevent the waterfront buildings of Nome from being undermined, also indicates a yearly transport of sediments eastward (Fig. 28). As the beaches are protected from waves and wind during the winter by a thick ice cover, the net transport along the beaches during the summer months represents total transport.



Figure 28.--The Snake River jetties showing accumulation of sediment on the west side and erosion on the east. Looking west with the town of Nome in the foreground.

## Ice

Ice has a major influence upon the beaches of Nome. In the fall, after the kaimoo develops, the beach becomes insulated from waves and wind and remains stable until spring. Sea-ice forms on the Bering Sea, in Norton Sound during the winter and curtails wave action until the spring. In the spring the sea-ice breaks up and is pushed ashore by wind pressure transporting with it sediments that are eventually left on the beach from the stranded, melting sea-ice. Sea-ice may on occasions remove sediment from the beach. When the kaimoo melts, microrelief develops and new sediment is added to the beach.

## V. OFFSHORE FEATURES

Two major features were observed during the summer of 1967 offshore of Nome. One was the formation and shifting of river mouth bars and spits. The other was the presence of a longshore bar with unusual relief.

### River Mouth Bars and Spits

Bars and spits formed at the mouths of Penny, Snake, and Nome Rivers and spits developed at the mouths of smaller streams late in the summer of 1967, when river and stream flow was reduced (Fig. 29). Very late in the summer, when the stream flow across the beach was low, the spits at the stream mouths developed into barrier spits and bars enclosing small lagoons (Fig. 30). At times during southerly storms the river mouth bars of Penny and Nome Rivers disappeared, only to reappear after the storm subsided. The



bar at Snake River was dredged regularly during the summer of 1967 and was never seen above sea level.



Figure 29.--A. River mouth bar off the Nome River in late July, 1967. Top of photo is north.



Figure 29.--B. A spit at the mouth of Cripple Creek in late July, 1967. The spit is developing into a barrier spit. Top of photo is west.

#### Longshore

A longshore bar was everywhere present along the Nome beaches. On several occasions, especially after southerly storms, slightly crescentic submarine bars developed on the longshore bar. These crescentic bars had a relief of about 1 to 2 feet; they were oriented with their long axes roughly perpendicular to the coastline. The bars usually occurred in groups of 2 or 3 and contained coarse gravel on their crests, resembling some type of lag deposit. The origin of these crescentic type bars is unknown.



Figure 30.--Barrier spit with small lagoon built at the mouth of a stream east of Nome in late July, 1967. Top of photo is east.

An ancestral barrier spit could still be seen at Penny River and the old river channel formed a small arm of the present day estuary (Fig. 31). The eskimos claim that several years ago a large storm from the north formed the barrier spit and the outlet of Penny River was shifted eastward to its present position.



Figure 31---Old barrier spit and previous outlet of Penny River can be seen as a small finger in the western edge of the present day estuary. Sledge Island in the background.

## VI. CONCLUSIONS

The Nome beaches are generally very coarse grained with very poor sorting and a random pattern of grain size distribution (Fig. 21). This is quite unusual for beaches at lower latitudes, but for an arctic beach, such as at Nome, these characteristics are to be expected. Beach dynamics of arctic beaches are influenced by ice, more than any one single factor. The pushing and grinding ashore of blocks of sea-ice that have gravel and sand frozen into them add some new sediment to the beach. Sea-ice obtains its sand and gravel from the ocean bottom by grounding and picking-up, through freezing, bottom sediment. After grounding several times there will be as many layers of sediment producing sizeable concentrations of material which eventually may be added to the beaches. Sediment is sometimes transported great distances before they may be dropped onto a beach. Transportation by sea-ice is one means of adding new material to arctic beaches and this process probably influenced the distribution of beach sediments at Nome; the quantitative importance of this, however, is unknown.

Melting of the kaimoo and snowbanks and drainage of the tundra onto the beaches also affect distribution of sediments on the Nome beaches and aid in producing a random pattern of grain sizes and sorting. Occasional "great storms" erode the shore-cliffs at the backshore and considerable amount of material is added to the beach at this time. Hopkins (written communication, 1968) reports that at Nome driftwood appears as though it has not been disturbed

for years on end, but believes that when it is disturbed, such as during a "great storm", cliffs are eroded and new material is added to the beach; this could be a major factor in nourishment of the beaches -- especially when the backshore is more disturbed than the lower foreshore. Insulation from the elements by ice during winter give little chance for wind and waves to act upon the beach material. Since the Seward Peninsula near Nome is a low energy coast, what waves and littoral currents affect the beach make little headway against the disturbances caused by ice. However, the period of observation did not include the most stormy periods. A coarse cobble and pebble, basal shingled layer found under most of the beach indicate that occasional storms deeply erode the beach. Also, during these occasional storms unconsolidated deposits and tills that makeup the bluffs at the backshore and underlie the foreshore contribute considerable coarse material to the beach. The boulders found along the beach indicate local areas where till is most likely close to the beach surface or makeup the bluffs at the backshore and may supply the beach with coarse material.

In the swash zone the sediments are fine grained and are generally well sorted because waves and littoral currents work on that part of the beach throughout the entire 6 months or so that the beach is not protected by ice. In fact, the best sorting and lowest median diameters on the beach were exhibited in samples taken from the swash zone. However, no grain size distribution pattern except for uniformity of the swash zone, evolved from this

study. Bimodal distributions are present in zone areas and indicate the effects of both ice and waves. Most histograms show a unimodal distribution skewed toward the fines indicating the effects of wave action.

The foreshore (or lower foreshore), backshore (or upper foreshore), and the kaimoo deposit overlying the foreshore are generally coarse grained, poorly sorted sand and gravel with a random grain size distribution. Most of these areas show a polymodal and bimodal distribution possibly indicating that two separate agents are equally at work on the beach. The two agents that affect the beach in these areas are ice and waves. Bimodal characteristics may also indicate inclusion of two strata in sample, the presence of wind blown sand filtered into clean gravel, and the filtering in of sand as wave energy is reduced. Ice transports and deposits a random agglomeration of sediments, some well sorted, others not so well sorted, some fine grained, others coarse grained, and the waves attempt to winnow out the fines and sort the sediments. Some samples exhibit polymodal distributions indicating that the dynamics at work on the beach in those areas are quite complex, most likely mixed by encroaching sea-ice.

The kaimoo ridge is very coarse grained, well sorted, and has a unimodal distribution skewed toward the coarse. This is to be expected as when the kaimoo forms only coarse, well sorted material is swept toward the back of the beach where the kaimoo ridge develops and normally extra large storms are required for the swash

to extend 100 feet, or so, onto the beach. Although, the kaimoo ridge is an ice deposited feature, the material that is included in the kaimoo originally was deposited by waves on the beach in the fall when the swash freezes. If the kaimoo ridge is not disturbed by ice push in the spring it will show the effects of only its depositing agent, which would be by wave action.

Micro-outwash deposits on the backshore (or upper foreshore) are fine grained, well sorted and have unimodal distributions. The one agent affecting this type of deposit is fluvial and brings fine material down onto the beach, and also acts to sort the beach material.

Offshore, on the longshore bar, sediments are fine grained, well sorted with a general unimodal distribution indicating the effects of waves and currents only. The longshore trough is coarse grained, very well sorted, and has a unimodal distribution indicating only one agent at work on it, the surf.

Terrestrial material is brought to the beaches by Penny, Snake, and Nome Rivers and by various small streams along the beach that drain the tundra area. The rivers generally add fine to coarse grained sands and the streams add very fine-grained sands and silt to the beach. However, the major source for the beach sediments is probably from the bluffs at the backshore with some material transported by sea-ice from offshore.

Longshore drift along the beaches is variable throughout the time the beaches are affected by littoral currents and waves.



However, a net transport eastward is indicated by deposition of sediments west of Nome River jetties and erosion on the east. It is not known where the sediments go from the beaches east of Nome, but it is suspected that beach material rounds Cape Nome and is deposited in and around Safty Lagoon, just east of Cape Nome.

Two Mean Size vs. Sorting plots were constructed from mean size and sorting data calculated by the Trask method (Figs. 23 and 32). These plots show, contrary to conclusions drawn by simple analysis of the cumulative curves, that the longshore bar, swash zone, and backshore portions of the beach can be easily delineated by comparing the median diameters with sorting coefficients (Fig. 23). Although ice has greatly disturbed the surface of the backshore area, the Mean Size vs. Sorting plots show that this area can be identified by grain size analysis and indicated that there was not as much ice disturbance on the backshore as was initially indicated. However, this is the only portion on the beach, with the exception of the swash zone, that can be identified in this manner. The foreshore, on the other hand, cannot be delineated and thus indicates that the effects of ice is greatest on the foreshore. There is an increase in median grain size and a decrease in good sorting from the longshore bar to the swash zone to the backshore, as illustrated in the Mean Size vs. Sorting plot (Fig. 23); this is a typical characteristic of most beaches found at lower latitudes.

A Mean Size vs. Sorting plot was also constructed from the calculated Trask data for the longshore trough, kaimoo deposit,

kaimoo ridge, and micro-outwash deposits (Fig. 32). Although most of the data points are scattered throughout the plot, the kaimoo ridge and micro-outwash deposits can be roughly outlined. One thing that is pretty well illustrated in this plot is that the micro-outwash material is generally finer grained, but not better sorted, than the kaimoo ridge deposits. This is to be expected as more energy is used in forming the kaimoo ridge deposit than is used in forming the micro-outwash deposit.

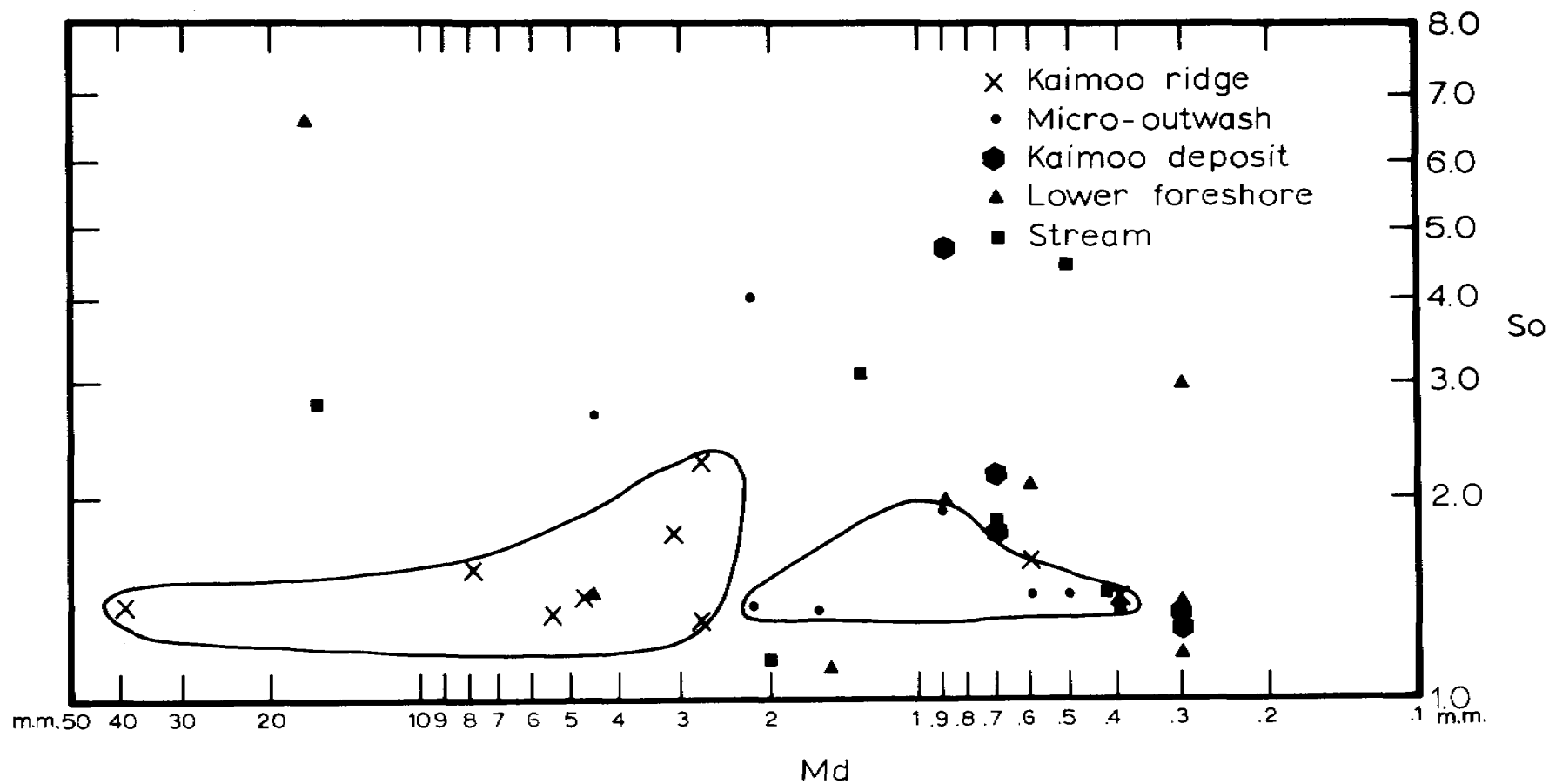


Figure 32--- Mean Size vs. Sorting plot for samples collected from the longshore trough, kaimoo deposit, kaimoo ridge, and micro-outwash deposit. Graph constructed by the Trask method.

### PART III

#### SEISMIC INVESTIGATION

##### I. INTRODUCTION

Portable refraction seismographs have been used by soil engineers and engineering geologists for many years in studying overburden thickness and physical properties at construction sites for highways, dams, buildings, and other such installations. The portable seismograph has been used in South Africa, Alaska, California and other countries in surveys of beaches and placer deposits. No seismic refraction investigation of the beaches of Nome, Alaska, however, had been attempted prior to this study.

As the seismic survey on the unfrozen beach was successful, a short experimental seismic line was completed inland to determine the usefulness of the portable refraction seismograph in areas of permafrost. The success of the Nome studies later led Tom E. Smith of the U.S. Geological Survey to investigate overburden thickness in another permafrost region using the same seismograph. He obtained interpretable seismograms in his investigation of the Kougarok gravel located in the interior of Seward Peninsula (Smith, oral communication, 1958).

##### II. EQUIPMENT AND PROCEDURES

The seismic records were obtained with an Electro-Tech Porta-Seis Refraction System (Model ER-75-12)--which is a self-contained, battery operated, portable seismic recording interval timer that

resembles several other commercially available instruments. Permanent seismic records were produced on Polaroid 4 x 5 inch film; the records contain 12 data traces, 1 shot break trace, and timing marks at 10 millisecond intervals. Accessory equipment included 6,000 feet of multiconductor geophone cable and 13 EVS-4 vertical moving coil geophones with a frequency of 7.5 cycles per second. The sound source was explosive.

#### Description of Equipment

The portable seismograph used was a light-weight system of 40 pounds, that may easily be carried by one person. At Nome, the equipment was transported by tracked vehicles and helicopter. The nickel-cadmium storage batteries were charged daily for efficient operation.

The field techniques used in the Nome beach study involved two men (a shooter-observer and his helper) for rapid, efficient operation. Duties for the shooter-observer entailed digging and loading the shot hole and readying the amplifier and recording oscillograph. Duties for the helper consisted of laying out the geophone cable, clipping geophones to the cable, and plugging the cable into the seismic amplifier. Upon completion of preparation, the shooter-observer detonated the charge to obtain a seismogram.

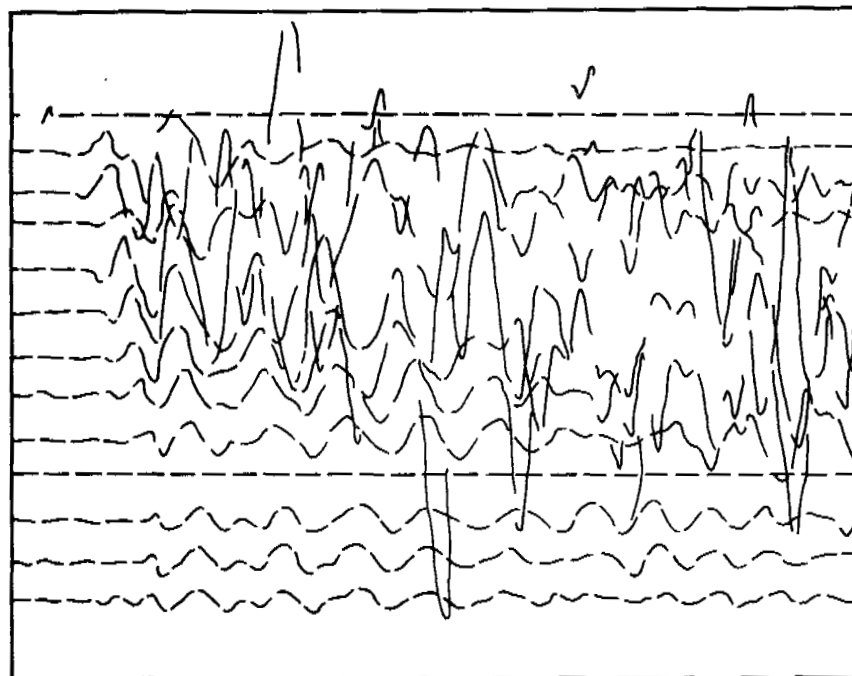
#### Procedures

A preliminary experimental survey was made before undertaking the investigation of the beach and tundra areas in order to determine the optimum sound source and geophone configuration.

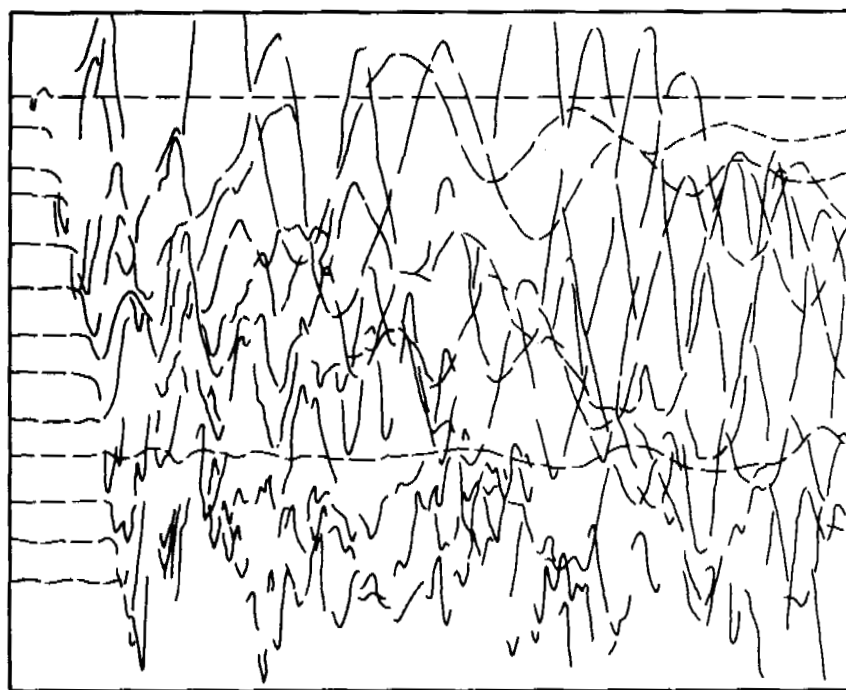
For shallow refraction work spread length determinations described by Griffiths is sufficient; "In refraction seismology the size of the shot is controlled mainly by the maximum range from shot to geophone, which must be at least twice the critical distance  $X_c$  if the second branch of the time-distance graph is to be properly defined. The critical distance in turn depends on the depth to the refraction of interest" (Griffiths and King, 1965, p. 101).

The results of the experimental survey indicated that 1 to 3 blasting caps, fired at depths of 2 feet beneath the beach surface, could not impart enough energy to the beach sands to give good signal response. However, 1/8 to 1/4 pound (1/4 to 1/2 stick) of 60% ditching dynamite detonated with a #6 Dupont instantaneous blasting cap in holes 2 to 3 feet deep and 3 to 5 feet above the water table was found to be adequate along most of the beach. Seismograms produced with blasting caps and dynamite-sound sources are compared in figure 33. On the tundra, dynamite was used exclusively. As in seismic reflection work, the explosive charges were buried at suitable depths, discussed later.

Profile shooting was used throughout the investigation. This method requires shot and detectors laid out in a straight line with equal spacing between detectors (Figs. 36D and 41B). Optimum geophone distances were determined during the pilot program. The length of the geophone spread is dependent on dip and depth to the lower horizon under study, and seismic velocities within overburden and bedrock. As long as the spread length is large enough to



A.



B.

Figure 33. Seismograms obtained with blasting caps (A) and dynamite sound sources (B).

determine the distance corresponding to the critical angle of refraction, good resolution of the bedrock and intermediate shallower layers are obtainable. A general rule established at Nome was to keep the spread length greater than twice the inferred depth to bedrock. Also, the shot-to-first-detector distance was kept about twice the critical distance length of the expected shallowest refraction horizon which was mistakenly thought to lie between 10 and 30 feet. A very low velocity surface layer, 5 to 12 feet thick, was disregarded during the field work and neglected during the first analysis of the data. This layer is thought to consist mostly of dry sands on the beach and peaty-soil in the tundra and in some cases probably absorbed so much energy that only later phases of the signal were recorded thus producing apparent velocities. Velocities of this surface layer should have been measured using closely spaced geophones and increased charge sizes. Whenever first arrival intercept times are very large, as is common in this case, a velocity study should be made.

Probable variations in the degree of saturation at the top of the water table in some locations caused differences in arrival times and produced apparent velocities (David Barnes, written communication, 1968). To distinguish between true velocities and apparent velocities overlapping spreads should be made and this was done at several stations (see Fig. 38, Station 33 overlaps Stations 103 and 104 of the detailed beach survey). Comparison with velocities obtained from the overlapping spreads and velocity



measurements obtained during the offshore reflection investigation indicate that most of the seismic velocities mentioned in this report may be considered as true velocities.

Preliminary shots indicated a bedrock depth of 20 to 60 feet beneath the beach and 20 to 100 feet under the tundra. Spread lengths of 120 to 240 feet with geophone spacings of 10 to 20 feet were experimented with on the beach, and spread lengths of 300 to 600 feet with geophone spacings of 25 to 50 feet were tried on the tundra. The distance of shot to first detector was kept at the same length as geophone spacings and in line with the geophone spread. For optimum resolution, it was discovered that spread lengths of 192 feet with geophone spacings and shot offsets of 16 feet were ideal for the beach; spread lengths of 300 feet with geophone spacings and shot offsets of 25 feet were suitable for the tundra survey. A detailed continuous seismic line was run on a section of the beach to delineate a buried stream channel believed to lie 60 feet beneath the surface (Fig. 36A, C). The detailed line was designed to investigate the probable extension of a deep channel that had been discovered in a prospecting shaft about a mile inland (oral communication from the late Mike Walsh to David M. Hopkins, 1961). The channel probably represents the pre-glacial course of the Snake River (Hopkins, oral communication, 1967). Experiments before shotting the detailed line showed that a spread length of 300 feet with shot offsets and geophone spacings of 25 feet gave good bedrock definition.

Signal-to-noise-ratio must be considered when determining the best technique to use in a seismic investigation. Strong winds and heavy surf action, especially along beaches, produce seismic noise that may interfere with the identification of refracted seismic signals. During the time of the survey no major storms occurred, difficult noise problems were not encountered. In trying to improve signal amplitude and poor signal response encountered during the preliminary survey, the geophones were placed at different depths below the beach surface. By burying the geophones approximately 6 inches beneath the surface, it was found that signal response was improved over that obtained when the geophones were simply exposed on the surface.

Shooting a seismic survey across tundra and permafrost areas creates unique problems. The ground in tundra areas near Nome commonly remains frozen throughout the year at depths below 30 inches, and frozen ground was encountered at 18 inches at the time of the tundra survey in July. It was feared that the increase in modulus of elasticity of the overburden caused by permafrost would increase its seismic velocity so much that a good velocity contrast might not be obtained between overburden and bedrock. However, a vertical velocity contrast did exist in the area of the tundra survey and the bedrock interface was definable. Most tundra areas are mantled by mosses and other acoustical absorbing organic matter; these act as an acoustical sponge, preventing returning signals from being recovered. To eliminate this problem, geophones were placed

in the thaw zone, in silt below the organic matter, and several inches above the permafrost surface, with the resulting signal amplitude found to be equivalent to or better than that obtained in the beach sands.

#### Summary

A 192-foot spread length and geophone spacing of 16 feet was used for the general beach investigation with all geophones buried approximately 6 inches beneath the beach surface. A 1/8 to 1/4 pound dynamite sound source buried in a 3 foot hole in wet sand 2 to 5 feet above the water table was employed. The shot was offset 16 feet from the first geophone and linear profiles were utilized. Experimental work showed that the detailed beach line should have a 300 foot spread length with a 25 foot geophone spacing and shot offset (Fig. 36E); the best sound source and geophone positions were determined to be the same as for the general beach study. By placing all geophones at equal elevations, terrain and elevation corrections were avoided. On the tundra, a 300 foot spread length with a 25-foot geophone spacing was used with all geophones positioned in the thaw zone just beneath the organic matter of the tundra. The best sound source was a 1/4 to 1/2 pound charge of dynamite buried about 2 feet beneath the tundra surface, on the permafrost, and offset 25 feet from the first geophone, in line with the spread (Fig. 41B).

Seismic beach stations were generally located approximately 1/2 mile apart (Fig. 36A). Once a station was established and

occupied a marker was erected and later located accurately by Raydist positioning equipment mounted in a helicopter. The geophone cable was first laid out in a line parallel to the coast line. After obtaining the initial seismogram, a reverse shot was made, fired at the opposite end of the spread to assist in dip determination of bedrock surface. On the detailed beach stations the reverse shot made for a previous spread was used at the shot point for a following line, making the survey continuous in nature. At 5 stations where the beach was wider than 200 feet a line was shot perpendicular to the coast line to better delineate bedrock topography.

The tundra seismic line was oriented by a Brunton traverse and extended from Dry Creek Road 1200 feet S40E across Dry Creek. It consisted of four sections (Fig. 41A). Elevation changes for this line were determined with a hand level. This survey was continuous, employing the same procedures used for the detailed beach line with the last shot of a spread used as the shot point for the following spread.

### III. INTERPRETATION OF SEISMOGRAMS

The object of refraction seismology "...is to build up a time-distance graph with adequate number of points on the branches corresponding to all refractors of interest..." (Griffiths, in Griffiths and King, 1965, p. 121). Interpretation of refraction seismograms consists of picking, correcting, and plotting on time-distance graphs all first-arrival times. From time-distance graphs seismic velocities can be calculated and depth determinations can

be made.

### Theory

Recovery of refracted and reflected sound waves produced by controlled seismic explosions usually produce a seismic record indicating one or more events that are caused by the change in velocity of the wave front. Seismic energy is represented by elastic waves and abrupt changes in the elastic properties through which the wave is propagated will cause the wave to be refracted or bent. The amount of bending is dependent upon Snell's Law; sine of the angle of incidence is equal to sine of the angle of refraction. Another way of representing this law is by the equation:

$$\frac{\sin i}{\sin r} = \frac{V_1}{V_2}$$

where  $i$  = angle of incidence

$r$  = angle of refraction

$V_1$  = velocity of transmission of elastic wave in incidence  
medium

$V_2$  = velocity of transmission of elastic wave in refraction  
medium.

An important concept in refraction work is that of the critical angle. When the angle of refraction equals  $90^\circ$  the sine of the angle of incidence equals  $V_1/V_2$ . This is a special case where the incident ray strikes the interface at the critical angle and the refracted wave travels parallel to the interface. A refracted wave acts as a first arrival when the time required for it to travel from the

source through the refraction layer to the detector is equal to, or greater than, the time required for the direct wave to travel from the source to the detector. Distance along the ground surface from the source to that point where the refracted wave and direct wave meet is called the critical distance  $X_c$  and, as shown later, is an important function in calculating depth of the refraction horizon (Fig. 34). The path that first arrival waves take is dependent upon the depth to the reference interface and distance between the first geophone and source.

When first arrival times are plotted on a time-distance graph a break in the slope of the time-distance curve will occur where the time taken for both direct and refracted waves to travel from source to detector are the same (Fig. 34). Velocities are obtained from the slope rate on the time-distance curve.

The following sources can be referred to for a more detailed discussion on refraction theory: Hodgson (1964) and Griffiths and King (1965) for a clear and concise elementary discussion of refraction seismology; Dobrin (1960), Nettleton (1952), and Dix (1940), for more technical and advanced approach to the subject.

#### Analysis of Data

First-arrival times were interpreted from seismograms by locating points where the Galvanometer traces first departed from a straight line drawn parallel to the first portion of the trace (Fig. 35A). Travel times were assigned to these points by reading differences in time between data traces and the shot time.

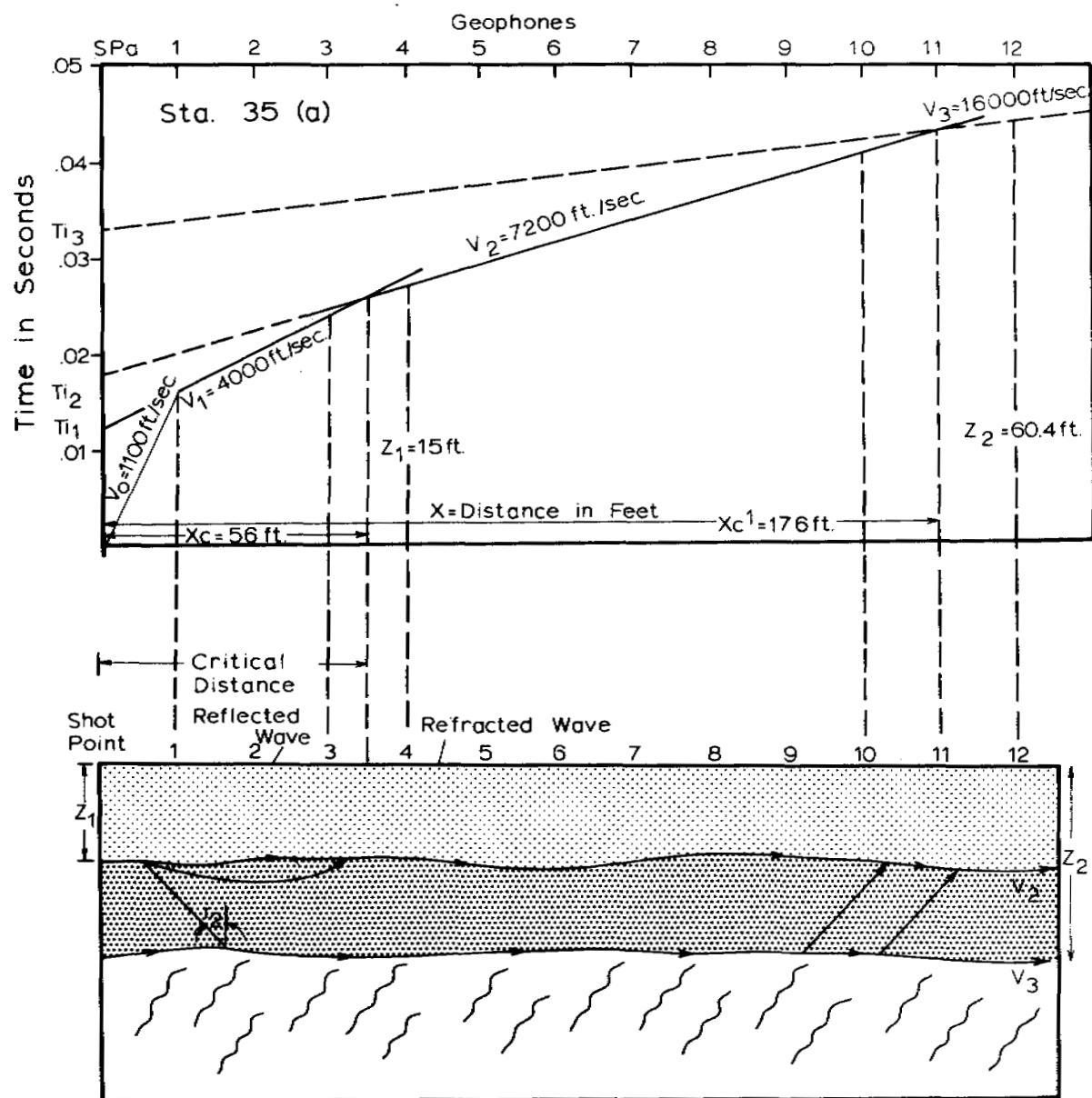


Figure 34.--Time-distance graph and schematic representation of refraction of seismic energy at three acoustical interfaces and the resultant time-distance graph.

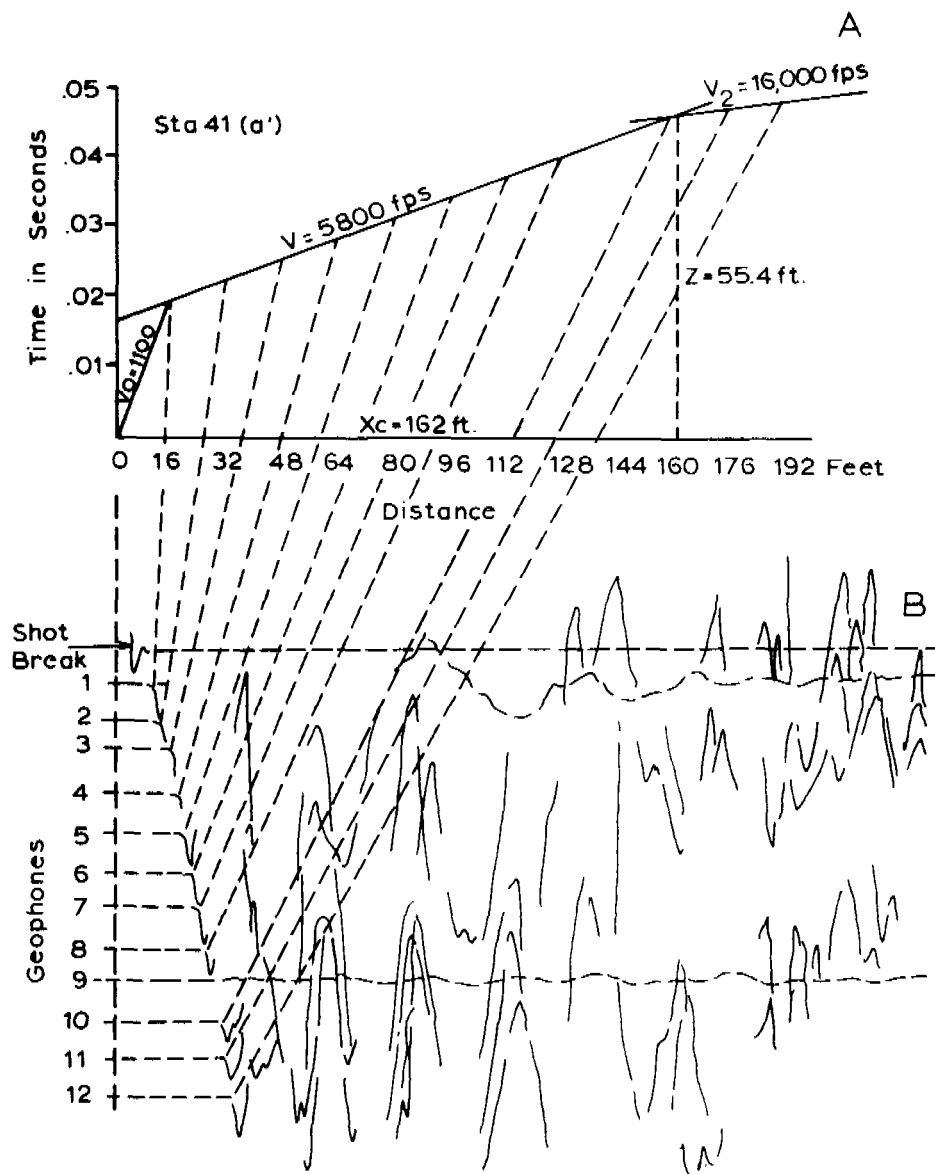


Figure 35. Refraction seismograms showing how first-arrival times are picked and plotted on a time-distance graph.



The first-arrival times obtained were then corrected by applying the difference in time between the shot break and the zero timing mark. A transparent timing plotter that could be laid over the seismogram and adjusted to read directly the corrected times from the seismic record was developed.

Once the first-arrival times were determined, they were plotted to a time-distance graph (Fig. 35B). By using the two equations:

$$\text{Velocity} = \frac{\text{Distance}}{\text{Time}} \quad (1)$$

$$Z = \frac{X_c}{2} \sqrt{\frac{V_2 - V_1}{V_2 + V_1}}, \quad (2)$$

where  $Z$  = depth to acoustic interface

$X_c$  = critical distance,

$V_1, V_2$  = velocities of first and second layers respectively.

Seismic velocities for each layer and depth to each acoustical interface shown on the seismograms were calculated from information developed on the time-distance graph. A third equation, utilizing intercept times, was used to check depths calculated by the critical distance method. This equation is given below:

$$Z = T_i \left( \frac{V_1 + V_0}{\sqrt{V_2 - V_0}} \right), \quad (3)$$

where  $Z$  = depth to acoustic interface

$T_i$  = intercept time

$V_0, V_1$  = velocity of first and second layers respectively.

The depth information obtained by both the intercept time and critical distance methods were used to construct contour maps and cross sections covering the investigation areas.

Four standard interpretation procedures are used by refraction seismologists: 1) Critical distance formulae, 2) Time intercept formulae, 3) Apparent-velocities-of-sloping-layers formulae, and 4) Delay time formulae. The choice of an interpretation technique depends on local conditions and the interpreter's judgment and experience (David Barnes, written communication, 1968). In this survey the first two techniques were used, but the more complex dipping beds method probably should have been used where sloping layers were encountered and might have changed the interpretation. However, where dipping interfaces were inclined at great angles the depths and velocity of those interfaces were checked by using the dipping beds formula and found to show no appreciable variation in the interpretation.

#### IV. RESULTS

##### General

Contour maps and cross sections of beach and tundra investigation areas were constructed from data obtained by the interpretation of the time-distance graphs which were correlated with offshore seismic reflection data and onshore drill hole information. Apparent velocities and depths of different refractors were calculated.

## Beach Profile

### Seismic velocities

Velocities observed in overburden were quite variable; probably reflecting differences in lithology within the stratigraphic unit. Sharp acoustical discontinuities in some seismograms clearly indicate that two or three velocity layers are present in the overburden; whereas a lack of discontinuities in other seismograms suggested the absence of any distinct interface within the overburden. All seismic records disclosed a well-defined bedrock interface.

A very low velocity surface layer extends across most of the beach area and has a range of 500 to 2400 fps with an arithmetic mean velocity of 1300 fps and a median of 1500 fps. For the upper layer in the overburden (Layer A) calculated velocities ranged from 4000 to 6000 feet per second (fps) with a mean of 4800 fps and a median of 5000 fps. Occasionally a low value was detected in Layer A with a range of 2000 to 3400 fps and a mean and median of 2700 fps. This low velocity zone was especially conspicuous near the mouths of rivers, as shown in seismograms from beach station 49 located along the river mouth bar of the Snake River (Figs. 36 and 37). The lower overburden layer (Layer B) exhibited variation in velocities from 9200 to 13,200 fps with a mean velocity of 11,700 fps and a median of 12,000 fps. Where there were no indications of layering in the overburden, the time-distance graphs showed seismic velocity from 6600 to 10,400 fps with an arithmetic mean of 8200 fps and a median of 8000 fps. Figures 38

and 39 show time-distance graphs where three-layer cases exist. For the acoustic basement, or bedrock, the velocities range from 14,000 to 18,500 fps with a mean of 16,200 and a median of 16,000 fps.

### Depths

Depths to different acoustical interfaces were calculated from the time-distance graphs and show an average of 6.5 feet to the base of the very low velocity surface layer, 18.6 feet to the first interface (thickness of Layer A), and an average 48.6 feet to bedrock. Thickness of the surface layer ranges from 3.5 feet to 9.0 feet; of the upper layer from 0 to 27 feet, and of the sediments overlying bedrock 34 to 80 feet.

The low velocity surface layer and the first acoustical interface (surface of Layer A) are shown in cross section (Fig. 36B). Structures of Layer A appears to be unrelated to the bedrock surface.

### Bedrock topography

Depth results were used to construct a basement contour map and cross sections along the beach (Fig. 34). Contours drawn from the depth information showed a bedrock surface topography that is undulating and correlatable with USSR&M's bedrock contours inland--established from drill hole data--and offshore bedrock contours--established by seismic reflection data (Fig. 36A).

The following four major subsurface channels are shown on the contour map and cross section: (1) Recent Snake River Channel, located about 1/2 mile west of the present outlet of the Snake River, (2) Offshore Channel located approximately 4 miles west of

# EXPLANATION

USSR and M basement contour from drill-hole data  
Long dashes where known, short dashes where approximate. Contour interval 20'. Datum is mean sea level.

Basement contours from seismic depth data  
Solid where known, dashed where approximate, dotted where inferred. Contour interval 10'. Datum is mean sea level.

Station number  
Note: Contours that extend offshore have been correlated with and drawn from offshore reflection data.

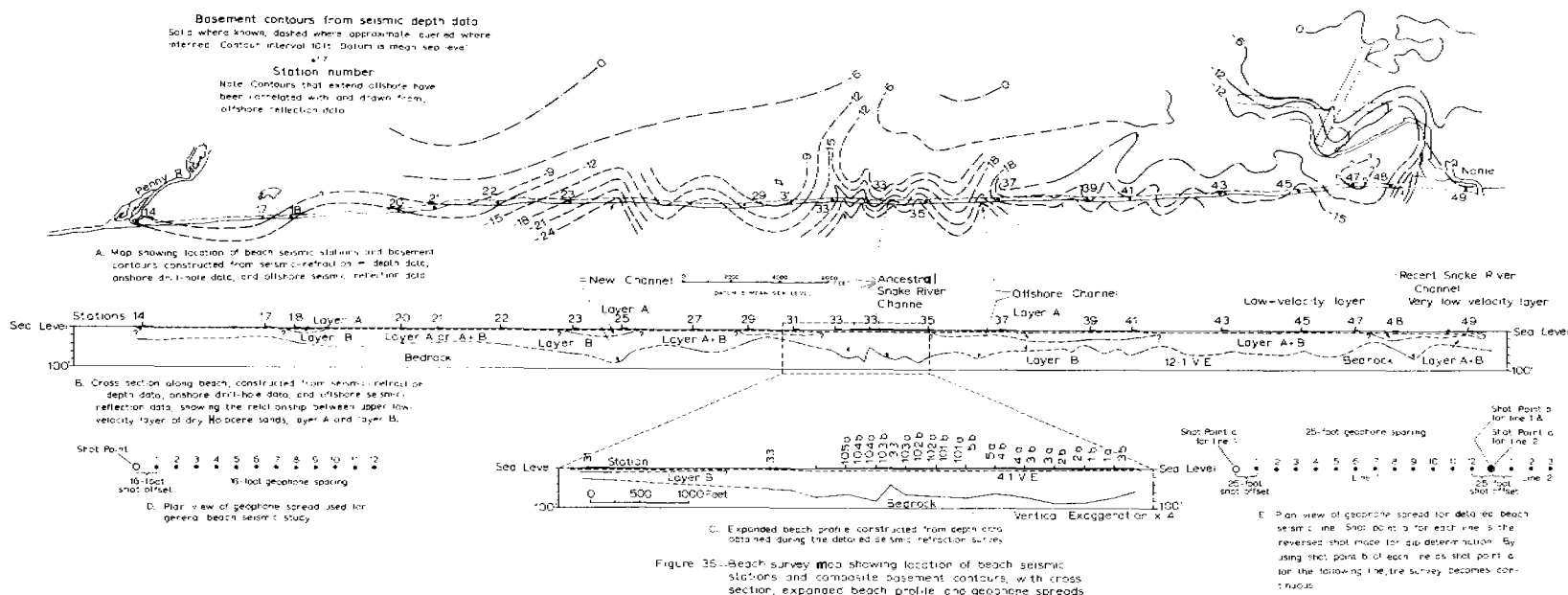


Figure 35. Beach survey map showing location of beach seismic stations and composite basement contours, with cross section, expanded beach profile, and geophone spreads.

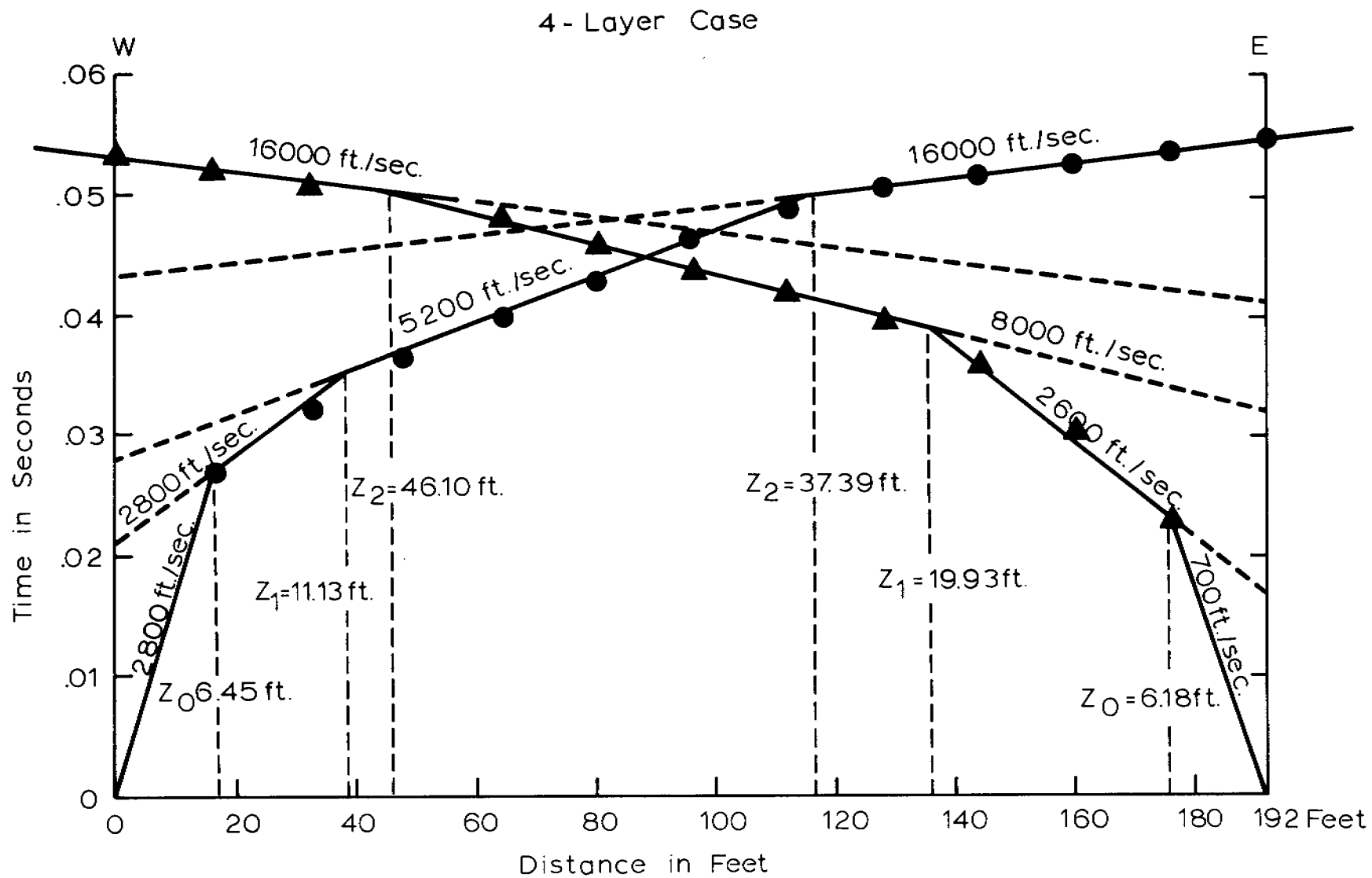


Figure 37. Time-distance graphs constructed from data of beach station 49.

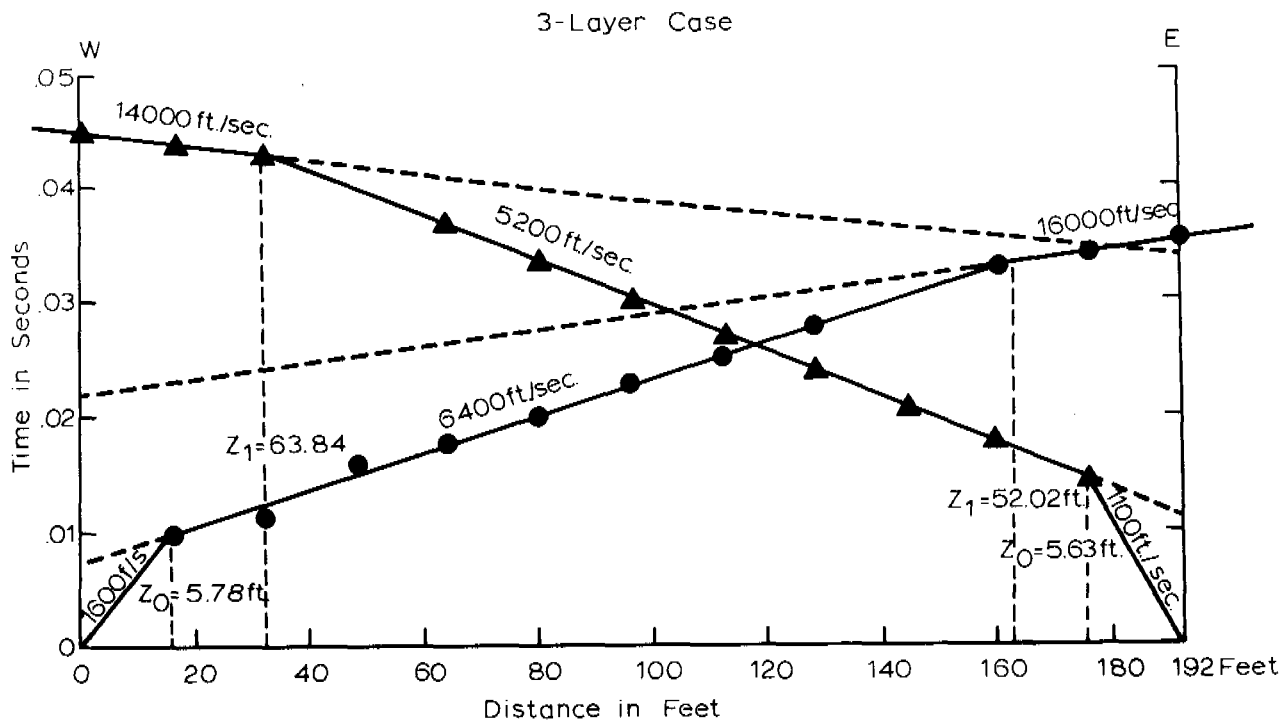


Figure 38. Time-distance graphs constructed from data of beach station 27.

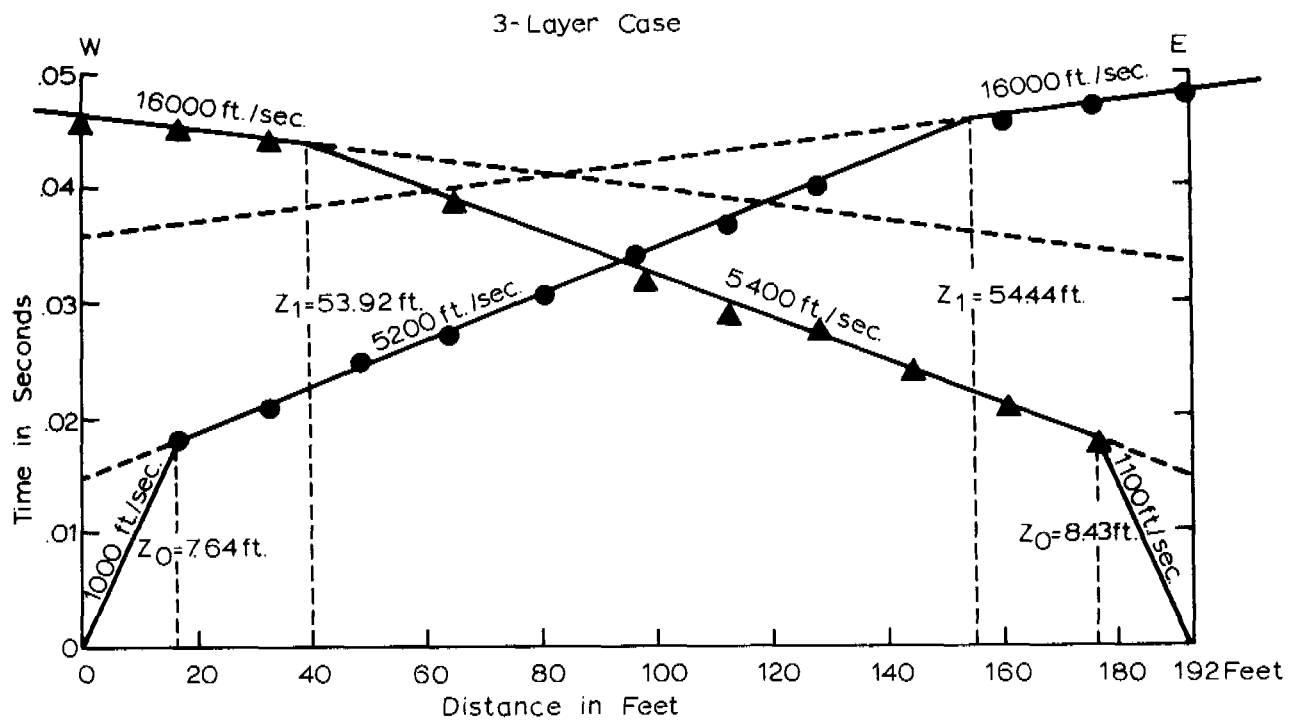


Figure 39. Time-distance graphs constructed from data of beach station 45.

the Snake River, (3) Ancestral Snake River Channel, located about 1/2 mile west of Offshore Channel and (4) New Channel, located about 3 miles east of Penny River (Fig. 36A, B). The subsurface Snake River channels appear to line up fairly well with onshore contours, but Offshore Channel does not agree with any onshore data and has been constructed solely from offshore reflection data. New Channel is not supported by onshore subsurface topography, possibly because of the lack of data. Between beach stations 31 and 35, a detailed seismic line was run to outline the Ancestral Snake River Channel. A cross section made from this line shows an old river channel consisting of two well-incised tributaries and one broad river bed cut into the bedrock surface (Fig. 36B, C). Figure 40 shows continuous travel-time curves of the detailed line that can be explained by the bedrock topography shown in the section.

#### Tundra Survey

##### Seismic velocities

Time-distance plots constructed from seismograms obtained on the tundra defined a well established bedrock interface with no additional acoustic discontinuities in the overburden except for the surface very low velocity layer. Seismic velocities in the low velocity layer range from 600 fps to 2300 fps with a mean of 1500 fps and a median of 1800 fps. Velocities in the overburden range from 5200 to 11,200 fps with an arithmetic mean of 9000 fps and a median of 9500 fps. The mean velocity for sediments overlying the tundra bedrock was 2900 fps greater than the mean velocity for



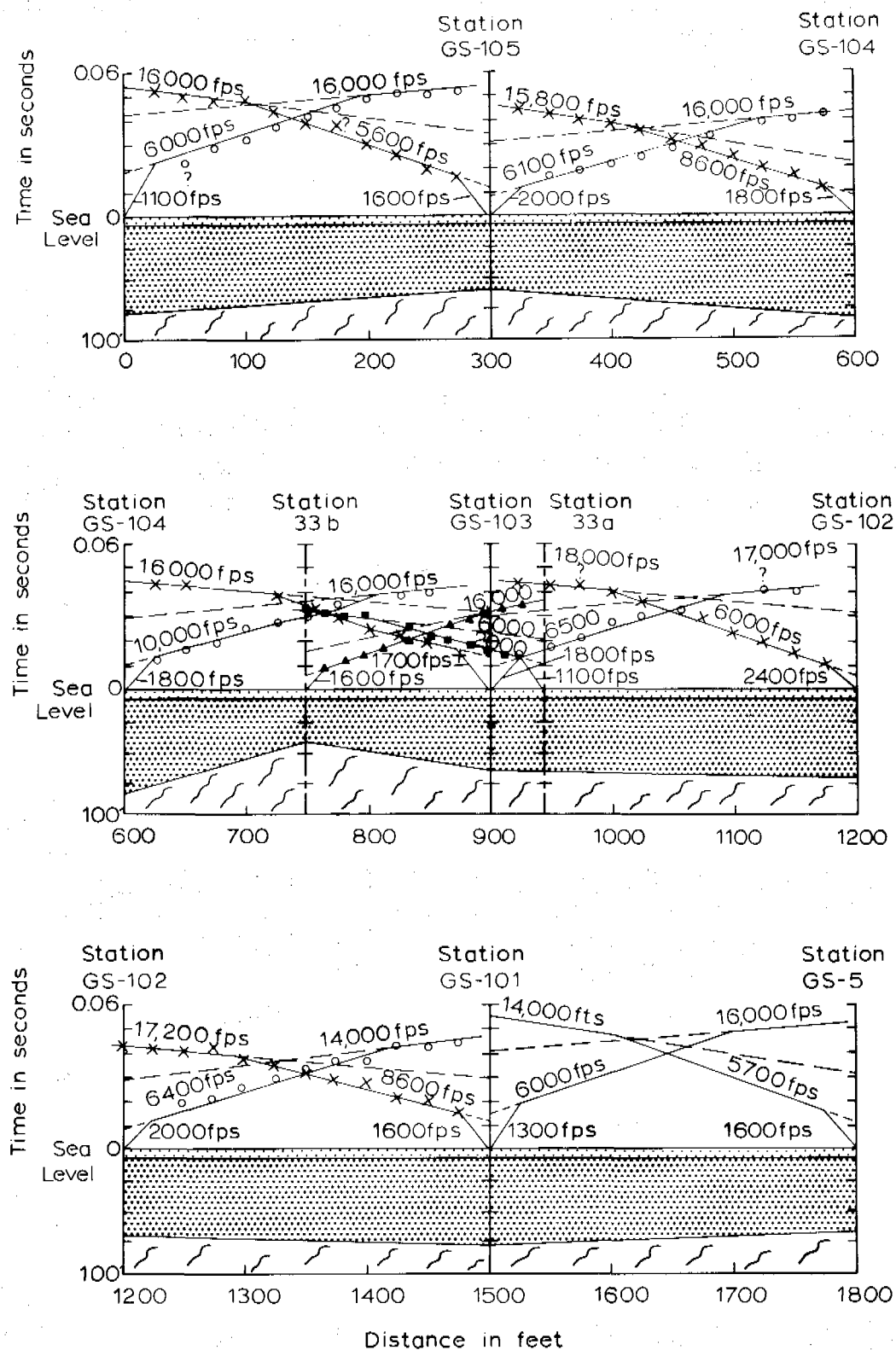
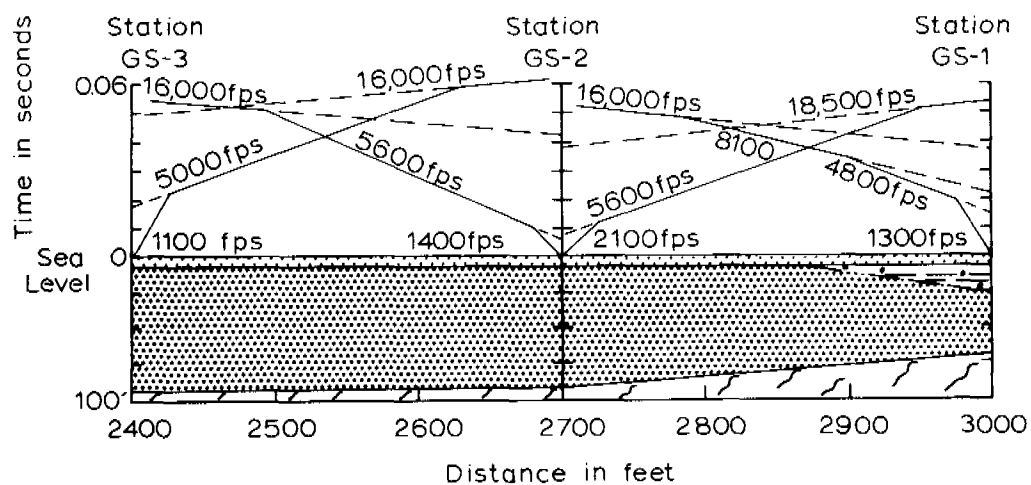
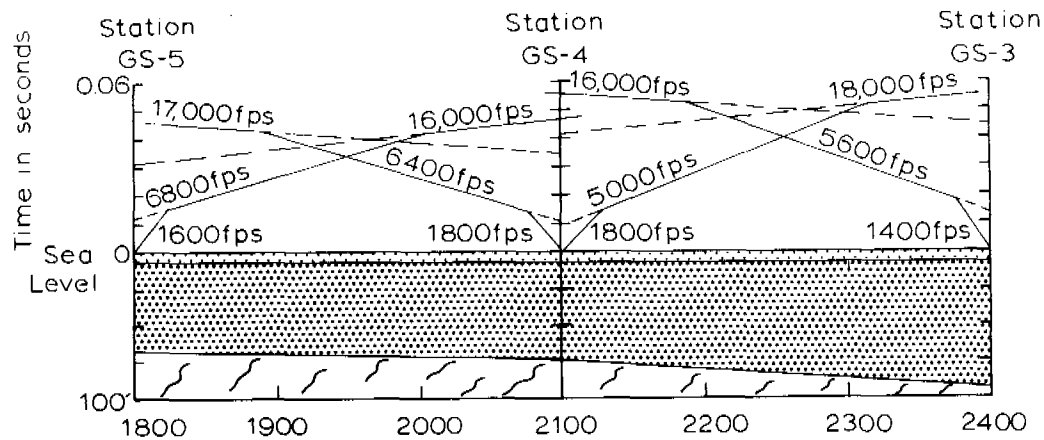




Figure 40.--Profile of detailed beach seismic refraction line



#### Explanation

  
Holocene sand and gravel

  
Illioian till

  
Sangamon poorly consolidated silt, clay, and sand

  
Paleozoic schist bedrock

relating travel-time curves to bedrock topography.

sediments overlying bedrock on the beach. The higher velocities probably reflect the presence, beneath part of the line, of perennially frozen overburden. Velocity within the acoustical basement of the tundra ranged from 14,000 to 18,500 fps with a mean of 16,300 fps and a median of 16,000 fps, which is nearly identical to the velocity of bedrock beneath the beach.

### Depths

Average depth to bedrock on the tundra was 48.8 feet with sediment thickness varying from 38 to 60 feet. The low velocity surface layer has an average thickness of 10 feet. Depth figures were used to construct a basement cross section and contour map (Fig. 41), which shows the bedrock surface dipping under Dry Creek, from both sides. Travel-time curves illustrated in figure 42 can be explained by the stratigraphy shown in the section and suggests that a channel has been cut into the bedrock surface. Drill-hole data obtained by USSR&M near the Dry Creek seismic line indicated an accuracy for the seismic data of  $\pm 4$  feet for bedrock depth. Comparisons of USSR&M's drill-hole data with cross section constructed from seismic information is shown in figure 42B.

## V. DISCUSSION AND CONCLUSIONS

### General

Heavy-mineral deposits, including gold placers, have a tendency to be concentrated on bedrock, and, if stream deposited, are likely to lie in bedrock channels. Beach deposits normally occur on flat bedrock surfaces seaward of a bedrock scarp. The

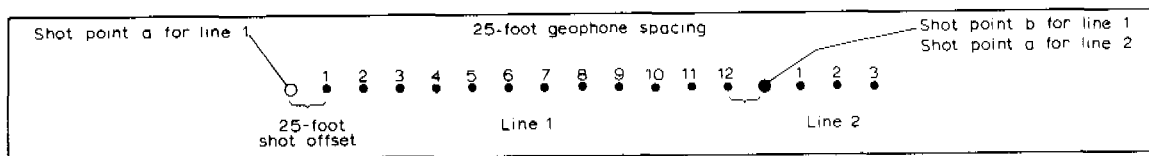
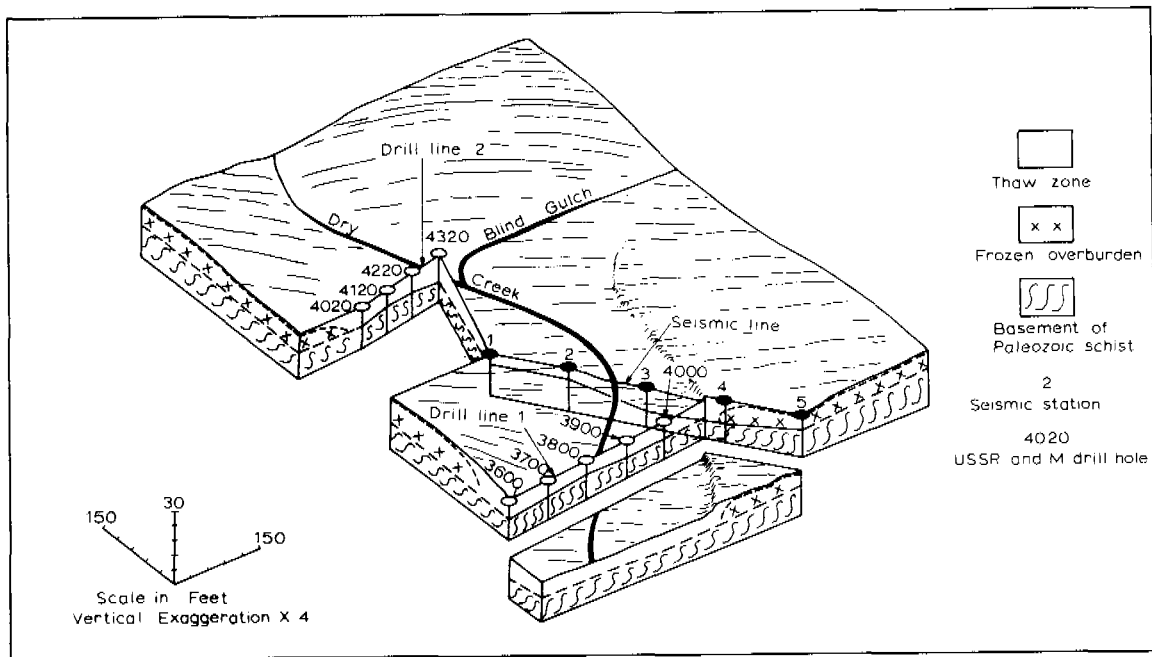
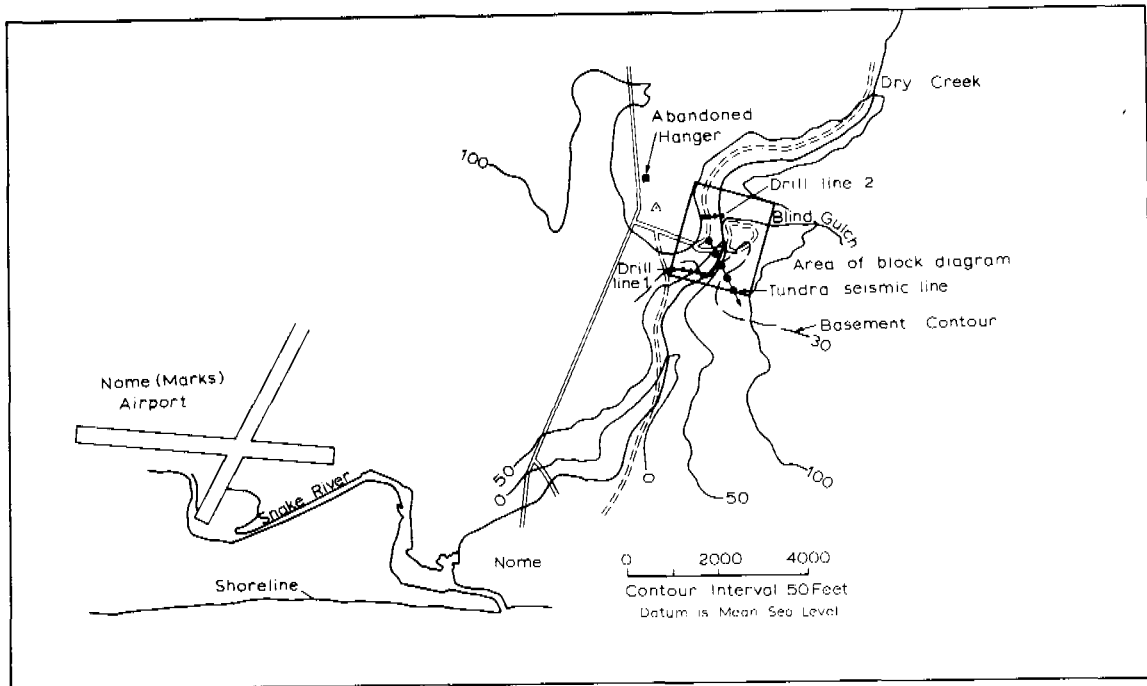


Figure 41.--Tundra survey Map showing location of tundra seismic line and USSR&M drill-hole lines with block diagram and geophone spread

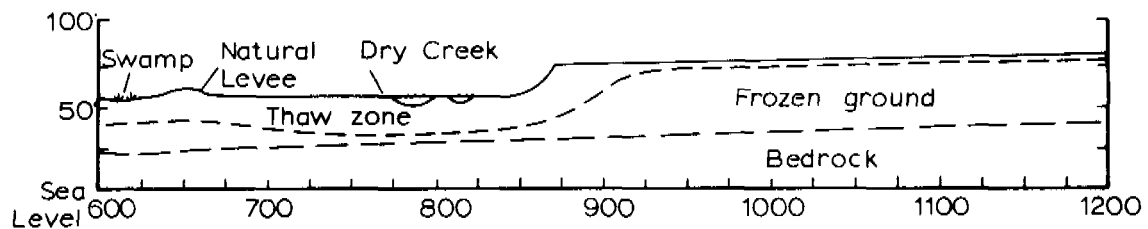
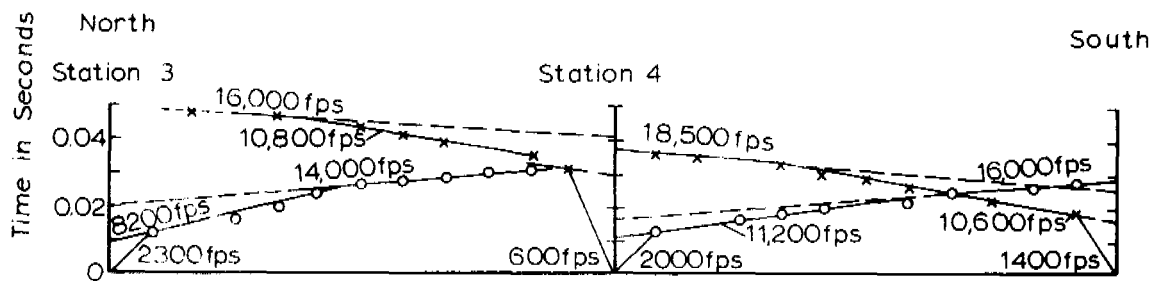
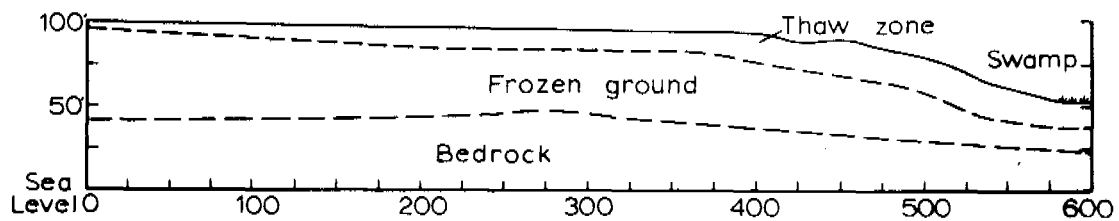
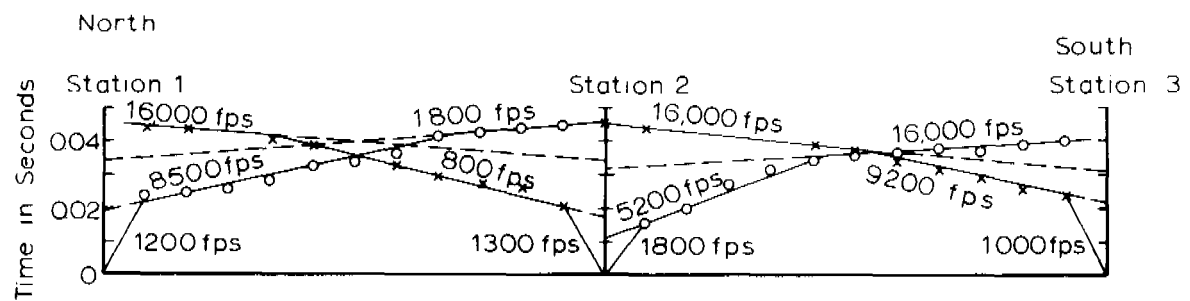


Figure 42.--Profile of tundra seismic refraction line relating travel-time curves with bedrock topography.

need has long been felt for a tool to locate buried stream channels and subsurface structures that attract the accumulation of detrital gold, and other heavy metals. An inexpensive and easy method to determine bedrock topography can be of great value in delimiting those areas likely to contain placers, and thus result in important economics in designing an exploratory placer-drilling program.

Results obtained with the portable refraction seismograph near Nome show that it is possible to acquire accurate data that can be used to determine locations and configurations of bedrock features that may be the site of placer accumulations. The technique established for the Nome survey can also provide information regarding internal stratigraphy of unconsolidated overburden. The bedrock at Nome can be delimited in both permafrost and unfrozen areas.

#### Interpretation

Interpretation of the Nome beach stratigraphy was made by comparing published geology with new observations, by studying information, and by correlating these studies with seismic data. Consideration of these factors led to the correlation of seismic velocities with interpreted stratigraphic units and has allowed reconstruction of geologic history with greater detail than previously allowed.

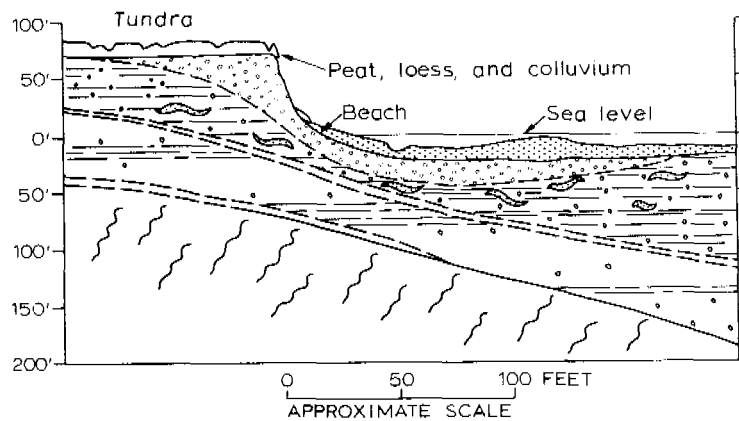
Variation of seismic velocity within overburden partly reflects differences within the stratigraphic unit. For example, a poorly consolidated till may give lower velocities than a well compacted

till, bouldery till, or tillite; this type of condition most likely exists at Nome. In the overburden at Nome a four layer case exists where the lower velocities of Layer A are caused by poorly consolidated post-till marine sand and silt of an offshore facies of Second Beach age, whereas higher velocities in Layer B are the result of well compacted, relatively fine-grained till with boulders. The thick, extremely low velocity layers, such as those found near river mouths, are thought to be caused by the accumulation of unconsolidated Holocene beach sand and gravel. The very low velocity surface layer found covering most of the beach consists of dry to damp Holocene sand and gravel that is probably in transport. Variation of seismic velocities in this layer is possibly due to the difference in water saturation. Several feet of dry sands above the wet sands found within the water table could produce the differential velocities. Where there is no velocity contrast in the overburden (only one acoustic layer present, not including the low velocity surface layer), seismic velocities appear to represent an average velocity of both Layer A and B. This may occur with compaction of both layers is nearly the same and boulders are lacking in the lower layer. Several places on the beach where this two-layer situation existed, outcrops of Sangamon silt and sand that accumulated in shallow-water offshore or estuarine environment were observed (D. M. Hopkins, oral communication, 1967). Along the beach near Station 35, a thin layer of beach sand and gravel covered sediment consisting of lagoonal deposits, peat, and iron oxidized

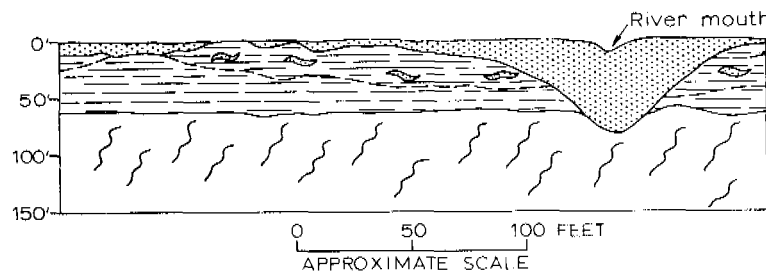
gravels, possibly of Sangamon age. This reconstruction leads to the conclusion that the unconsolidated beach sand and gravel included in Layer A have a velocity of 2000 to 3400 fps and the dry sand and gravel surface layer covering most of the beach has a velocity of 500 to 2000 fps. Drilling offshore and mining onshore show that bedrock underlying the beach and tundra consists of mica or graphite schist. A seismic velocity of 16,000 fps is typical for this type of rock.

Final interpretation with reference to the Nome geology led to the construction of a stratigraphic column and idealized stratigraphic cross-sections for beach and tundra (Fig. 43). The stratigraphic sections show a thin layer (0-15 feet) of unconsolidated beach sand and gravel overlying a silt and clay bed. Locally, the beach sand and gravel unit increases in thickness in the vicinity of river mouths. Beneath the beach material is a layer of Sangamonan outwash and, at places, estuarine deposits that vary in thickness where present. Underlying the Sangamonan sediments is a relatively thick layer (20-30 feet) of Illinoian till and outwash which overlies bedrock. Layer A consists of unconsolidated marine silty sands of Sangamonan (Second Beach) age. Layer B consists of well-compacted Illinoian till and outwash. Bedrock is a mica or graphite schist. On the tundra the section consists of Wisconsinan peat, loess, and colluvium overlying Illinoian till and outwash (Hopkins, 1960).





CROSS SECTION OF BEACH AND TUNDRA



TRANSVERSE PROFILE OF BEACH

AGE	LITHO- LOGY	DESCRIPTION	SEISMIC VELOCITIES	APPROX SCALE IN FT.
Holocene		Dry beach sand and gravel	Very low 50 to 2400fps	25
		Wet beach sand and gravel	Low 2000 to 3400 fps	
Pleistocene	Saginawan	Poorly consolidated near-shore silt, clay, and sand of Second Beach age	Layer A 4000 to 6000 fps	50
	Illinoian	Illinoian till (Nome River Glaciation)	Layer B 200 to 13,200fps	75
		Near-shore silt, clay, and sand of Intermediate Beach age (middle Pleistocene)		
		Iron Creek till, well compacted		100
Pliocene		Near-shore silt, sand, and clay of Submarine Beach age	Basement 14,000 to 18,500 fps	125
Paleozoic		Schist		

Figure 43.--Idealized cross sections and stratigraphic column of Nome Beach and tundra survey areas.

### Potential Placer Sites

Application of the seismic technique in the Nome area established the position of a former channel of the Snake River and several other channels not anticipated. These channels have not been tested by drilling, but they may contain workable gold placers.

### Conclusions

Successful operation of the refraction seismograph throughout the Nome survey demonstrated the usefulness of such an instrument in locating possible sites of heavy metal placers. Application of the seismic method used at Nome should contribute to the success of future exploration for heavy mineral placer deposits on beaches and in regions of permafrost.

## PART IV. SUMMARY

Beaches of Nome, Alaska, during the summer of 1967 contained many micro-topographic structures. Due to unusual spring and summer weather conditions these features persisted throughout the summer and many were probably preserved in the stratigraphic cross section of the beach.

Microrelief features develop in the spring and early summer as the result of dynamic processes associated with the break-up of sea-ice and the melting or thawing of the kaimoo, permafrost, snow-banks, and blocks of ice stranded on the beach. Resulting microrelief form in two zonal areas which were defined by the originating mechanisms of the microrelief features. The lower beach zone is restricted to the swash zone where the interaction of wave deposition and melting of stranded gravel and sand-rich brash ice produce ice-pushed ridges, kaimoo ridge and deposits, sea-ice kettles, and sea-ice sand and sea-ice gravel cones. The upper beach zone is restricted to the upper foreshore or backshore where fluvial processes form microfluvial features consisting of micro-outwash deposits and microdeltaic deposits.

A grain size distribution map constructed from the sediment data clearly shows that the sediment distribution along the beach is random with no direction of increasing or decreasing median diameters, sorting coefficients, or sand-gravel percentages. Generally, the swash zone and offshore area sampled with the use of SCUBA showed the best sorting and most uniform grain size distribution. The foreshore and backshore of the beaches exhibited bimodal or polymodal distribution and were commonly coarse grained.

The coast of the Seward Peninsula is a relatively low energy coast and the beaches are usually insulated from the elements by ice for about 6 months per year. During the fall, when sea-ice is breaking up, the beach is disturbed by ice-push. This disturbance is indicated by the random grain size distribution.

Sea-ice is also responsible for bringing some new sediment to the beach, but the quantitative importance of this is not known. It appears that new sediment is added to the Nome beaches by Cripple Creek, Penny River, Snake River, Nome River, and streams that empty out onto the beach. Erosion of the wave-cut cliffs at the backshore during storms contribute considerable amounts of coarse material.

Longshore drift varied from east to west between June and September, 1967 with a net sediment transport toward the east. This net eastward transport was indicated by accumulation of sediment on the west side of the Snake River jetties and erosion on the east. An eastward trail of tin cans from the Nome dumps, located on the beach, also indicated a net eastward longshore drift.

A seismic refraction study was made of the beach and tundra gold placer areas near Nome, Alaska, using a small light-weight portable seismograph system. Geophone configuration and type of sound source for this investigation were determined during a preliminary experimental survey.

As the beach study was successful, a short experimental seismic line was completed inland to determine the usefulness of a portable refraction seismograph in permafrost areas near Nome. The basic

problems in permafrost areas are the high seismic velocities in the overburden caused by the increased elastic modulus of frozen ground and by the acoustical absorption and variable thickness of the overlying tundra. The increase in sediment velocity reduces the possibility of a good velocity contrast at the bedrock-overburden interface, and the organic material of the tundra absorbs returning seismic energy. These problems were reduced by setting the seismic explosion off on the permafrost surface and by placing the geophones in the thaw zone of silt beneath the spongelike matter of the tundra. The results of this survey suggest that a refraction seismograph investigation of permafrost areas near Nome can be made successfully.

Results of the beach survey indicated that internal stratigraphy of the overburden could be interpreted and seismic velocities assigned to the different units. A very low velocity dry-to-damp layer of Holocene sands covering most of the beach showed seismic velocities of 500 to 2400 fps. Low velocity layers included in the overburden and especially conspicuous near river mouths exhibited velocities of 2000 to 3400 fps. Below the very low velocity layer, a Sangamonian poorly consolidated nearshore or estuarine silt, clay, and sand layer gave velocities of 4000 to 6000 fps. Beneath the estuarine material is an Illinoian till that has a velocity of 9200 to 13,200 fps. Bedrock was well defined in all seismograms and exhibited velocities from 14,000 to 18,500 fps.

Several buried channels were identified that may be sites of possible gold placer deposits. Results of the tundra survey illustrate the feasibility of the portable seismograph as a tool for placer prospecting.

## **BIBLIOGRAPHY**

## BIBLIOGRAPHY

- Brooks, A. H., Richardson, G. B., and Collier, A. J., 1901, Reconnaissances in the Cape Nome and Norton Bay regions, Alaska, in 1900: U.S. Geol. Survey Bull. 222 p.
- Collier, J. A., Hess, F. L., Smith, P. S., and Brooks, A. H., 1908, The gold placers of parts of Seward Peninsula, Alaska including the Nome, Council, Kougarok, Port Clarence, and Goodhope precincts: U.S. Geol. Survey Bull. 328, 343 p.
- Dix, C. H., 1940, Seismic prospecting for oil: New York, Harper & Brothers, 414 p.
- Dobrin, M. B., 1960, Introduction to geophysical prospecting, 2nd ed: New York, McGraw Hill, 446 p.
- Emery, K. O., 1938, Rapid method of size analysis: Jour. Sed. Pet., V. 8, No. 3, p. 105-111.
- Griffiths, D. H., and King, R. F., 1965, Applied geophysics for engineers and geologists: New York, Pergamon Press, 223 p.
- Hodgson, J. H., 1964, Earthquakes and earth structures: Englewood, N. J., Prentice-Hall, 166 p.
- Hopkins, D. M., MacNeil, F. S., and Leopold, E. B., 1960, The coastal plain at Nome, Alaska - A Late Cenozoic type section for the Bering Strait region: Internat. Geol. Cong. 21st, Copenhagen 1960, pt. 4, p. 46-57.
- Hopkins, D. M., 1967, Quaternary marine transgressions in Alaska; in Hopkins, D. M., ed, The Bering Land Bridge: Stanford, California, Stanford Univ. Press, 495 p.
- Hume, J. D., and Schalk, M., 1964, The effects of ice-push on arctic beaches: Amer. Jour. Science, V. 262, p. 267-273.
- Johnson, D. W., 1919, Shore Processes and Shoreline Development: John Wiley and Sons, 584 p.
- King, Cuchlaine A. M., 1961, Beaches and Coasts: Edward Arnold LTD., London, 403 p.
- Kuenen, Ph. H., 1948, The formation of beach cusps: Jour. Geol., V. 56, No. 1, p. 34-40.

- MacNeil, S. F., Mertie, J. B., Jr., and Philsby, H. A., 1943, Marine invertebrate faunas of the buried beaches near Nome, Alaska: Jour. Paleon., V. 17, No. 1, p. 69-96.
- Moffit, F. H., 1913, Geology of the Nome and Grand Central quadrangles, Alaska: U.S. Geol. Survey Bull. 533, 140 p.
- Moore, G. W., 1966, Arctic beach sedimentation: Environment of the Cape Thompson Region, Alaska: Oak Ridge, Tenn., U.S. Atomic Energy Comm., Wilimovsky, N. J., and Wolfe, J. N., eds, p. 587-608.
- Nettleton, L. L., 1952, Geophysical prospecting for oil: New York, McGraw-Hill, p. 245-279.
- Nichols, R. L., 1961, Characteristics of beaches formed in polar climates: Amer. Jour. Sci., V. 259, p. 697.
- Poole, David M., 1957, Size analysis of sand by a sedimentation technique: Jour. Sed. Pet., V. 27, No. 4, p. 460-468.
- Poole, D. M., Butcher, W. S., and Fisher, R. L., 1951, The use and accuracy of the Emery settling tube for sand analysis: Beach Erosion Board, Tech. Memo, No. 23 Corps of Engineers.
- Rex, R. W., 1964, Arctic beaches, Barrow, Alaska: In Papers in Marine Geology, MacMillan Co., New York, Miller, R. L., ed, p. 384-400.
- Roberts, James A., Bleistein, Donald M., and Dolan, Robert, 1967, Investigation of marine processes and coastal landforms near Crescent City, California: Vol. I, Tech. Discussion, Earth Sci. Division, Dept. of the Army, U.S. Army Natick Lab., Natick, Mass., 71 p.
- Schalk, M., 1961, Sea-ice movement of beach material in the vicinity of Point Barrow, Alaska: Jour. Geophys. Res., V. 66, p. 2558-2559.
- Sharp, R. P., 1949, Studies of superglacial debris on valley glaciers: Amer. Jour. Sci., V. 247, p. 299.
- Shepard, Francis, P., 1963, Submarine Geology: Harper and Row, New York, 557 p.
- Trask, Parke D., 1932, Origin and environment of source sediments for Petroleum, Houston: Amer. Pet. Inst., Gulf Publ. Col., p. 323.



## APPENDIX

TABLE I  
GRAIN SIZE ANALYSIS OF NOME BEACH SEDIMENT SAMPLES

Sample No.	Size Class in mm -- Fractional %/Cumulative %							
	32.0	16.0	8.00	4.00	2.00	1.00	.707	.500
G-14-1a						35.3	13.6	15.7
						35.3	48.9	64.6
G-14-2a		2.0	17.4	10.4	6.6	22.0	10.7	8.9
		2.0	19.4	29.8	36.4	58.4	69.1	78.0
G-14-4	21.6	9.5	12.6	9.5	8.7	18.6	2.4	7.2
	21.6	31.1	43.7	53.2	61.9	80.5	82.9	90.1
G-17-2a			4.5	13.0	13.6	27.1	7.4	3.9
			4.5	17.5	31.0	58.1	65.5	69.4
G-17-3		6.3	5.8	6.7	5.2	6.8	4.1	4.8
		6.3	12.1	18.8	24.0	30.8	34.9	39.7
G-20-1		0.6	0.0	0.5	0.9	16.5	7.3	11.9
		0.6	0.6	1.1	2.0	18.5	25.8	37.7
G-20-2			4.0	4.2	4.8	25.4	10.2	13.3
			4.0	8.2	13.0	38.4	48.6	61.9
G-20-3b						46.0	7.8	10.8
						46.0	53.8	64.6
G-20-5						9.0		12.6
						9.0		21.6

TABLE I  
(Continued)

Sample No.	.350	Size Class in mm (continued) -- .250	.180	Fractional %/Cumulative % .125	.088	.062	.031	<.031
G-14-1a	13.6	17.3	3.4	1.1				
	78.2	95.5	98.9	100.1				
G-14-2a	14.2	4.1	3.0	0.6				
	92.2	96.3	99.3	99.9				
G-14-4	6.6	1.9	1.0	0.5				
	96.7	98.6	99.6	100.1				
G-17-2a	14.7	7.4	6.8	1.7				
	84.1	91.5	98.3	100.0				
G-17-3	4.8	10.9	21.9	21.9	0.7			
	44.5	55.4	77.3	99.2	99.9			
G-20-1	22.6	27.7	10.2	1.2	0.6			
	60.3	88.0	98.2	99.4	100.0			
G-20-2	21.0	12.7	4.4					
	82.9	95.6	100.0					
G-20-3b	10.8	16.7	5.9	2.0				
	75.4	92.1	98.0	100.0				
G-20-5		41.0	24.2	11.6		1.5	0.1	
		62.6	86.8	98.4		99.9	100.0	

TABLE I  
(Continued)

Sample No.	Md.	Moment Measures -- Trask			Q <sub>3</sub>	Percentage	
		So.	Sk.	Q <sub>1</sub>		Gravel	Sand
G-14-1a	0.70	1.80	1.06	0.40	1.30		100
G-14-2a	1.3	3.10	2.06	0.60	5.80	36.4	63.3
G-14-4	5.00	4.47	1.25	1.25	25.00	61.9	38.1
G-17-2a	1.20	2.48	0.82	0.44	2.70	31.0	69.0
G-17-3	0.30	3.08	3.80	0.19	1.80	24.0	76.0
G-20-1	0.42	1.53	1.19	0.30	0.70	2.0	98.0
G-20-2	0.70	1.87	1.14	0.40	1.40	13.0	87.0
G-20-3b	0.90	1.93	0.56	0.35	1.30		100
G-20-5	0.33	1.63	0.79	0.18	0.48	9.0	91.0

TABLE I  
(Continued)

Sample No.	32.0	Size Class in mm 16.0	8.00	Fractional %/Cumulative % 4.00	2.00	1.00	.707	.500
G-21-1		1.3	6.1	12.5	41.4	29.9	2.1	0.9
		1.3	7.4	12.9	61.3	91.2	93.3	94.2
G-21-2			0.9	58.0	22.8	13.5	1.2	1.1
			0.9	58.9	81.7	95.2	96.4	97.5
G-22-1						9.9	18.8	20.8
						9.9	28.7	49.5
G-22-2a					12.8	71.2	7.0	3.8
					12.8	84.0	91.0	94.8
G-22-3			4.8	8.6	12.8	39.9	8.5	7.4
			4.8	13.4	26.2	66.1	74.6	82.0
G-23-1		19.9	38.9	11.2	2.5	4.4	3.3	2.0
		19.9	58.8	70.0	72.5	76.9	80.2	82.2
G-23-2a						44.9	10.1	8.0
						44.9	55.5	63.0
G-23-3	6.2	1.9	5.3	1.5	0.7		0.9	8.3
	6.2	8.1	13.4	14.9	15.7		16.6	24.9
G-25-1	8.7	29.4	15.6	5.0	3.9	21.8	6.2	2.1
	8.7	38.1	53.7	58.7	62.6	84.4	90.6	92.7

TABLE I  
(Continued)

Sample No.	Size Class in mm (continued) -- Fractional %/Cumulative %						
	.350	.250	.180	.125	.088	.062	.031 <.031
G-21-1	13.6	17.3	3.4	1.1			
	78.2	95.5	98.9	100.1			
G-21-2	1.7	0.5	0.2	0.1			
	99.2	99.7	99.9	100.0			
G-22-1	25.7	20.8	3.5	0.5			
	75.2	96.0	99.5	100.0			
G-22-2a	3.2	2.1					
	98.0	100.1					
G-22-3	10.5	5.0	2.5				
	92.5	97.5	100.0				
G-23-1	5.6	6.9	5.1	0.2			
	87.8	94.7	99.8	100.0			
G-23-2a	11.6	13.6	10.9	1.4			
	74.6	87.6	98.5	99.9			
G-23-3	15.6	38.4	19.2	1.9			
	40.5	78.9	98.1	100.0			
G-25-1	5.5	1.8					
	98.2	100.0					

TABLE I  
(Continued)

Sample No.	Md.	Moment Measures -- Trask			Q <sub>3</sub>	Percentage	
		So.	Sk.	Q <sub>1</sub>		Gravel	Sand
G-21-1	2.8	1.52	0.76	1.60	3.70	61.3	38.7
G-21-2	4.5	1.45	0.70	2.61	5.50	81.7	18.3
G-22-1	0.5	1.51	1.12	0.35	0.80		100
G-22-2a	1.5	1.19	0.91	1.2	1.7	12.8	87.2
G-22-3	1.2	1.77	1.07	0.70	2.20	26.2	73.8
G-23-1	9.0	3.16	0.28	1.5	15.0	72.5	27.5
G-23-2a	0.90	2.00	0.60	0.35	1.40		100
G-23-3	0.32	1.51	1.07	0.22	0.50	15.7	84.3
G-25-1	10.0	4.18	0.25	1.2	21.0	62.6	37.4

TABLE I  
(Continued)

Sample No.	32.0	Size Class in mm --		Fractional %/Cumulative %				
		16.0	8.00	4.00	2.00	1.00	.707	.500
G-25-3a		11.1	25.0	7.1	17.0	23.4	4.1	7.0
		11.1	36.1	43.2	60.2	83.6	87.7	94.7
G-25-4						12.3	14.8	9.7
						12.3	27.1	36.8
G-27-1a		19.8	14.6	12.9	3.6	26.7	7.3	6.3
		19.8	34.4	47.3	50.9	77.6	84.9	91.2
G-27-2			0.5	6.1	46.7	44.6	1.5	1.3
			0.5	6.6	53.3	97.9	99.4	100.0
G-27-3		5.8	48.3	44.0	1.7	0.2		
		5.8	54.1	98.1	99.8	100.0		
G-27-4						10.0	9.2	8.3
						10.0	19.2	27.5
G-27-5		9.6	30.6	28.8	4.2	2.5	0.86	3.2
		9.6	40.2	69.0	73.2	75.7	76.6	79.8
G-27-6			2.4	7.6	7.8	9.8	3.6	11.7
			2.4	10.0	17.8	27.6	31.2	42.9
G-29-1a						18.1	19.4	15.0
						18.1	37.5	52.5



TABLE I  
(Continued)

Sample No.	Size Class in mm (continued) -- Fractional %/Cumulative %							
	.350	.250	.180	.125	.088	.062	.031	<.031
G-25-3a	4.1	1.2						
	98.8	100.0						
G-25-4	17.4	14.8	27.1	3.9				
	54.2	69.0	96.1	100.0				
G-27-1a	6.8	1.0	1.0					
	98.0	99.0	100.0					
G-27-2								
G-27-3								
G-27-4	13.3	26.7	27.5	5.0				
	40.8	67.5	95.0	100.0				
G-27-5	4.3	8.1	5.4		1.8	0.09		
	84.1	92.2	97.6		99.5	99.6		
G-27-6	10.6	27.9	14.0		3.7	0.1		
	53.7	81.6	95.6		99.3	99.4		
G-29-1a	28.8	15.6	3.1					
	81.3	96.9	100.0					

TABLE I  
(Continued)

Sample No.	Md.	Moment Measures -- Trask			Q <sub>3</sub>	Percentage	
		So.	Sk.	Q <sub>1</sub>		Gravel	Sand
G-25-3a	3.0	2.98	1.80	1.35	12.0	60.2	39.8
G-25-4	0.38	1.77	1.25	0.24	0.75		100
G-27-1a	3.0	3.44	1.59	1.1	13.0	50.9	49.1
G-27-2	2.2	1.41	0.93	1.5	3.0	53.3	46.8
G-27-3	8.5	1.25	0.89	6.4	10.0	99.8	0.2
G-27-4	0.32	1.50	1.27	0.24	0.54		100
G-27-5	4.80	2.41	0.25	1.00	5.80	73.2	26.8
G-27-6	0.38	2.07	2.33	0.28	1.20	17.8	82.2
G-29-1a	0.55	1.52	1.11	0.38	0.88		100

TABLE I  
(Continued)

Sample No.	32.0	Size Class in mm --		Fractional %/Cumulative %				
		16.0	8.00	4.00	2.00	1.00	.707	.500
G-29-2a			20.7	53.8	22.3	1.6	0.3	0.3
			20.7	74.5	96.8	98.4	98.7	99.0
G-29-3a			9.2	19.7	30.3	28.5	3.7	1.7
			9.2	28.9	59.2	87.7	91.4	93.1
G-29-4		2.3	4.3	3.6	9.3	9.4	3.4	2.7
		2.3	6.6	10.2	19.5	28.9	32.3	35.0
G-31-1a		8.2	1.6	0.3	5.1	25.6	8.7	8.0
		8.2	9.8	10.1	15.3	40.9	49.6	57.6
G-31-2a(1)						25.5	18.1	9.6
						25.5	43.6	53.2
G-31-3		1.2	3.4	7.3	3.8	1.3	9.4	6.9
		1.2	4.6	11.9	15.7	17.0	26.4	33.3
G-33-1a(1)							15.6	36.4
							15.6	52.0
G-33-2		3.1	18.9	18.9	8.8	16.2	5.6	6.2
		3.1	22.0	40.9	49.6	65.8	71.4	77.6
G-33-3							4.0	8.0
							4.0	12.0

TABLE I  
(Continued)

Sample No.	Size Class in mm (continued) -- Fractional %/Cumulative %					
	.350	.250	.180	.125	.088	.062 .031 <.031
G-29-2a	0.6 99.6	0.3 99.9				
G-29-3a	3.2 96.3	1.7 98.0	0.7 98.7	1.2 99.9		
G-29-4	4.7 39.7	21.5 61.2	33.4 94.6	5.4 100.0		
G-31-1a	23.4 81.0	14.6 95.6	4.4 100.0			
G-31-2a(1)	17.0 70.2	14.9 85.1	10.9 95.7	4.3 100.0		
G-31-3	16.4 49.7	31.4 81.1	15.1 96.2	3.1 99.3	0.6 99.9	
G-33-1a(1)	36.4 88.4	11.7 100.1				
G-33-2	7.5 85.1	10.0 95.1	4.3 99.4	0.6 100.0		
G-33-3	18.0 30.0	43.0 73.0	23.0 96.0	3.0 99.0	1.0 100.0	

TABLE I  
(Continued)

Sample No.	Md.	Moment Measures -- Trask			Q <sub>3</sub>	Percentage	
		So.	Sk.	Q <sub>1</sub>		Gravel	Sand
G-29-2a	5.5	1.37	0.99	4.0	7.5	96.8	3.2
G-29-3a	2.5	1.75	1.03	1.45	4.45	59.2	40.8
G-29-4	0.27	2.33	4.28	0.24	1.30	19.5	80.5
G-31-1a	0.70	2.01	1.13	0.37	1.50	15.3	84.7
G-31-2a(1)	0.60	1.71	0.94	0.34	1.00		100
G-31-3	0.35	1.63	1.59	0.27	0.72	15.7	84.3
G-33-1a(1)	0.52	1.28	0.98	0.40	0.66		100
G-33-2	2.00	1.15	0.10	0.56	0.74	49.6	50.4
G-33-3	0.28	1.24	1.13	0.24	0.37		100

TABLE I  
(Continued)

Sample No.	32.0	16.0	8.00	4.00	2.00	1.00	.707	.500
G-33-4						6.5		2.4
						6.5		8.9
G-34-1	24.0	23.1	12.8	8.9	6.7	4.9	1.8	1.3
	24.0	47.2	60.0	68.9	75.5	80.4	82.2	83.5
G-34-8I						3.3	16.7	53.3
						3.3	20.0	73.3
G-35-1a				2.0	12.9	35.7	4.6	12.8
				2.0	14.9	50.6	55.2	68.0
G-35-5b						11.7	14.8	39.5
						11.7	26.5	66.0
G-35-6a				5.1	35.3	32.0	7.3	7.8
				5.1	40.4	72.4	79.7	87.5
G-35-7		1.7	3.3	2.9	7.8	24.7	6.1	4.8
		1.7	5.0	7.9	15.8	40.5	46.6	51.4
G-35-8								37.7
								37.7
G-37-1								11.0
								11.0

TABLE I  
(Continued)

Sample No.	Size Class in mm (continued) -- Fractional %/Cumulative %						
	.350	.250	.180	.125	.088	.062	.031 <.031
G-33-4		24.3	32.9	30.9		2.9	0.1
		33.2	66.1	97.0		99.9	100.0
G-34-1	0.6	1.3	1.9	4.9	4.5	1.1	2.3
	84.1	85.4	87.3	92.2	96.7	97.8	100.1
G-34-8I	23.3	3.3					
	96.6	99.9					
G-35-1a	17.4	11.9	2.7				
	85.4	97.3	100.0				
G-35-5b	29.6	4.3					
	95.6	99.9					
G-35-6a	11.9	0.5					
	99.4	99.9					
G-35-7	15.1	21.9	8.9	2.0	0.7		
	66.5	88.4	97.3	99.3	100.0		
G-35-8		46.3	9.6	5.8		0.5	0.1
		84.0	93.6	99.4		99.9	100.0
G-37-1		70.1	15.7	2.9		0.2	0.1
		81.1	96.8	99.7		99.9	100.0

TABLE I  
(Continued)

Sample No.	Md.	Moment Measures -- Trask			Percentage	
		So.	Sk.	$Q_1$	$Q_3$	Gravel Sand
G-33-4	0.22	1.29	1.12	0.18	0.30	100
G-34-1	13.0	3.73	0.44	2.3	32.0	75.5 24.5
G-34-8I	0.60	1.18	0.97	0.50	0.70	100
G-35-1a	1.00	1.83	0.68	0.45	1.50	14.9 85.1
G-35-5b	0.54	1.25	1.14	0.46	0.72	100
G-35-6a	1.80	1.70	0.72	0.90	2.60	40.4 59.6
G-35-7	0.7	2.17	0.98	0.32	1.50	15.8 84.2
G-35-8	0.43	1.37	0.91	0.30	0.56	100
G-37-1	0.40	1.27	0.79	0.28	0.45	100



TABLE I  
(Continued)

Sample No.	32.0	Size Class in mm -- 16.0	8.00	Fractional %/Cumulative % 4.00	2.00	1.00	.707	.500
G-37-2a		3.8	9.2	33.9	26.5	18.6	1.9	0.7
		3.8	13.0	46.9	73.4	92.0	93.9	94.6
G-37-3	58.8	39.5	1.7					
	58.8	98.3	100.0					
G-37-4a						3.2	12.7	7.9
						3.2	15.9	23.8
G-37-5a	21.5	31.1	8.0	2.2	1.4	7.9	3.1	2.4
	21.5	52.6	60.6	62.8	64.2	72.1	75.2	77.6
G-37-6a		10.7	1.4					
		10.7	12.1					
G-39-1a			17.3	31.0	16.8	18.8	3.8	3.0
			17.3	48.3	65.1	83.9	87.7	90.7
G-39-2a		14.0	14.0	6.3	7.9	30.2	7.7	10.0
		14.0	28.0	34.3	42.2	47.4	55.1	65.1
G-39-3a						12.3	11.6	15.9
						12.3	23.9	39.8
G-39-4a		1.8	18.0	15.9	8.8	17.8	7.3	5.3
		1.8	19.8	35.7	44.5	62.3	69.6	74.9

TABLE I  
(Continued)

Sample No.	Size Class in mm (continued) -- Fractional %/Cumulative %						
	.350	.250	.180	.125	.088	.062	.031 <.031
G-37-2a	1.0 95.6	1.0 96.6	1.7 98.3	1.2 99.5	0.5 100.0		
G-37-3							
G-37-4a	26.2 50.0	30.2 80.2	14.3 94.5	4.8 99.3	0.8 100.1		
G-37-5a	5.9 83.5	5.5 98.0	7.9 96.9	2.8 99.7	0.4 100.1		
G-37-6a	3.9 16.0	11.1 27.1	35.8 62.9	36.5 99.4	0.6 100.0		
G-39-1a	5.5 96.2	2.9 99.1	0.8 99.9	0.2 100.1			
G-39-2a	15.6 80.7	10.9 91.6	5.4 97.0	3.1 100.1			
G-39-3a	30.5 70.3	21.1 91.4	7.2 98.6	1.4 100.0			
G-39-4a	6.6 81.5	6.9 88.4	8.3 96.7	3.0 99.7	0.3 100.0		

TABLE I  
(Continued)

Sample No.	Md.	Moment Measures -- Trask			Q <sub>3</sub>	Percentage	
		So.	Sk.	Q <sub>1</sub>		Gravel	Sand
G-37-2a	3.50	1.78	0.93	1.90	6.00	73.4	26.6
G-37-3	40.0	1.41	0.78	25.0	50.0	100	
G-37-4a	0.35	1.39	1.06	0.26	0.50		100
G-37-5a	17.0	6.55	0.07	0.7	30.0	64.2	35.8
G-37-6a	0.20	1.26	1.15	0.17	0.27	12.1	87.9
G-39-1a	3.8	2.24	0.59	1.3	6.5	65.1	34.9
G-39-2a	0.9	4.74	4.44	0.4	9.0	42.2	57.9
G-39-3a	0.43	1.46	1.25	0.33	0.70		100
G-39-4a	1.5	3.63	1.47	0.5	6.6	44.5	55.5

TABLE I  
(Continued)

Sample No.	Size Class in mm -- Fractional %/Cumulative %								
	64.0	32.0	16.0	8.00	4.00	2.00	1.00	.707	.500
G-39-5a	3.3	6.6	39.0	16.5	6.7	4.2	9.9	3.2	5.1
	3.3	9.9	48.9	65.4	72.1	76.3	86.2	89.4	94.5
G-40-1a			20.4	18.3	11.0	9.1	20.9	3.7	4.3
			20.4	38.7	49.7	58.8	79.7	83.4	87.7
G-40-2b							27.8	11.5	16.4
							27.8	39.3	55.7
G-40-3d							2.0		6.5
							2.0		8.5
G-40-4a							3.9		18.1
							3.9		22.0
G-43-1a			1.7	6.6	17.3	12.8	16.2	7.5	6.8
			1.7	8.3	25.6	38.4	54.6	61.1	67.9
G-43-3			7.0	47.9	20.9	4.7	6.2	1.4	2.0
			7.0	54.9	75.8	80.5	86.7	88.1	90.1
G-43-4a					0.27	0.53	0.97	0.41	2.7
					0.3	0.8	1.8	2.2	5.0
G-45-1a				1.8	4.5	20.2	51.7	5.9	5.3
				1.8	6.3	26.3	78.2	84.1	89.4

TABLE I  
(Continued)

Sample No.	Size Class in mm (continued) -- Fractional %/Cumulative %						
	.350	.250	.180	.125	.088	.062	.031 <.031
G-39-5a	1.9 96.4	2.7 99.1	0.5 99.6	0.3 99.9			
G-40-1a	6.1 93.8	4.3 98.1	1.2 99.3	0.6 99.9			
G-40-2b	27.9 83.6	11.5 95.1	3.3 98.4	1.6 100.0			
G-40-3d		41.0 49.5	35.4 84.9	13.0 97.9		2.0 99.9	0.1 100.0
G-40-4a		30.2 52.2	31.5 83.7	13.7 97.4		1.4 98.8	0.1 98.9
G-43-1a	13.1 81.0	7.5 88.5	6.8 95.3	3.1 98.4	0.6 100.0		
G-43-3	3.6 93.7	1.4 95.1	3.3 98.4	1.6 100.0			
G-43-4a	6.8 12.0	28.1 40.1	31.2 71.0		28.6 99.6	0.19 99.8	
G-45-1a	5.9 95.3	2.4 97.7	2.3 100.0				

TABLE I  
(Continued)

Sample No.	Md.	Moment Measures -- Trask			Q <sub>3</sub>	Percentage	
		So.	Sk.	Q <sub>1</sub>		Gravel	Sand
G-39-5a	16.0	2.83	0.20	2.5	20.0	76.3	23.7
G-40-1a	4.0	3.57	0.96	1.1	14.0	58.8	41.2
G-40-2b	0.56	1.70	1.33	0.38	1.10		100
G-40-3d	0.25	1.19	1.31	0.24	0.34	2.0	98.0
G-40-4a	0.27	1.50	1.24	0.20	0.45	3.9	96.1
G-43-1a	1.2	3.16	1.11	0.4	4.0	38.4	61.6
G-43-3	8.0	1.55	0.72	4.4	10.5	80.5	19.5
G-43-4a	0.23	1.19	0.97	0.19	0.27	0.8	99.2
G-45-1a	1.6	1.35	0.86	1.1	2.0	26.5	73.5

TABLE I  
(Continued)

Sample No.	32.0	Size Class in mm -- 16.0	8.00	Fractional %/Cumulative % 4.00	2.00	1.00	.707	.500
G-45-2a			14.1	23.7	21.5	16.9	5.1	4.2
			14.1	37.8	59.3	76.2	81.3	85.5
G-45-3a								8.2
								8.2
G-45-4a	4.7	22.8	4.5	0.3	0.2		0.7	2.7
	4.7	27.5	32.0	32.3	32.5		33.2	35.9
G-46-1a			9.1	21.6	27.9	27.2	5.1	3.6
			9.1	30.7	58.6	85.8	90.9	94.5
G-46-2		2.5	20.5	41.4	29.9	5.4	0.2	0.1
		2.5	23.0	64.4	94.3	99.7	99.9	100.0
G-46-3a	9.6	7.1	8.7	12.2	14.8	14.0	3.7	4.1
	9.6	16.7	25.4	37.6	52.4	66.4	70.1	74.2
G-46-4b		2.7	3.6	3.6	5.8	24.6	9.0	14.2
		2.7	6.3	9.9	15.7	40.3	49.3	63.5
G-46-5a		0.2	2.6	3.4	2.9	9.2	7.4	13.5
		0.2	2.8	6.2	9.1	18.3	25.7	39.2
G-47-1			0.8	18.5	42.0	27.2	4.3	1.4
			0.8	19.3	61.3	88.5	92.5	94.2

TABLE I  
(Continued)

Sample No.	Size Class in mm (continued) -- Fractional %/Cumulative %						
	.350	.250	.180	.125	.088	.062	.031 <.031
G-45-2a	7.5 93.0	2.3 95.3	3.3 98.6	1.4 100.0			
G-45-3a		43.6 51.8	35.8 87.6	11.2 98.8		1.1 99.9	0.1 100.0
G-45-4a	7.4 43.3	22.3 65.6	29.0 94.6	4.7 99.3	0.7 100.0		
G-46-1a	3.0 97.5	1.5 99.0	0.6 99.6	0.3 99.9			
G-46-2	0.1 100.1						
G-46-3a	10.2 84.4	8.6 93.0	4.1 97.1	2.9 100.0			
G-46-4b	20.8 84.3	7.1 91.4	5.6 97.0	2.4 99.4	0.5 99.9		
G-46-5a	23.4 62.6	19.6 82.2	14.7 96.9	3.1 100.0			
G-47-1	2.2 96.4	1.4 97.8	1.4 99.2	0.7 99.9			



TABLE I  
(Continued)

Sample No.	Md.	Moment Measures -- Trask			Q <sub>3</sub>	Percentage	
		So.	Sk.	Q <sub>1</sub>		Gravel	Sand
G-45-2a	2.8	2.32	0.88	1.1	5.9	59.3	40.7
G-45-3a	0.25	1.29	1.18	0.21	0.35	8.2	91.8
G-45-4a	0.30	8.42		0.24	17.00	32.5	67.5
G-46-1a	2.5	1.96	1.04	1.3	5.0	58.6	41.3
G-46-2	4.8	1.52	1.15	3.4	7.8	94.3	5.7
G-46-3a	2.2	4.00	0.83	0.5	8.0	52.4	47.6
G-46-4b	0.70	1.80	1.23	0.43	1.40	15.7	84.3
G-46-5a	0.42	1.58	1.11	0.28	0.70	9.1	90.9
G-47-1	2.1	1.23	0.98	1.6	2.7	61.3	36.7

TABLE I  
(Continued)

Sample No.	32.0	Size Class in mm -- 16.0	8.00	Fractional %/Cumulative % 4.00	2.00	1.00	.707	.500
G-47-2a		2.4	24.9	26.3	9.0	14.8	4.8	2.2
		2.4	27.3	53.6	62.6	77.4	82.2	84.4
G-47-3			1.6	27.3	33.0	21.5	5.4	3.2
			1.6	28.9	61.8	83.3	88.7	91.9
G-47-4a			2.3	1.4	0.9	2.4	9.5	4.8
			2.3	3.7	4.6	7.0	16.5	21.3
G-47-5a						20.1		14.6
						20.1		34.7
G-R-48-1a			0.2	0.3	2.5	16.0	11.4	39.1
			0.2	0.5	3.0	19.0	30.9	69.5
G-R-48-2a		9.7	18.0	25.8	7.0	1.7	0.58	2.15
		9.7	27.7	53.5	60.5	62.2	62.8	65.0
G-R-48-3b			1.5	4.6	4.4	17.4	5.1	21.5
			1.5	6.1	10.5	27.9	33.0	54.5
G-48-4a						10.3		26.7
						10.3		37.0
G-R-49-1a					0.8	10.5	9.0	47.4
					0.8	11.3	20.3	67.7

TABLE I  
(Continued)

Sample No.	Size Class in mm (continued) -- Fractional %/Cumulative %						
	.350	.250	.180	.125	.088	.062	.031 <.031
G-47-2a	6.1 90.5	3.0 93.5	3.9 97.4	2.2 99.6	0.4 100.0		
G-47-3	3.2 95.1	2.1 97.2	1.1 98.3	1.6 99.9			
G-47-4a	16.7 38.0	30.9 68.9	22.7 91.6	7.2 98.8	1.2 100.0		
G-47-5a		31.5 66.2	24.1 90.3	7.8 98.1		1.9 100.0	
G-R-48-1a		25.4 94.9	3.6 98.5	1.4 99.9		0.1 100.0	
G-R-48-2a		8.1 73.1	11.7 84.8	13.3 98.1	1.8 99.9	0.1 100.0	
G-R-48-3b		18.5 73.0	10.1 83.1	13.9 97.0	2.6 99.6	0.1 99.7	
G-48-4a		27.1 64.1	24.6 88.7	10.1 98.8		1.1 99.9	0.1 100.0
G-R-49-1a		29.3 97.0	2.2 99.2	0.64 99.8	0.10 99.9	0.1 100.0	

TABLE I  
(Continued)

Sample No.	Md.	Moment Measures -- Trask			Q <sub>3</sub>	Percentage	
		So.	Sk.	Q <sub>1</sub>		Gravel	Sand
G-47-2a	4.5	2.71	0.44	1.1	8.1	62.6	37.4
G-47-3	3.2	1.79	0.62	1.4	4.5	61.8	38.2
G-47-4a	0.31	1.37	1.03	0.23	0.43	4.6	95.4
G-47-5a	0.33	1.89	1.73	0.23	0.82	20.1	79.9
G-R-48-1a	0.56	1.29	1.22	0.48	0.80	3.0	97.0
G-R-48-2a	5.00	5.92	0.08	0.24	8.40	60.5	39.5
G-R-48-3b	0.56	2.14	0.84	0.24	1.10	10.5	89.5
G-48-4a	0.35	1.83	1.09	0.20	0.67	10.3	89.7
G-R-49-1a	0.52	1.17	1.17	0.48	0.66	0.8	99.2

TABLE I  
(Continued)

Sample No.	32.0	Size Class in mm -- 16.0	8.00	Fractional %/Cumulative % 4.00	2.00	1.00	.707	.500
G-R-49-2a				0.2	1.47	5.1	2.4	14.9
				0.2	1.6	6.6	9.0	23.9
G-R-49-3a		4.0	1.5	0.56	6.2	9.0	1.6	9.2
		4.0	5.5	6.1	12.3	21.3	22.9	32.1
L-1-1 1'						94.2		2.1
						94.2		96.3
L-1-2						3.0	3.0	0.8
						3.0	6.0	6.8
L-1-3								
L-1-4								
L-1-5								
L-1-6								
L-2-1					86.6			2.4
					86.6			89.6

TABLE I  
(Continued)

Sample No.	Size Class in mm (continued) -- Fractional %/Cumulative %						
	.350	.250	.180	.125	.088	.062	.031 <.031
G-R-49-2a		48.8	18.6	7.4	0.8		
		73.0	91.5	98.9	99.7		
G-R-49-3a	19.9	22.4	19.5		5.5	0.00	
	52.0	74.4	93.9		99.4		
L-1-1 1'		1.5	0.9	1.0		0.3	
		97.8	98.7	99.7		100.0	
L-1-2	2.3	5.3	15.0	42.8	27.1	0.8	
	9.1	14.4	29.4	72.2	99.3	100.1	
L-1-3	2.8	2.8	5.6	40.3	48.6		
	2.8	5.6	11.2	51.5	100.1		
L-1-4		2.3	6.8	54.5	33.0	3.4	
		2.3	9.1	63.6	96.6	100.0	
L-1-5	1.0	1.1	7.4	33.7	55.8	1.0	
	1.0	2.1	9.5	43.2	99.0	100.0	
L-1-6		1.1	2.3	21.6	72.7	2.3	
		1.1	3.4	25.0	97.7	100.0	
L-2-1		5.7	3.7	1.1		0.4	
		94.7	98.4	99.5		99.9	

TABLE I  
(Continued)

Sample No.	Md.	Moment Measures -- Trask			Q <sub>3</sub>	Percentage	
		So.	Sk.	Q <sub>1</sub>		Gravel	Sand
G-R-49-2a	0.35	1.41	1.02	0.25	0.50	1.6	98.4
G-R-49-3a	0.35	1.55	1.22	0.25	0.60	12.3	87.7
L-1-1 1'	1.4	1.19	1.04	1.2	1.7	94.2	5.8
L-1-2	0.15	1.32	1.12	0.12	0.21		100
L-1-3	0.125	1.17	1.06	0.11	0.15		100
L-1-4	0.13	1.08	0.99	0.12	0.14		100
L-1-5	0.12	1.22	1.04	0.10	0.15		100
L-1-6	0.12	1.12	0.87	0.10	0.125		100
L-2-1	2.8	1.20	0.97	2.3	3.3	86.6	13.4

TABLE I  
(Continued)

Sample No.	32.0	16.0	8.00	4.00	2.00	1.00	.707	.500
L-2-2								0.6
								0.6
L-2-4								
L-3-2								



TABLE I  
(Continued)

Sample No.	Size Class in mm (continued) -- Fractional %/Cumulative %						
	.350	.250	.180	.125	.088	.062	.031 <.031
L-2-2	0.6	2.3	18.6	55.8	22.1		
	1.2	3.5	22.1	77.9	100.0		
L-2-4	1.1	2.3	6.9	29.9	56.3	3.4	
	1.1	3.4	10.3	40.2	96.5	99.9	
L-3-2			6.0	48.2	45.8		
			6.0	54.2	100.0		

TABLE I  
(Continued)

Sample No.	Md.	Moment Measures -- Trask			Q <sub>3</sub>	Percentage	
		So.	Sk.	Q <sub>1</sub>		Gravel	Sand
L-2-2	0.160	1.20	0.88	0.125	0.180		100
L-2-4	0.12	1.23	1.04	0.10	0.15		100
L-3-2	0.13	1.27	0.95	0.10	0.16		100

## APPENDIX B

TABLE II

TEXTURAL ANALYSIS OF NOME BEACH SEDIMENT SAMPLES  
BY FOLK AND WARD METHOD

Sample No.	$\phi 5$	$\phi 16$	$\phi 50$	$\phi 84$	$\phi 95$	$M_z$	$\delta 1$	$Sk_i$
G-17-3	-4.32	-2.46	2.26	2.47	2.74	0.76	2.30	-0.89
G-20-5	-0.44	1.35	1.6	2.32	2.84	1.76	0.74	0.12
G-22-3	-3.0	-1.81	0.26	1.03	1.74	-0.17	1.43	-0.42
G-23-3	-5.32	2.55	1.64	2.06	2.25	2.08	1.02	-1.78
G-25-4	-0.48	0.15	1.39	2.18	2.32	1.24	0.93	-0.28
G-27-6	-1.81	-1.07	1.39	2.03	2.47	0.78	1.42	-0.54
G-29-4	-3.32	-1.26	1.88	2.18	2.56	0.93	1.75	-0.80
G-31-3	-3.0	-0.58	1.52	2.03	2.32	0.99	1.46	-0.65
G-33-4	-0.27	1.52	2.18	2.52	2.84	2.07	0.72	-0.45
G-34-8	0.15	0.45	0.73	1.15	1.43	0.78	0.37	0.15
G-35-8	0.52	0.74	1.22	2.0	2.64	1.32	0.64	0.29
G-37-6	-4.65	1.52	2.32	2.6	2.78	2.15	1.40	-0.68
G-39-4	-3.81	-3.17	-0.57	1.69	2.32	-0.68	2.14	-0.06
G-40-3	0.5	1.43	2.0	2.47	2.89	1.97	0.62	-0.18
G-43-4	1.0	1.6	2.12	2.74	3.12	2.15	0.61	0.02
G-45-4	-5.0	-4.32	1.74	2.15	2.56	-0.14	2.76	-0.83
G-46-5	-2.58	-0.2	1.26	2.03	2.32	1.03	1.30	-0.44
G-47-5	-0.77	-0.14	1.6	2.33	2.64	1.26	1.13	-0.40
G-48-4	-0.48	0.23	1.52	2.64	2.84	1.46	1.11	-0.14
G-49-3	-3.46	-0.58	1.52	2.18	2.64	1.04	1.61	-0.58

TABLE II  
(Continued)

Sample No.	$\phi_5$	$\phi_{16}$	$\phi_{50}$	$\phi_{84}$	$\phi_{95}$	$M_z$	$\delta_1$	$Sk_1$
L-1-2	0.32	2.06	2.74	3.12	3.33	2.64	0.72	-0.45
L-1-3	2.0	2.56	3.0	3.33	3.45	2.96	0.41	-0.26
L-1-4	2.18	2.64	2.94	3.18	3.45	2.92	0.33	-0.15
L-1-5	2.25	2.64	3.06	3.34	3.45	3.01	0.36	-0.28
L-1-6	2.56	2.89	3.06	3.38	3.47	3.11	0.26	0.10
L-2-2	2.18	2.33	2.64	3.18	3.38	2.72	0.39	0.25
L-2-4	2.18	2.47	3.06	3.34	3.47	2.96	0.41	-0.36
L-2-2	2.25	2.47	2.94	3.35	3.50	2.92	0.41	-0.09
L-1-1	-0.93	-0.77	-0.49	-0.14	0.15	-0.47	0.32	0.15
L-2-3	-1.97	-1.82	-1.48	-1.07	2.0	-1.46	0.79	0.42